technische universität
dortmund

2022

SCIENTIFIC HIGHLIGHTS

Annual Report

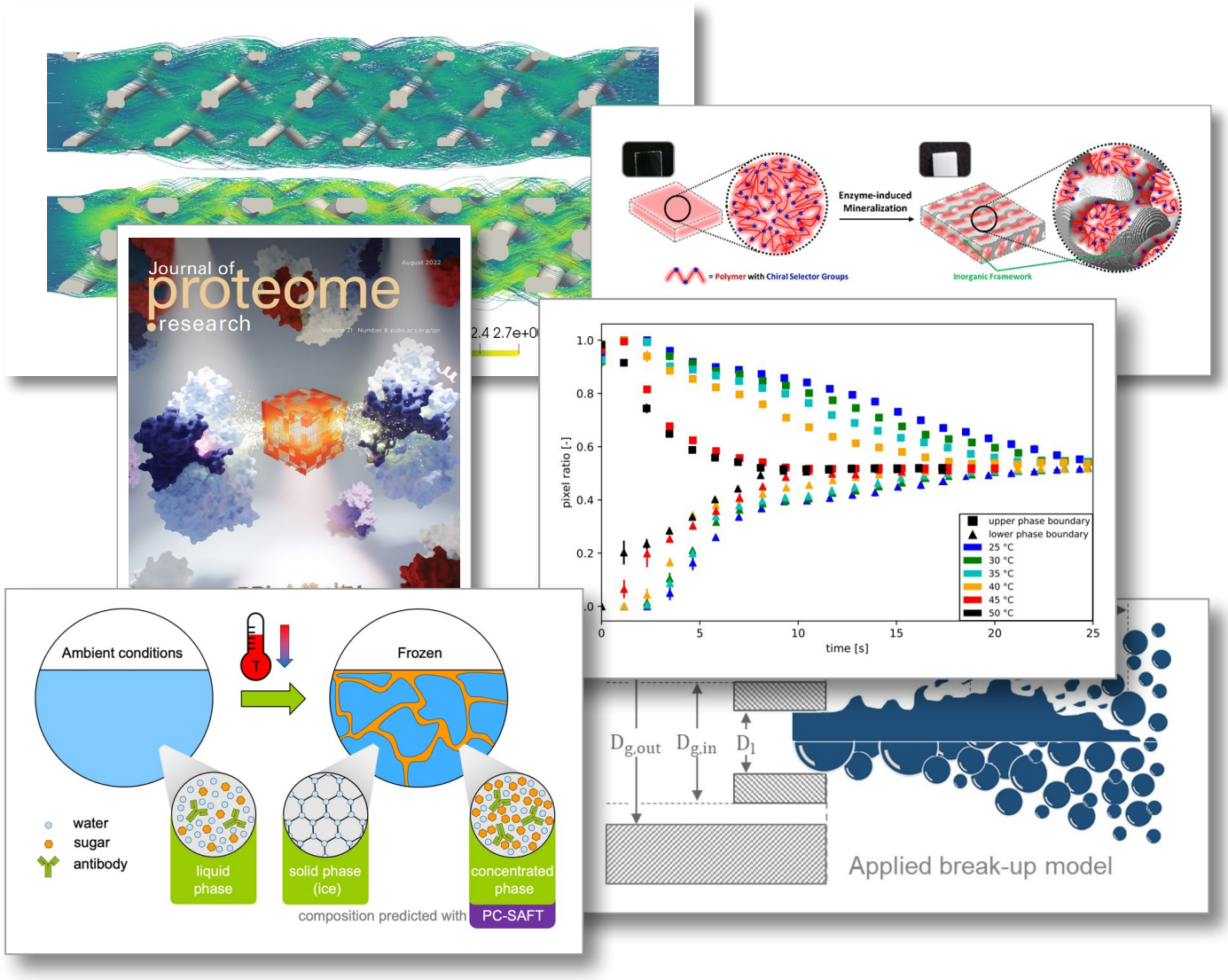

Fakultät Bio- und
Chemieingenieurwesen

Content

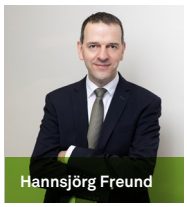
Hannsjörg Freund

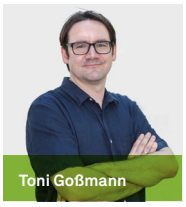
Toni Goßmann


Christoph Held


Oliver Kayser

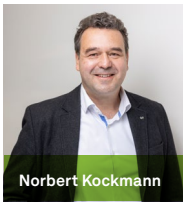
Norbert Kockmann

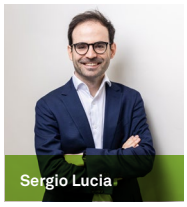
Sergio Lucia

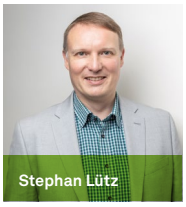
Stephan Lütz


Markus Nett

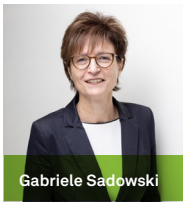
Gabriele Sadowski

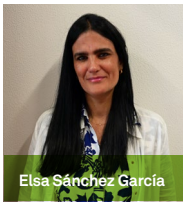
Elsa Sánchez García


Gerhard Schembecker


Markus Thommes

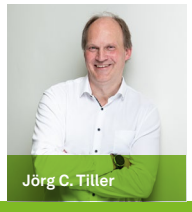
Jörg C. Tiller


Dieter Vogt

Department of BCI

Preface

Dear Reader,

I proudly present the Scientific Highlights of 2022 of the Department of Bio- and Chemical Engineering (BCI). This year of transitions after the fortunate end of the pandemic and the way back to “normal”, i.e., from “home office” back to lab or lecture hall, turned out to be challenging for some. Yet, we could successfully move forward enabling our Postdocs, Ph.D., Master, and Bachelor students to be scientifically inspired and productive. The here presented highlights are testament to these scientific achievements. The transitions took also place in the faculty. We say farewell to Prof. Germann, who followed a call to the University of Stuttgart, and warmly welcome our new colleagues Prof. Toni Goßmann (Computational Systems Biology) and Prof. Elsa Sánchez García (Computational Bioengineering) and wish them an excellent start. The present collection of excellent science is not only meant to show off, but also to inspire to readers to future become collaboration partners. This is of great importance, because the interdisciplinary, applied science of the faculty BCI ranging from process engineering over chemistry to systems biology is only possible with joint forces.

Enjoy the reading,

Joerg C. Tiller

Equipment Design (AD)

Ontology Development for Catalytical Reactions

Alexander S. Behr, Julia Surkamp, Norbert Kockmann

Catalytic data lacks standardized terms and conditions, making it difficult to retrieve, compare, and reuse. Machine-readable annotations are essential for leveraging advances in artificial intelligence AI and machine learning ML. Although complex datasets can now be retrieved and relevant information extracted, standardized data readability remains a challenge. To address this issue, we have developed an iterative approach that uses ontologies to define standardized terms and semantic relationships. This approach aims to improve the discoverability, accessibility, interoperability, and reuse of digital resources in catalysis.

The power of ontology description languages such as SKOS or OWL is that they are both based on Resource Description Framework (RDF), which allows for linking and connecting of concepts in human- and machine-readable form. As an example in Fig. 1, an enzyme can be thought of, or "conceptualized" as a protein-based catalyst, which in turn is a substance, while a biocatalytic reaction is some kind of a catalytic reaction, which in turn can be summarized with other (bio)chemical reactions by a super class called reaction. Every reaction in turn has some reactants, which each can be described as a substance. A catalytic reaction has the specification of at least one catalyst as a necessary reactant. Assuming, that a researcher has conducted a biocatalytic reaction in a certain well of a multiwell plate, this real-world realization of the biocatalytic reaction concept can be described as an individual of the latter class. This short (and incomplete) example of a, yet still not fully formalized, ontology is depicted in Fig. 1.

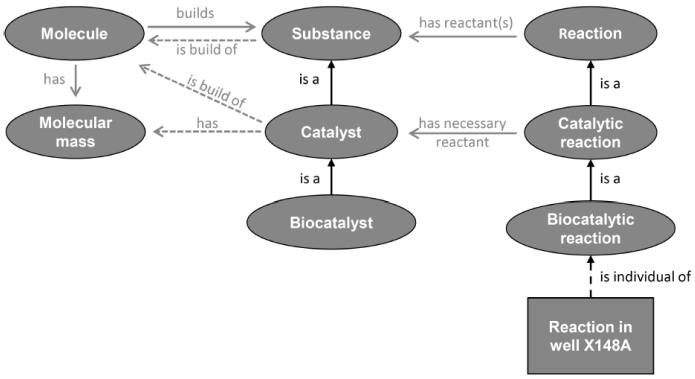

Figure 1: Short example of an ontology. Concepts in ellipsoids denote classes, black arrows hierarchical relations and grey arrows denote relationships between classes, dashed, grey arrows denote inferred relations.

The full use of ontologies lies within the structured data handling, ranging from experiments to simulations. This helps in interconnecting data from different sources. In an overall data flow depicted in Fig. 2, the data obtained from the experiments is described via an ontology. The ontology gets evaluated via a python script to obtain the data from the experiments together with their corresponding metadata derived from the ontology. Additionally, a database was created from the generated experimental data. In the database, the generated tables of the laboratory experiments are stored and assigned database IDs. These IDs are linked to individuals of the ontology, thus enabling data access.

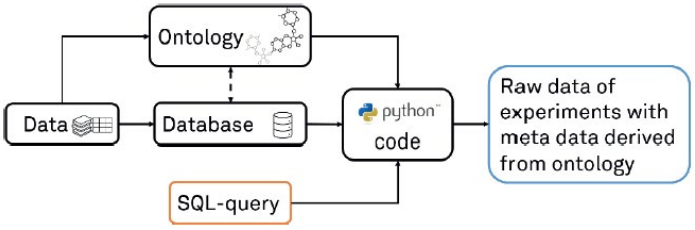

Figure 2: : Overall data flow from raw data to structured queries on ontologies to gain meta data.

Contacts:
alexander.behr@tu-dortmund.de
norbert.kockmann@tu-dortmund.de

Publications:
M.J. Menke, A.S. Behr, K. Rosenthal, D. Linke, N. Kockmann, U.T. Bornscheuer, M. Dörr, Chem. Ing. Technik, 94(11), 1827-1835, 2022, DOI: 10.1002/cite.202200066.
J. Grühn, A.S. Behr, T. Eroglu, V. Trögel, K. Rosenthal, N. Kockmann, Chem. Ing. Technik, 94 (6), 852-863, 2022, DOI:10.1002/cite.202100177.

Development of an Automatable Affinity Purification Process for DNA Encoded Chemistry

Katharina Götte, Robin Dinter, Leon Justen, Norbert Kockmann, Andreas Brunschweiger

Reaction screening can be assisted by DNA-labelled substrate marking, the DNA encoded library (DEL) setup. These DEL technologies can benefit from high throughput, automatable platforms for chemistry development, building block rehearsal, and library synthesis. An affinity based process based on dispersive solid phase extraction (DSPE) and Watson Crick interactions was developed that enables purification of DNA tagged compounds under washing conditions with multiple solvents. The lab equipment for purification of DNA conjugate was constructed by 3D printing and tailored for parallel automation with open source hardware in combination with an automated dosing system (ADoS).

In DSPE, the solid phase is dispersed in an agarose matrix with a covalently bound azide functionality, as shown in Figure 1. A 14mer DNA single strand **DNA 1** is loaded with low density to the matrix by copper-catalyzed alkyne azide cycloaddition reaction to obtain **capture DNA 1**. The complementary DEL-DNA-single strand **DNA 2** is added to the dispersion with the sorbent and mixed, as shown in Figure 1B. **DNA 2** is bound to the solid phase by annealing via Watson–Crick interactions. The contaminants are separated from the product by washing the matrix with water, an aqueous EDTA solution to remove metal contaminants, and various aqueous mixtures of organic solvents to remove further contaminants. The product **DNA 2** is eluted from the affinity matrix via denaturing the double strand using an aqueous ammonia solution.

The repetitive and laborious washing and elution steps of the newly established DNA conjugate purification process performed by a 3D printed microwell filter plate device (Figure 1B). To evaluate the automatability of the DNA conjugate purification process, the head to head comparison of the microwell filter plate device and batch procedure shows that both provided similar recovery of the **DNA 2**. The microwell filter plate device is successfully validated for parallel purification of multiple **DNA 2** products by purifying 10 **DNA 2** products without contaminations. Finally, the potential of the 3D printed microwell filter plate device is demonstrated for automation using the ADoS. The head to head comparison of the quantitative results of these experiments shows that the ADoS reproduces the manually performed washing steps with the same amount of purified **DNA 2** products (Fig. 2).

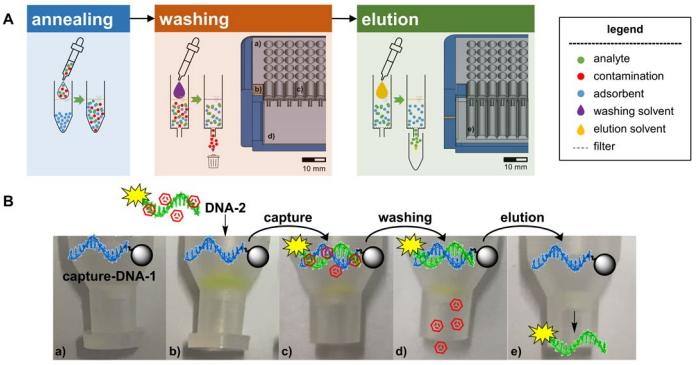

Figure 1: Affinity based purification process for DNA encoded chemistry. A) Design of the tailored 3D printed vacuum chambers for washing and elution with (a) a 96 microwell filter plate with 35 µm pore size; (b) silicon sealing; (c) filter; (d) waste container; (e) 96-microwell plate for collecting the cleaned product DNA. B) Pictures of the **capture DNA 1** in filter columns (a) after capturing **DNA 2** (b, c), washing with several solvents (d), and elution of **DNA 2**.

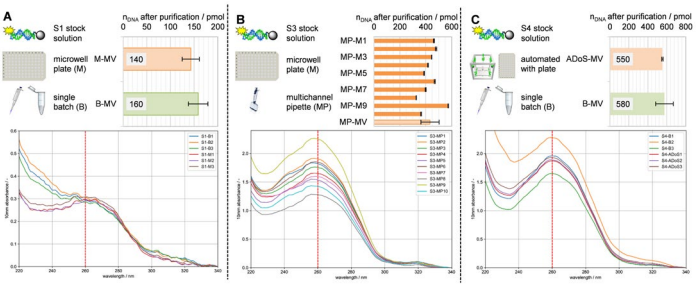

Figure 2: Evaluation of the automatability of the DNA-conjugate purification process in three individual experiments. (A) Comparison of the microwell filter plate device (M) and single batch procedure (B) with stock solution S1. (B) Validation of the parallelization of the microwell filter plate device with the tailored 3D-printed equipment using stock solution S3 and a multichannel pipette (MP) manually. (C) Validation of the automated microwell filter plate washing steps using stock solution S4.

Publications:
K. Götte, R. Dinter, L. Justen, N. Kockmann, A. Brunschweiger, ACS Omega. 7(32), 28369–28377, 2022.
J. Bobers, L.K. Hahn, T. Averbeck, A. Brunschweiger, N. Kockmann, Chem. Ing. Technik, 94(5), 780-785, 2022.

Contacts:
robin.dinter@tu-dortmund.de
norbert.kockmann@tu-dortmund.de

Measuring Kinetics in Flow Using Isoperibolic Flow Calorimetry

Timothy Aljoscha Frede, Moritz Greive, Nick Nikbin, Norbert Kockmann

Continuous flow calorimeters are a promising tool in process development and safety engineering, especially for flow chemistry applications to characterize the heat release and kinetic parameters of rapid chemical reactions. An automated isoperibolic flow calorimeter was developed with digital accompaniment for characterization of exothermic reactions and mixing progress. Reaction enthalpy is determined via an energy balance of the entire calorimeter. Characterization of reaction kinetics is carried out via a local balancing of the individual Seebeck elements using measurements with different flow rates. To support experimental planning and evaluation, computational fluid dynamic simulations are carried out for single-phase flow in the microreactor.

The calorimeter's setup and its peripheral equipment have been described in previous works of Reichmann et al. and Frede et al. In the current development step, the oxidation of sodium thiosulfate with hydrogen peroxide was chosen as a test reaction to study the assessment of kinetics in flow using micro calorimetry because of its ease of use and high exothermicity. Additionally to calorimetric measurements, the coupling of CFD and reactor performance estimation is shown. The focus is put on the simplification and acceleration of estimation of temperature and conversion profiles. This leads to an integration of CFD simulations into a microcalorimeter's software-guided workflow reducing the experimental effort regarding the determination of thermokinetic data.

Using the local balancing of the individual Seebeck elements, five automated runs resulted in 48 data points for the Arrhenius plot (Figure 1). The activation energy was determined to be 62.2 kJ mol^{-1} and the frequency factor to be 2.6 × 109 L mol^{-1} s^{-1}. In general, the calculated kinetic parameters are in the range of literature values. The predicted conversion and temperature profiles are compared to experimental data obtained in the microcalorimeter for volumetric flow rates between 0.03 and 0.30 mL min^{-1} (Figure 2). All in all, the calculations of conversion and temperature profiles lead to good agreement with experimental results with this approach for volumetric flow rates up to 0.17 mL min^{-1} and enable predictions of suitable experimental settings for microreactor used. The kinetic data can be easily varied, since only the reactor performance has to be recalculated, not the flow behavior with residence time distribution.

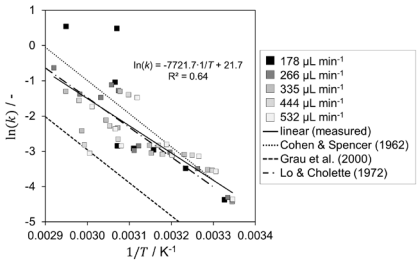

Figure 1: Arrhenius plot for sodium thiosulfate oxidation using hydrogen peroxide in LTF-MS in comparison with literature.

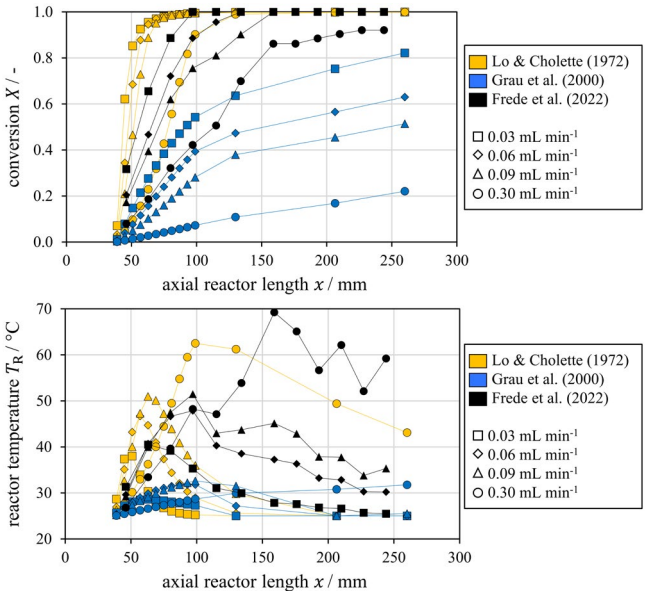

Figure 2: Comparison of experimental data by Frede et al. (2022) and predicted conversion and temperature in the LTF-MS reactor with kinetic parameters of Lo & Cholette, Can. J. Chem. Eng. (1972) and Grau et al., Chem. Eng. Process. (2000) for c_(NaTS,0) = 1 M and T_in = T_ambient = 25 °C and different volumetric flow rates.

Contacts:
timothy.frede@tu-dortmund.de
norbert.kockmann@tu-dortmund.de

Publications:
T.A. Frede, M. Greive, N. Kockmann, Reactions. 3(4), 525-536 (2022).
T.A. Frede, N. Nikbin, N. Kockmann, J. Flow Chem. (2022).

Cooling Crystallization with Complex Temperature Profiles on a Quasi-Continuous and Modular Plant

Stefan Höving, Bastian Oldach, Phil Bolien, Norbert Kockmann

Increasing demands for quality and fast availability of specialty chemical products led to the rise of small-scale, integrated, and modular continuous processing plants. Particularly, cooling crystallization is part of this trend as a significant unit operation used for product isolation and purification. A modular filter belt crystallizer was developed and characterized regarding crystal size distribution. It was found that seed crystal properties are the most important parameter. Further, an oscillating temperature profile has a narrowing effect on the particle size distribution. The integrated, small-scale, and modular setup of the filter belt crystallizer offers high degrees of flexibility, process control, and adaptability to cope with future market demands

The modular, small-scale and integrated quasi-continuous filter belt crystallizer (QCFBC) combines cooling crystallization, solid-liquid separation, and drying on a single apparatus (cf. Figure 1). The presented research shows the general working principle, different operation modes, and possibilities of temperature control with the modular setup. For precise temperature control in cooling crystallization, Peltier elements show promising results in a systematic study of different operation parameters, where sucrose/water was used as a model substance system.
Cooling crystallization of sucrose dissolved in water was investigated in detail for different seed crystal sizes, seed crystal amount, process time, and three different temperature profiles (cf. Figure 2). Although temperature control via Peltier elements is quite common for microfluidic applications, literature on temperature control in cooling crystallization of comparable dimensions, as presented here, is scarce. The developed temperature module with Peltier elements enables precise temperature control with deviations smaller than 0.5 K from the target temperature in the range from 20 °C to 60 °C. The modular setup is supported by a 3D-printed container lid that holds a temperature sensor and two-pitch blade stirrers responsible for suspending the crystals. As the temperature is precisely controlled on the crystallization modules, investigation of the progressive and the oscillating temperature profiles has shown that refraining from the classical linear profile has beneficial effects on the product properties (cf. Figure 2). Particularly the oscillating temperature profile substantially narrows the product size distribution without major drawbacks regarding product size or yield.

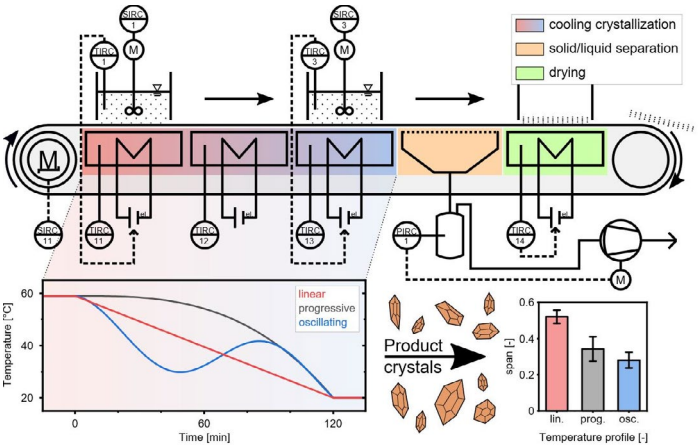

Figure 1: Simplified Piping and Instrumentation Diagram of the quasi-continuous filter belt crystallizer. Process containers are incrementally moved from left to right, passing each module.

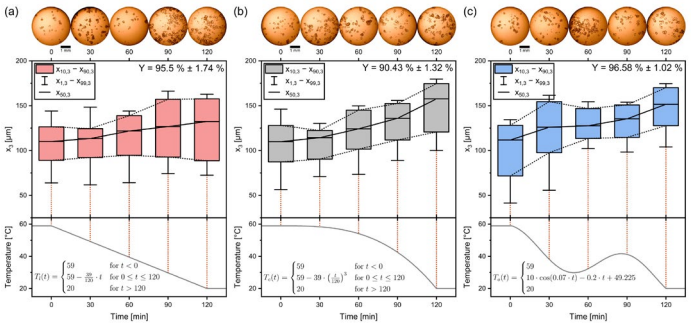

Figure 2: Boxplots of the crystallization of sucrose for the discussed temperature profiles. (a) shows the linear, (b) the progressive, and (c) the oscillating temperature profile. Yields are indicated in the top right. Quantiles are averages from triple experiments. The temperature profiles are plotted in the bottom panels. Process time $t_{process}$ = 120 min, seed crystal amount Ω_{SC} = 0.025 g·g_{ECM}^{-1}, seed sieve size: 90–125 µm.

Publications:
[1] S. Höving, B. Oldach, N. Kockmann, Cooling Crystallization with Complex Temperature Profiles on a Quasi-Continuous and Modular Plant, MDPI processes, 10(6) 1047, 2022, doi.org/10.3390/pr10061047
[2] J. Sonnenschein, M. Hermes, S. Höving, N. Kockmann, K. Wohlgemuth, Population balance modeling of unstirred cooling crystallization on an integrated belt filter, Comp. & Chem. Eng., 167, 108024, 2022, doi.org/10.1016/j.compchemeng.2022.108024

Contacts:
Stefan.Hoeving@tu-dortmund.de
Norbert.Kockmann@tu-dortmund.de

AI-based Image Recognition for Process Analysis and Supervision

Laura Neuendorf, Pia Kolloch, Tobias Kock, Christian Bergeest, Md Jahangir Alam, Norbert Kockmann

Fast on-line analysis of chemical processes requires new methods of analysis for liquid-liquid systems. The development is inevitably linked to optimized data acquisition of chemical systems. In order to visualize the complex interplay of two-phase systems, AI-based methods are advantageous for process monitoring techniques. In addition, improved process monitoring leads to more process parameters being determined live, enabling new ways of online process control. Automated process control based on image analysis using convolutional neural networks is therefore developed.

Artificial Intelligence (AI)-based process supervision and process control methods were developed with the goal of developing new analysis methods for laboratory measurement processes based on AI-assisted camera sensor technology.

First, properties of crystals were analyzed using AI-based image analysis. Here, the 2D properties of crystals such as diameter and Q3 distribution were investigated in a flow cell under the light microscope. Based on this, 3D analytics were developed to additionally determine the Waddell sphericity in the cluster of crystals in the microcomputed tomograph (a) in Figure 1). Secondly, an artificial neural network and the associated post-processing were developed for a cost-effective, easy-to-use online measurement method to determine various substance parameters of liquids, e.g. density and interfacial tension. These substance parameters can be determined iteratively with high accuracy from rising single droplets by solving a force balance seen in (b) in Figure 1). A third laboratory analysis method was developed, where the coalescence behavior of liquid-liquid substance systems is investigated using a convolutional neural network indicated as c) in Figure 1. The coalescing time of different chemicals under varying temperatures was accurately determined, indicated in Figure 2. From this, recommendations for the optimal scale-up of phase separation processes can be derived.

Further image recognition with convolutional neural networks was used for process monitoring of an extraction column. With the help of the additional camera sensor and CNN, the undesired operating state "flooding" can be detected and delimited from the regular operation (d) in Figure 1).

Furthermore, the diameters of the rising droplets in the extraction column can be determined and averaged using Mask RCNN (e) in Figure 1). The average droplet size parameter enables reliable process control at the optimum operating point, since a defined optimum droplet size correlates directly with the best possible separation efficiency of the extraction

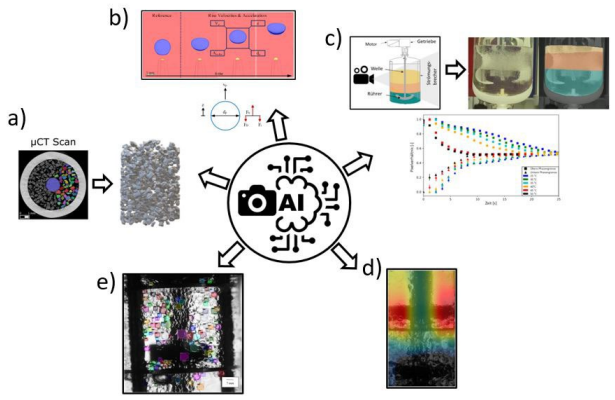

Figure 1: Different use cases of AI-based image analysis in the field of process analysis a)-c) and online process monitoring and control d), e).

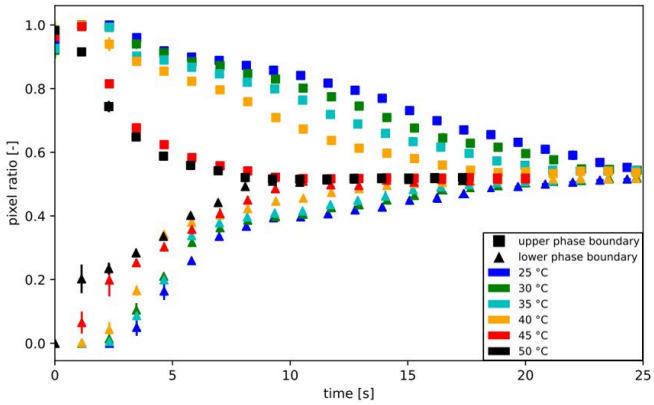

Figure 2: Results of the influence of temperature on the coalescence behavior of n-butyl acetate/water. The course of the coalescing, upper phase boundary (UPB, squares) and the sedimenting, lower phase boundary (LPB, triangles) over time is depicted.

Contacts:
laura.neuendorf@tu-dortmund.de
norbert.kockmann@tu-dortmund.de

Publications:
[1] S. Höving, L. Neuendorf, T. Betting, N. Kockmann, Determination of Crystal Size Distributions of Bulk Samples using Micro-Computed Tomography and Artificial Intelligence, MDPI Materials, accepted 2022
[2] L. Neuendorf, P. Müller, C. Bergeest, C. Schlander, A. Meijer, N. Kockmann, Künstliche Intelligenz (KI)-basierte optische Sensorik für flüssig-flüssig Systeme, 16. Dresdner Sensor-Symposium 2022, DOI: 10.5162/16dss2022/P50
[3] L. Neuendorf, F.Z. Baygi, P. Kolloch, N. Kockmann, Implementation of a control strategy of a stirred liquid–liquid extraction column based on convolutional neural networks, ACS Engineering Au, 2(4), 369–377, 2022, doi.org/10.1021/acsengineeringau.2c00014
[4] R. de Cerqueira, O. Bayomie, L. Neuendorf, K. Lammers, I. Kornijez, S. Kieling, T. Sandermann, N. Kockmann, Detecting flooding state in extraction columns: convolutional neural networks vs. a white-box approach for image-based soft sensor development, Comp. & Chem. Eng., 164 (107904), 2022, doi.org/10.1016/j.compchemeng.2022.107904
[5] V. Khaydarov, L. Neuendorf, T. Kock, N. Kockmann, L. Urbas, MTPPy: Open-Source AI-friendly Modular Automation, 2022 IEEE 27th International Conference on Emerging Technologies and Factory Automation (ETFA), Stuttgart, DOI: 10.1109/ETFA52439.2022.9921713

AI support for drawing piping and instrumentation diagrams in DEXPI

Jonas Oeing, Wolfgang Welscher, Niclas Krink, Lars Jansen, Fabian Henke, Norbert Kockmann

The design and engineering of piping and instrumentation diagrams (P&ID) is a very time-consuming and labor-intensive process. With support from machine learning (ML) tools, it is possible to recognize typical patterns and to make them available for the development and the drawing process of P&IDs. In order to achieve this, P&ID data is made accessible for AI applications through the DEXPI format (Data EXchange in Process Industry) as a machine-readable, manufacturer-independent exchange standard. It is demonstrated how ML models trained with P&ID data can support the drawing and engineering of P&IDs to decrease labor time and costs.

This is achieved by assisted prediction of equipment in P&IDs based on recurrent neural networks as well as consistency checks based on graph neural networks. Fig. 1 shows the two use cases identified for AI-assisted P&ID synthesis and their respective modeling approaches. In the first use case, a node prediction generates suggestions about subsequent components based on a recurrent neural network (RNN). These suggestions can support the user and decrease the time of the drawing process. The second approach uses graph neural networks (GNN), which are neural networks especially developed for the modeling of graphs. They can learn the topologies of process plants, which are stored in the form of a graph, and enable a consistency check during drawing by comparing the models with drawn P&IDs.

Graph-based P&ID formats are a promising way to improve the machine-readability of important process information. The standardized DEXPI format, which is continuously improved by the DEXPI Initiative, is able to store the topology of process plants as well as all apparatus specifications in a structured way and make them available in a machine-interpretable manner. This standardization enables the retrieval of information and a simple application of ML models. Primarily, it is recommended to suggest components during P&ID synthesis and to identify and reduce possible errors through validation. In addition, further AI solutions can be developed that recognize functional groups in P&IDs. This includes safety assessment and HAZOP studies, where machine-readable HAZOP scenarios could be mapped to graph-based plant topologies using deterministic search algorithms. In the future a possible detection of subgraphs in P&IDs i.e. functional equipment assemblies could facilitate the mapping between process simulations based on unit operations and P&IDs.

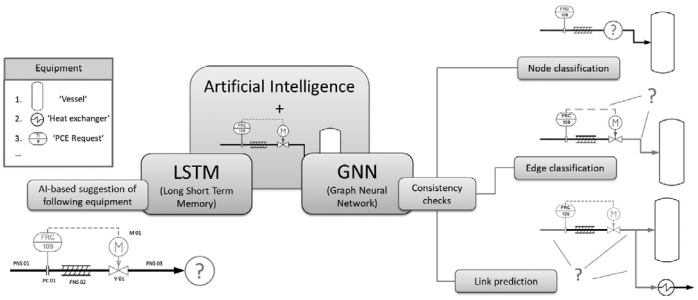

Figure 1: Use cases of artificial intelligence to accelerate and improve the synthesis of P&IDs using Recurrent Neural Networks as well as Graph Neural Networks.

Publications:
J. Oeing, W. Welscher, N. Krink, L. Jansen, F. Henke, N. Kockmann, Digital Chemical Engineering, 4, 100038, 2022

Contacts:
jonas.oeing@tu-dortmund.de
norbert.kockmann@tu-dortmund.de

Publications 2020 – 2022

2022

Peer-reviewed Journal Articles

- J. Sonnenschein, M. Hermes, S. Höving, N. Kockmann, K. Wohlgemuth
  Population balance modeling of unstirred cooling crystallization on an integrated belt filter
  Comp. & Chem. Eng., 167, 108024 (2022) DOI:10.1016/j.compchemeng.2022.108024

- M.J. Menke, A.S. Behr, K. Rosenthal, D. Linke, N. Kockmann, U.T. Bornscheuer, M. Dörr
  Ontology development in Biocatalysis
  Chem. Ing. Technik, 94(11), 1827-1835, (2022) DOI: 10.1002/cite.202200066

- T. A. Frede, M. Greive, N. Kockmann,
  Measuring Kinetics in Flow Using Isoperibolic Flow Calorimetry
  MDPI reactions, 3(4), 525-536, (2022) DOI: 10.3390/reactions3040035

- R. de Cerqueira, O. Bayomie, N. Kockmann, L. Neuendorf, K. Lammers, I. Kornijez, S. Kieling, T. Sandermann
  Detecting flooding state in extraction columns: convolutional neural networks vs. a white-box approach for image-based soft sensor development
  Comp. & Chem. Eng., 164 (107904), (2022) DOI: 10.1016/j.compchemeng.2022.107904

- A. Klose, J. Lorenz, L. Bittorf, K. Stark, M. Hoernicke, A. Stutz, H. Weinhold, N. Krink, W. Welscher, M. Eckert, S. Unland, A. Menschner, P. da Silva Santos, N. Kockmann, L. Urbas
  Orchestration of modular plants: Procedure and application for orchestration engineering
  atp, 63(9), 68-77, (2022) DOI: 10.17560/atp.v63i9.2599

- K. Götte, R. Dinter, L. Justen, N. Kockmann, A. Brunschweiger
  Development of an Automatable Affinity Purification Process for DNA-Encoded Chemistry
  ACS Omega, 7(32), 28369-28377, (2022) DOI: 10.1021/acsomega.2c02906

- L.M. Neuendorf, F.Z. Baygi, P. Kolloch, N. Kockmann
  Implementation of a control strategy of a stirred liquid-liquid extraction column based on convolutional neural networks
  ACS Engineering Au, 2(4), 369-377, (2022) DOI: 10.1021/acsengineeringau.2c00014

- P. Sakthithasan, N. Gerdes, M. Venhuis, N. Kockmann
  Investigation of strong asymmetric pulsation patterns in a stirred-pulsed extraction measurement cell
  Chem. Eng. Proc - PI, 180, 108757, (2022) DOI: 10.1016/j.cep.2021.108757

- J. Oeing, W. Welscher, N. Krink, L. Jansen, F. Henke, N. Kockmann
  Using artificial intelligence to support the drawing of piping and instrumentation diagrams in DEXPI standard
  Digital Chemical Engineering, 4, 100038, (2022) DOI: 10.1016/j.dche.2022.100038

- A. Markaj, A. Fay, N. Kockmann
  Definition, characterization, and modeling of hybrid modular-monolithic process plants
  Chem. Ing. Technik, 94(8), 1117-1130, (2022) DOI: 10.1002/cite.202200048

- J. Schuler, J. Herath, N. Kockmann
  X-ray based Tomographic Imaging for the Investigation of Laminar Mixing in Capillaries
  Chem. Eng. & Technol., 45(7), 1247-1254, (2022) DOI: 10.1002/ceat.202100530

- S. Höving, B. Oldach, N. Kockmann
  Cooling Crystallization with Complex Temperature Profiles on a Quasi-Continuous and Modular Plant
  MDPI processes, 10(6) 1047, (2022) DOI: 10.3390/pr10061047

- S. Höving, J. Bobers, N. Kockmann
  Open-source multi-purpose sensor for measurements in continuous capillary flow
  J. Flow Chem., 12, 185-196, (2022) DOI: 10.1007/s41981-021-00214-w

- J. Grühn, A. Behr, K. Rosenthal, N. Kockmann
  From coiled flow inverter to stirred tank reactor - Bioprocess development and ontology design
  Chem. Ing. Technik, 94 (6), 852-863, (2022) DOI: 10.1002/cite.202100177

- A. Frede, M. Maier, N. Kockmann, H. Gruber-Wölfler
  Advances in continuous flow calorimetry
  Org. Proc. R&D, 26(2), 267-277, (2022) DOI: 10.1021/acs.oprd.1c00437

- J. Bobers, L.K. Hahn, T. Averbeck, A. Brunschweiger, N. Kockmann
  Reaction Optimization of a Suzuki-Miyaura Cross-Coupling using Design of Experiments
  Chem. Ing. Technik, 94(5), 780-785, (2022) DOI: 10.1002/cite.202100194

- M. Schmalenberg, L. Mensing, S. Lindemann, T. Krell, N. Kockmann
  Miniaturized Draft Tube Baffle Crystallizer for Continuous Cooling Crystallization
  Chem. Eng. R&D, 178, 232-250, (2022) DOI: 10.1016/j.cherd.2021.12.024

Peer-reviewed Conference Papers

- R. Dinter, L. Helwes, M. Pillath, N. Kockmann
  Electrical Conductivity Sensor with Open-Source Hardware for the Microfluidic Determination of Reaction Parameters
  Poster-Beitrag, 16. Dresdner-Sensor Symposium, 5.-7.12.2022

- L. Neuendorf, P. Müller, C. Bergeest, A. Meijer, C. Schlander, N. Kockmann
  Künstliche Intelligenz (KI)-basierte optische Sensorik für flüssig-flüssig Systeme
  Poster-Beitrag, 16. Dresdner-Sensor Symposium, 5.-7.12.2022

- I. Burke, A.S. Youssef, N. Kockmann
  Design of an AI-supported Sensor for Process Relevant Parameters in Emulsification Processes
  Poster-Beitrag, 16. Dresdner-Sensor Symposium, 5.-7.12.2022

- A. Behr, H. Borgelt, N. Kockmann
  Modelling knowledge with ontologies for catalysis research, invited talk, Machine Learning and Modelling
  Seminar, Charles University, Prague, 29.09.2022

- L. Korel, M. Holena, A. Behr, N. Kockmann
  Using Artificial Neural Networks to Determine Ontologies Most Relevant to Scientific Texts, oral talk, Machine Learning and Modelling
  Seminar, Charles University, Prague, 29.09.2022

- U. Yorsh, A. Behr, N. Kockmann, M. Holena
  Text-to-Ontology Mapping via Natural Language Processing Models, oral talk, Machine Learning and Modelling
  Seminar, Charles University, Prague, 29.09.2022

- R. Dinter, S. Willems, M. Hachem, M. Mittelstädt, A. Brunschweiger, N. Kockmann
  Two-Phase Flow Reaction System for Amide Coupling Towards Automated DNA-Encoded Chemistry
  ProcessNet Annual Meeting, Aachen, 12.-15.09.2022

- R. Dinter, L. Helwes, M. Pillath, N. Kockmann
  Reaction Kinetic Investigation with Open-Source Microfluidic Conductivity Sensor, poster presentation, Micro Flow and Interfacial Phenomena
  µFIP 2022 Conference, Irvine, USA, 20-23 June 2022

- I. Burke, S. Derkum, N. Kockmann
  Light Dependent Resistor for Online Dispersion Point In Time Detection in Emulsification Processes via Minichannel Bypass, oral presentation, Micro Flow and Interfacial Phenomena
  µFIP 2022 Conference, Irvine, USA, 20-23 June 2022

- L. Neuendorf, C. Bergeest, C. Schlander, A. Meijer, N. Kockmann
  Liquid-Liquid Interphase Tracking During Coalescence for Process Scale Up, oral presentation, Micro Flow and Interfacial Phenomena
  µFIP 2022 Conference, Irvine, USA, 20-23 June 2022

- B. Oldach, C. Helwing, K.F. Buchhorn, N. Kockmann
  Micro-Computed Tomography for 3D-Imaging of Liquid-liquid Interfaces in Capillary Flow, oral presentation, Micro Flow and Interfacial Phenomena
  µFIP 2022 Conference, Irvine, USA, 20-23 June 2022

Book chapters

- N. Kockmann, D.W. Agar,
  Liquid-Liquid Processes - Mass Transfer Processes and Chemical Reactions,
  in V. Ranade, R. Utikar (eds.) Multiphase Flows for Process Industries: Fundamentals and Applications Vol. 2, Wiley-VCH, Weinheim, 2022, ISBN 978-3-527-34377-5, doi.org/10.1002/9783527812066.ch5

2021

Peer-reviewed Journal Articles

- J. Oeing, L. Neuendorf, L. Bittorf, W. Krieger, N. Kockmann
  Flooding Prevention in Distillation and Extraction Columns with Aid of Machine Learning Approaches
  Chem. Ing. Technik, 93(12), 1917-1929, (2021) DOI: 10.1002/cite.202100051

- M. Wiedau, G. Tolksdorf, J. Oeing, N. Kockmann
  Towards a systematic data harmonization to enable AI application in the process industry
  Chem. Ing. Technik, ,93(12), 2105-2115, (2021) DOI: 10.1002/cite.202100203

- J. Oeing, F. Henke, N. Kockmann
  Machine Learning based suggestions of separation units for process synthesis in process simulation
  Chem. Ing. Technik, 93(12), 1930-1936, (2021) DOI: 10.1002/cite.202100082

- F. Reichmann, J. Herath, L. Mensing, N. Kockmann
  Gas-liquid mass transport intensification for bubble breakup employing micronozzles
  J. Flow Chem., 11(3), 429-444, (2021) DOI: 10.1007/s41981-021-00180-3

- T.A. Frede, M. Dietz, N. Kockmann
  Software-Guided Microscale Flow Calorimeter for Efficient Acquisition of Thermokinetic Data
  J. Flow Chem, 11(3), 321-332, (2021) DOI: 10.1007/s41981-021-00145-6

- M. Schmalenberg, L. Weick, N. Kockmann
  Nucleation for Continuous Flow Cooling Sonocrystallization for Coiled Capillary Crystallizers
  J. Flow Chem, 11(3), 303-319, (2021) DOI: 10.1007/s41981-020-00138-x

- V. Fath, P. Lau, C. Greve, P. Weller, N. Kockmann, T. Röder
  Simultaneous self-optimisation of yield and by-product formation through successive combination of inline FT-IR spectroscopy and online mass spectrometry
  J. Flow Chem., 11(3), 285 – 302, (2021) DOI: 10.1007/s41981-021-00140-x

- J. Schuler, J. Herath, N. Kockmann
  3D Investigation of Laminar Mixing and Diffusion in Helically Coiled Capillaries by Micro-Computed Tomography
  J. Flow Chem, 11(3), 217-222, (2021) DOI: 10.1007/s41981-021-00161-6

- A. Kulkarni, R. Hartman, N. Kockmann
  Editorial of Special Issue on Engineering Aspects in Flow Chemistry
  J. Flow Chem, 11(3), 211-212, (2021) DOI: 10.1007/s41981-021-00197-8

- L. Bittorf, K. Pathak, N. Kockmann
  Spinning band distillation column – rotating element design and vacuum operation
  Ind.&Eng. Chem. Res., 60(30), 10854-10862, (2021) DOI: 10.1021/acs.iecr.1c01326

- C. Wulf, M. Beller, T. Boenisch, O. Deutschmann S. Hanf, N. Kockmann, R. Kraehnert, M. Oezaslan, S. Palkovits, S. Schimmler, S.A. Schunk, K. Wagemann, D. Linke
  A Unified Research Data Infrastructure for Catalysis Research - Challenges and Concepts
  ChemCatChem, 13(14), 3223-3236, (2021) DOI: 10.1002/cctc.202001974R2

- L. Bittorf, N. Böttger, D. Neumann, A. Winter, N. Kockmann
  Characterization of an automated spinning band column as a module for laboratory distillation
  Chem. Eng. & Technol., 44(9), 1660-1667, (2021) DOI: 10.1002/ceat.202000602

- M. Schmalenberg, S. Kreis, L. Weick, C. Haas, F. Sallamon, N. Kockmann
  Continuous Cooling Crystallization in a Coiled Flow Inverter Crystallizer Technology—Design, Characterization, and Hurdles
  Processes, 9, 1537, (2021) DOI: 10.3390/pr9091537

- T. Klement, S. Hanf, N. Kockmann, F. Wolff, S.A. Schunk, T. Röder
  Oscillating droplet reactor – Towards Kinetic Screening for Heterogeneous Catalysis in Hydrogenation Reaction
  Reac. Chem. Eng., 6, 1023-1030, (2021) DOI: 10.1039/D0RE00466A

- A. Bamberg, M. Bortz, N. Kockmann, S. Bröcker, L. Urbas
  The Digital Twin – Your ingenious companion for process engineering and smart production
  Chem. Eng. Technol., 44(6), 954-961, (2021) DOI: 10.1002/ceat.202000562

- T.A. Frede, I. Burke, N. Kockmann
  Software- guided Microfluidic Reaction Calorimeter Based on Thermoelectric Modules
  Chem. Ing. Technik, 93(5), 802-808 (2021) DOI: 10.1002/cite.202000223

- T. Klement, N. Kockmann, C. Schwede, T. Röder
  Kinetic measurement of acryl acid polymerization at high concentrations under nearly isothermal conditions in a pendula slug flow reactor
  Ind. Eng. Chem. Res, 60(11), 4240-4250, (2021) DOI: 10.1021/acs.iecr.0c04732

- J. Grühn, M. Vogel, N. Kockmann
  Digital Image Processing of Gas- Liquid Reactions in Coiled Capillaries
  Chem. Ing. Technik, 93(5), 825-829, (2021) DOI: 10.1002/cite.202000240

- J. Bobers, E. Forys, B. Oldach, N. Kockmann
  Application of Polyimide- based Microfluidic Devices on Acid-catalyzed Hydrolysis of Dimethoxypropane
  Chem. Ing. Technik, 93(5), 796-801, (2021) DOI: 10.1002/cite.202000224

- M. Schmalenberg, T.A. Frede, C. Mathias, N. Kockmann
  Efficient Short-cut Method for Determining the Process Window in Stirred-pulsed Extraction Columns
  Chem. Ing. Technik, 93(3), 466-472, (2021) DOI: 10.1002/cite.202000066

- J. Schuler, L.M. Neuendorf, K. Petersen, N. Kockmann
  Micro-Computed Tomography for the 3D Time-Resolved Investigation of Monodisperse Droplet Generation in a Co-Flow Setup
  AIChE J, 67(2) e17111, (2021) DOI: 10.1002/aic.17111

Peer-reviewed conference papers

- J. Schuler, N. Gumbiowski, J. Herath, L.M. Neuendorf, N. Kockmann,
  Micro-Computed Tomography for 3D-Imaging of of Laminar Dispersion and Multiphase Transport Phenomena in Capillary Flow,
  1st micro FIP conference, 7.-9. June 2021

- L.M. Neuendorf, P. Müller, N. Kockmann,
  Single Droplet Generation and Rising Velocity Analysis with Convolutional Neural Networks (CNNs) to Estimate Fluid Properties,
  1st micro FIP conference, 7.-9. June 2021

Book chapters

- M. Schlüter, F. Kexel, A. von Kameke, M. Hoffmann, S. Herres-Pawlis, P. Klüfers, M. Oßberger, S. Turek, O. Mierka, N. Kockmann, W. Krieger,
  Visualization and Quantitative Analysis of Consecutive Reactions in Taylor Bubble Flows,
  pp 507-543 in M. Schlüter, S. Herres-Pawlis, U. Nieken, (Eds.) Reactive Bubble Flow. Fluid Mechanics and Its Applications, vol 128. Springer, Cham, 2021, doi.org/10.1007/978-3-030-72361-3_21

- N. Kockmann,
  Historischer Abriss zur Entstehung und Entwicklung der Chemischen Reaktionstechnik,
  in W. Reschetilowski (Ed.) Handbuch Chemische Reaktoren, Springer, Berlin, 2021, doi.org/10.1007/978-3-662-56444-8_1-2

2020

Peer-reviewed Journal Articles

- M.M. Awad, D. Attinger, A. Bejan, A. Beskok, G.P. Celata, S. Colin, V.K. Dhir, P. Di Marco, S.V. Ekkad, S. Garimella, M. Kawaji, M.R. King, N. Kockmann, J. Kriegel, S.K. Mitra, S. Moghaddam, Y.S. Muzychka, V. Narayanan, G. Ribatski, S.A. Sherif, M. Shoji, P. Stephan, J.R. Thomé, P.B. Weisensee
  Professor Satish G. Kandlikar on His 70th Birthday
  J. Therm. Sci.&Eng. Appl., 12, 060301-1 - 3, (2020) DOI: 10.1115/1.4048813

- N. Kockmann
  Der Schnellstart in die digitale Lehre unter Corona-Randbedingungen
  Chem. Ing. Technik, 92(12), 1877-1886, (2020) DOI: 10.1002/cite.202000206

- J. Bobers, J. Grühn, S. Höving, T. Pyka, N. Kockmann,
  Two-phase Flow in Coiled Flow Inverter – Process Development and Scale-out From Batch to Continuous Flow
  Org. Proc. R&D, 24(10), 2094-2105, (2020) DOI: 10.1021/acs.oprd.0c00152

- V. Fath, P. Lau, C. Greve, N. Kockmann, T. Röder
  Efficient Kinetic Data Acquisition and Model Prediction in Continuous Flow Microreactors using Inline FT-IR Spectroscopy combined with SMCR Technique
  Org. Proc. R&D, 24(10), 1955-1969, (2020) DOI: 10.1021/acs.oprd.0c00037

- J. Schuler, L.M. Neuendorf, K. Petersen, N. Kockmann
  Micro-Computed Tomography for the 3D Time-Resolved Investigation of Monodisperse Droplet Generation in a Co-Flow Setup
  AIChE J., 67(2) e17111, (2020) DOI: 10.1002/aic.17111

- V. Fath, N. Kockmann, J. Otto, T. Röder
  Self-Optimising Processes and Real-Time-Optimisation of Organic Syntheses in a Microreactor System using Nelder-Mead and Design of Experiments
  Reac. Chem. & Eng., 5(7), 1281-1299, (2020) DOI: 10.1039/D0RE00081G

- N. Kockmann
  Gewusst wie! Entwurf und Betrieb eines Rohrreaktors mit enger Verweilzeitverteilung
  Chem. Ing. Technik, 92(6), 685-691, (2020) DOI: 10.1002/cite.202000028

- C.V. Benzin, N. Kockmann, T. Röder
  Lab-Scale Microreactor Plant for the Study of Methylations with Liquid Chloromethane
  Chem. Eng. & Technol., 43(9), 1733-1740, (2020) DOI: 10.1002/ceat.202000011

- W. Krieger, E. Bayraktar, O. Mierka, L. Kaiser, R. Dinter, J. Hennekes, S. Turek, N. Kockmann
  Arduino based slider setup for gas-liquid mass transfer investigation
  AIChE J., 66(6), e16953, (2020) DOI: 10.1002/aic.16953

- J. Bobers, M. Klika Škopić, R. Dinter, P. Sakthithasan, L. Neukirch, C. Gramse, R. Weberskirch, A. Brunschweiger, N. Kockmann
  Design of an Automated Reagent-Dispensing System for Reaction Screening and Validation with DNA-tagged Substrates
  ACS Combinatorial Science, 22(3), 101-108, (2020) DOI: 10.1021/acscombsci.9b00207

- J. Grühn, I. Burke, N. Neuhaus, N. Kockmann
  Investigations on selectivity of gas-liquid reactions in capillaries
  Chem. Ing. Technik, 92(5), 624-628, (2020) DOI: 10.1002/cite.201900144

- N. Steinfeldt, N. Kockmann
  Experimental and Numerical Characterization of Transport Phenomena in a Falling-film Microreactor with Gas-Liquid Reaction
  Ind. Eng. Chem. Res., 59(9), 4033-4047, (2020) DOI: 10.1021/acs.iecr.9b04154

- J. Schuler, N. Kockmann
  Micro-Computed Tomography for the investigation of stationary liquid/liquid and liquid/gas interfaces in capillaries
  AIChE J., 66(4), e16890, (2020) DOI: 10.1002/aic.16890

- M. Schmalenberg, A. Nokon, N. Kockmann
  Design and Hydrodynamic Characterization of a Lab-scale Draft Tube Baffle Crystallizer
  Chem. Ing. Technik, 92(3), 288-294, (2020) DOI: 10.1002/cite.201900078

- A. Bamberg, M. Bortz, N. Kockmann, S. Bröcker, L. Urbas
  Was den digitalen Zwilling zum genialen Kompagnon macht
  Chem. Ing. Technik, 92(3), 192-198, (2020) DOI: 10.1002/cite.201900168

Peer-reviewed conference papers

- M. Schmalenberg, F. Sallamon, C. Haas, N. Kockmann
  Temperature-Controlled Minichannel Flow-Cell for Non-Invasive Particle Measurements in Solid-Liquid Flow
  ICNMM2020, Orlando, USA, 17. July 2020

- J. Schuler, L.M. Neuendorf, K. Petersen, N. Kockmann
  3D Investigation of Droplet Generation in a Miniaturized Coflowing Device Using Micro-Computed Tomography
  ICNMM2020, Orlando, USA, 17. July 2020

Plant and Process Design (APT)

Image Analysis supporting Retention Determination in Centrifugal Partition Chromatography

New algorithm drastically improves the understanding of hydrodynamics in this promising chromatographic technology.

F. Buthmann, F. Pley, G. Schembecker, J. Koop

The main goal in Centrifugal Partition Chromatography is to compensate for the downsides of classical chromatographic processes by replacing the solid stationary phase with a liquid immiscible to the (liquid) mobile phase. This is achieved with the help of centrifugal force. Accurate knowledge of the amount of liquid stationary phase immobilized in the apparatus is crucial when optimizing separation performance in Centrifugal Partition Chromatography. Due to bleeding, i.e., the loss of stationary phase caused by hydrodynamic phenomena, its proportion changes over time. To date, an imprecise manual evaluation was the standard technique for determining the amount of stationary phase in the apparatus. Therefore, an image processing algorithm was developed, allowing for quick and highly accurate online evaluation of stationary phase retention by image analysis.

In Centrifugal Partition Chromatography (CPC), both mobile and stationary phases are liquid. The stationary phase is immobilized within a cascade of chambers and channels embedded in a rotor, whereas the second liquid is actively pumped as the mobile phase. Thus, when compared to conventional liquid chromatography, the solid stationary phase is replaced by a second liquid immiscible with the mobile phase that is kept in the CPC apparatus by centrifugal force.

A partially transparent rotor was used to ensure the visibility of the chambers and channels. This rotor was filmed with the help of a highspeed-camera. In contrast to stacked rotor versions, which are used for actual separation tasks (stacked and interconnected individual discs ensure a higher number of theoretical stages), the rotor mentioned is suitable for visual fluid flow detection. To enhance the contrast between both liquid phases, the mobile phase was dyed selectively (methylene blue). For actual retention determination, the mobile phase pump was stopped temporarily. Next, a video of the resting liquid phases in the chambers and ducts was recorded.

The raw data for the new algorithm was still images extracted from the footage mentioned (Figure 1-A). The edge detection algorithm “Canny” was then applied to the greyscale images (Figure 1-B). The resulting binary images were post-processed with different tools to repair unclosed contours and reduce artifacts, before enclosed areas were filled (Figure 1-C and 1-D). Subsequently, chambers and channels were separated to distinguish between the stationary phase left within both geometries and the retention value was calculated. Comparing the manual and automated measurement methods, the average discrepancy between both is below 1 %, which can be considered negligible. Besides, there is no proportional bias evident. It can be stated that the methods provide the same accuracy, with the automated method offering more precise data. Besides, the effort for processing the data given is cut from several hours to just about one minute.

Those main advantages allow for new process monitoring and control potentials. Identifying the current operating status of a Centrifugal Chromatograph is a huge step towards the implementation of those novel apparatuses in industry. Furthermore, the data can be used to control the operating parameters of the apparatus to prevent progressive flooding with the mobile phase, enabling long-term operability.

Compared with different approaches for measuring the retention in Centrifugal Partition Chromatography (for example phase separation at the device outlet and subsequent ratio determination of mobile and stationary phase), the innovative approach presented enables local resolution of bleeding within the rotor. Thus, the exact location of discharged stationary phase and consequently local hydrodynamic causes can be identified.

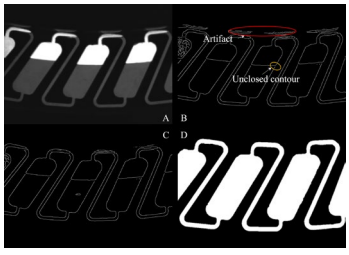

Figure 1: (A) Unprocessed still image—extracted from video files of the high-speed camera. (B) Binary image after editing with Canny edge algorithm. Highlighted: Artifact due to reflections (red) and unclosed contour (yellow). (C) Binary image after filtering with the help of a circular mask and edge closure. (D) Enclosed areas are filled.

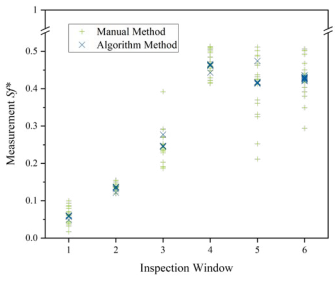

Figure 2: : Retention values (Sf*) at different inspection windows of the semi-transparent rotor. Results processed with the automated method are indicated with crosses, plus signs represent manually determined retention values.

Contacts:
felix.buthmann@tu-dortmund.de
gerhard.schembecker@tu-dortmund.de

Publications:
J. Koop, J. Merz, G. Schembecker
Journal of Biotechnology 334, 11-25 (2021).

Inert Gassing Crystallizing for Improved Product Separation of Oleo-Chemicals toward an Efficient Circular Economy

Astrid I. Seifert, Justin Simons, Jan Gutsch, Kerstin Wohlgemuth

The development of new chemical processes based on renewable resources plays an important role in the change toward sustainable chemistry and circular economy. The efficient transformation of oleo-chemicals, derived from natural fats and oils, to functionalized intermediate chemicals is enabled by the use of homogeneous catalysts. These catalysts typically contain expensive precious metals, so that a separation and recycling is required for an economic application. One promising separation method is crystallization, where the functionalized chemical is selectively precipitated as a solid product phase and then separated from the liquid reaction mixture containing the homogeneous catalyst. Key to an efficient recycling process by crystallization is the isolation of a pure product by precise control of the crystallization process while maintaining an inert atmosphere to prevent deactivation of the oxygen-sensitive catalyst. In this work, we demonstrate that a controlled crystallization by introducing inert argon gas to the crystallizer improves the particle properties of the crystalline product for an efficient separation in the subsequent filtration and washing steps. Finally, we verify that gassing crystallization with argon offers a considerable benefit for the isolation of a pure crystalline product while maintaining inert operating conditions required for recycling of oxygen-sensitive catalysts.

Isolation of a pure crystalline product requires precise control of the crystallization process. Assuming that the nucleation step is crucial for the control of particle properties of the crystalline product and the related efficiency of downstream separation by filtration and washing, we systematically investigated the effect of controlled nucleation by gassing with argon on these quantities, using the oleo-chemical model system, 1,12-dimethyl dodecanedioate / methanol. We demonstrated that by gassing with argon, the nucleation step can be initiated at lower supersaturation compared to uncontrolled cooling crystallization with spontaneous nucleation, despite the comparably small metastable zone width of the investigated model system in the range of 1–3 K. Consequently, less nuclei are formed that grow to larger and less agglomerated product crystals, as depicted in Figure 1.

By adding a color tracer to the mother liquor, we could quantify that crystals obtained from gassing crystallization are more efficiently separated by filtration and washing compared to crystals from cooling crystallization, due to better accessibility of mother liquor in the filter cake pores. As shown in Figure 2, the colored mother liquor was efficiently displaced from the white crystals by washing with approximately one pore volume of pure methanol in each washing step. After two washing steps, mother liquor leaching to the isolated product from gassing crystallization was significantly reduced to nearly 100 ppm.

Finally, we demonstrated the feasibility and considerable benefit of inert gassing crystallization for isolation of a pure product including subsequent filtration and washing, enabling the reuse of expensive homogeneous catalysts in a circular economy environment.

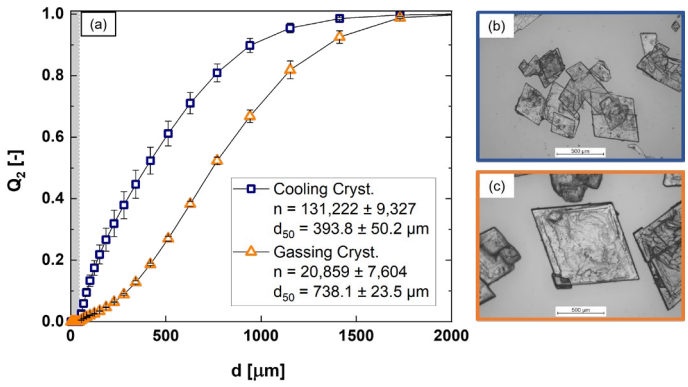

Figure 1: Q_2 particle size distributions (a) and microscope images of cooling crystallization (b) and gassing crystallization (c). Mean values and standard deviations of three experiments each.

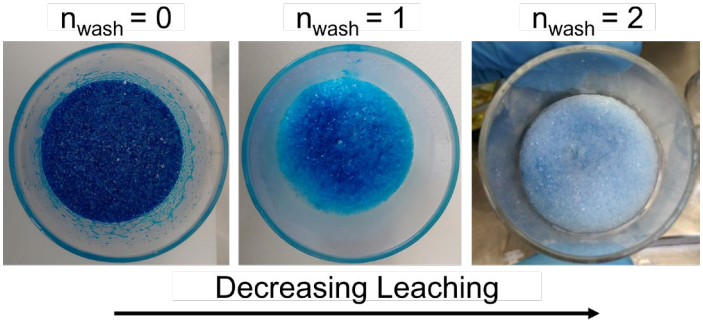

Figure 2: Photos of filter cake from gassing crystallization after zero, one, and two wash cycles (from left to right).

Reprinted with permission from Org. Process Res. Dev. 2023, 27, 1, 136–147.
 Our research receives funding by the German Research Foundation (Deutsche Forschungsgemeinschaft–DFG)–Project No. 424535516.

Publications:
Astrid I. Seifert, Justin Simons, Jan Gutsch, Kerstin Wohlgemuth, Org. Process Res. Dev. 27 (1), 136–147 (2023).
Publication Date: December 9, 2022

Contacts:
astridina.seifert@tu-dortmund.de
kerstin.wohlgemuth@tu-dortmund.de

Strategy for Fast Decision on Material System Suitability for Continuous Crystallization Inside a Slug Flow Crystallizer

Astrid I. Seifert, Justin Simons, Jan Gutsch, Kerstin Wohlgemuth

The growing interest in two-phase flow in micro- or mini-structured apparatuses has led to increased attention towards crystallization as a separation technique. However, achieving high-quality products in such apparatuses poses a challenge. The slug flow pattern, despite laminar flow conditions, offers significant advantages such as narrow residence time distribution, intensified mixing and heat exchange, and enhanced particle suspension. Exploiting these features, the slug flow crystallizer (SFC) shows promise for small-scale continuous crystallization, particularly for producing high-quality active pharmaceutical ingredients (APIs). To address this problem efficiently and with minimal experimental effort, a time-efficient strategy is developed. This strategy involves heuristics-based pre-selection of solvent or solvent mixtures, verification of slug flow stability by viewing static three phase contact angle and dynamic flow behavior, and modeling temperature-dependent solubility using perturbed chain statistical associating fluid theory (PC SAFT) for the material system considered. The strategy is successfully validated for binary and ternary systems of amino acids L alanine and L arginine, as well as the API paracetamol, demonstrating its applicability as a general approach for different material systems in the SFC.

Selecting a new and suitable material system for crystallization in the SFC is challenging and linked to many constraints to maintain slug flow stability, a narrow residence time distribution (RTD), and consequently obtain uniform and reproducible product yield with particles of desired size, a narrow width of particle size distribution, and a high purity at the end of the apparatus. Therefore, a systematic approach to decide on material system suitability as fast as possible and with low experimental effort in order to enable the continuous operation of the desired product using cooling crystallization inside the SFC is presented.

This structured procedure includes the selection of a suitable solvent for the desired solid via a screening of different solvents and tubing materials and the evaluation of the suitability for the SFC reviewing the static three phase contact angle θ_{stat}. For slug flow stability, a poorly wetting system ($\theta_{stat} > 90°$) is preferred, indicating convex formed slugs and a negligible wall film present. In a next step, the suitability of the selected solvent/tubing material combination is validated by examining the dynamic behavior in the apparatus with regard to flow stability by image analysis. According to the results of image analysis depicted in Figure 1, a significant difference in slug shape can be seen for the different solvents tested. The rounded shape of the gas bubbles can lead to the fact that in the presence of crystals in the liquid phase, the crystals can migrate between neighboring slugs and, thus, significantly broaden the RTD of the solid phase, which is unfavorable for the crystallization process. It has become clear that the static contact angle can be used to confirm the suitability of the tested combination of material system and the wall material via a high contact angle ($\theta_{stat} > 90°$), but the unsuitability cannot be approximated via the static behavior. For this purpose, the dynamic contact angle and the evaluation of the slug shape during operation are required to limit the operating window for successful and continuous crystallization. Based on this, the possible operating range of the SFC has been cosiderably extended by reviewing and correlating the static and dynamic contact angle behavior with the Capillary number Ca.

As the last step, the temperature-dependent solute's solubility in the solvent is modeled and predicted to evaluate the possible yield for crystallization processes for binary (solute/water and solute/ethanol, Figure 2), and ternary (solute/water/ethanol, Figure 3) systems. The modeling results and the experimental data (from literature, as well as from gravimetric measurements performed in this work) are in very good agreement. Thus, PC-SAFT shows a high capability in predicting solubilities in pure solvent and solvent mixtures at different temperatures.

With the help of this strategy, it is possible to ensure the crystallization of a new material system in the SFC within four steps for binary and ternary systems.

Strategy for Fast Decision on Material System Suitability for Continuous Crystallization Inside a Slug Flow Crystallizer

Astrid I. Seifert, Justin Simons, Jan Gutsch, Kerstin Wohlgemuth

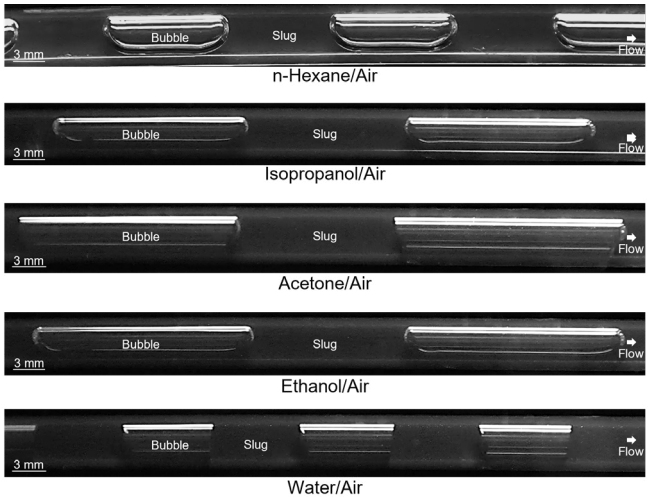

Figure 1: Images of slugs at the end of the apparatus (L = 7.5m) during operation with different solvents in a fluoroethylene propylene (FEP) tubing. The liquid and gas flow rates were set to Q = 10 mL min^{-1} each. The experiments were conducted at ambient temperature ($\vartheta_{amb} \approx$ 22 °C).

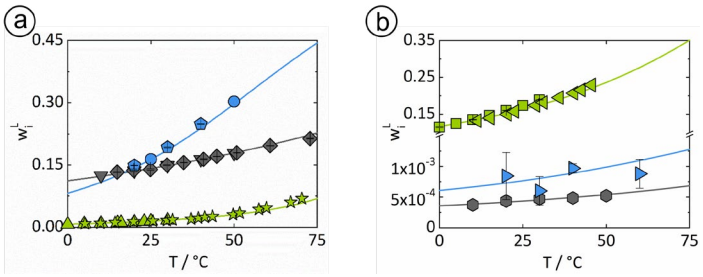

Figure 2: Solubilities of l-alanine (gray), l-arginine (blue), and paracetamol (green) in water (a) and ethanol (b) at 0.1 MPa: Down-pointing triangles, diamonds, circles, up-pointing triangles, and stars depict measured solubilities in water from An et al. [1], Grosse Daldrup et al. [2], Amend and Helgeson [3],

Granberg and Rasmuson [4], and Grant et al. [5]. Hexagons, squares, and left-pointing triangles denote solubility measurements in ethanol from An et al. [1], Granberg and Rasmuson [6], and Matsuda et al. [7]. Pentagons and right-pointing triangles are measurements in water and in ethanol performed in this work, respectively. The solid lines are modeled solubility lines using PC-SAFT.

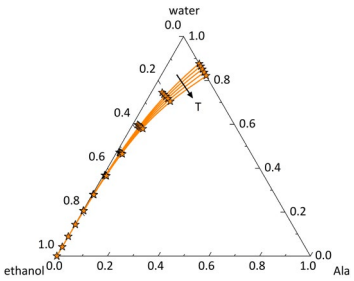

Figure 3: Ternary phase diagram of l-alanine/water/ethanol at 0.1 MPa with compositions given in mass fractions. Solubility lines were predicted using PC-SAFT, and symbols denote solubility measurements from An et al. [1]. The arrow indicates the direction of increasing temperature from 10 °C to 20 °C, 30 °C, 40 °C, and 50 °C.

Publications:
A.C. Kufner, A. Krummnow, A. Danzer, K. Wohlgemuth, Micromachines. 13(10), 1795 (2022)

References:

[1] An, M.; Qiu, J.; Yi, D.; Liu, H.; Hu, S.; Han, J.; Huang, H.; He, H.; Liu, C.; Zhao, Z.; et al. Measurement and Correlation for Solubility of l-Alanine in Pure and Binary Solvents at Temperatures from 283.15 to 323.15 K. J. Chem. Eng. Data 2020, 65, 549–560.
[2] Daldrup, J.-B.G.; Held, C.; Ruether, F.; Schembecker, G.; Sadowski, G. Measurement and Modeling Solubility of Aqueous Multisolute Amino-Acid Solutions. Ind. Eng. Chem. Res. 2010, 49, 1395–1401
[3] Amend, J.P.; Helgeson, H.C. Solubilities of the common L-a-amino acids as a function of temperature and solution pH. Pure Appl. Chem. 1997, 69, 935–942
[4] Granberg, R.A.; Rasmuson, C. Solubility of Paracetamol in Binary and Ternary Mixtures of Water + Acetone + Toluene. J. Chem. Eng. Data 2000, 45, 478–483
[5] Grant, D.; Mehdizadeh, M.; Chow, A.-L.; Fairbrother, J. Non-linear van't Hoff solubility-temperature plots and their pharmaceutical interpretation. Int. J. Pharm. 1984, 18, 25–38
[6] Granberg, R.A.; Rasmuson, C. Solubility of Paracetamol in Pure Solvents. J. Chem. Eng. Data 1999, 44, 1391–1395
[7] Matsuda, H.; Mori, K.; Tomioka, M.; Kariyasu, N.; Fukami, T.; Kurihara, K.; Tochigi, K.; Tomono, K. Determination and prediction of solubilities of active pharmaceutical ingredients in selected organic solvents. Fluid Phase Equilibria 2015, 406, 116–123

Contacts:
anne.kufner@tu-dortmund.de
kerstin.wohlgemuth@tu-dortmund.de

Publications 2020 – 2022

2022

Peer-reviewed Journal Articles

- F. Buthmann, F. Pley, G. Schembecker, J. Koop
  Automated Image Analysis for Retention Determination in Centrifugal Partition Chromatography
  Separations (2022)

- MM. Etmanski, M. Breloer, M. Weber, G. Schembecker, K. Wohlgemuth
  Interplay of Particle Suspension and Residence Time Distribution in a Taylor-Couette Crystallizer
  Crystals 12 (12), 1845 (2022)

- T.Pyka, J. Koop, C. Held, G. Schembecker
  Dry Pressure Drop in a Two-Rotor Rotating Packed Bed
  Industrial and Engineering Chemistry Research 61(46), 17156-17165 (2022)

- AI. Seifert, J. Simons, J. Gutsch, K. Wohlgemuth
  Inert gassing crystallization for improved product separation of oleo-chemicals towards an efficient circular economy
  Organic Process Research & Development (2/09/2022)

- AC. Kufner, A. Krummnow, A. Danzer, K. Wohlgemuth
  Strategy for fast decision on material system suitability for continuous crystallization inside a Slug Flow Crystallizer
  Micromachines (2022),

- J. Sonnenschein, M. Hermes, St. Höving, N. Kockmann, K. Wohlgemuth
  Population balance modeling of unstirred cooling crystallization on an integrated belt filter
  Journal Computers and Chemical Engineering (2022)

- R. Loll, L. Runge, J. Koop, C. Held, G. Schembecker
  Zickzack Packings for Deaeration in Rotating Packed Beds-Improved Rotor Design to Counter Bypass Flows
  Industrial and Engineering Chemistry Research 61(32), 11934-11946 (2022)

- M. Schreiber, G. Schembecker
  Development of an Automated Adsorbent Selection Strategy for Liquid–Phase Adsorption
  Chemical Engineering and Technology 45 (6), 1124–1132 (2022)

- J. Lins, U. Ebeling, K. Wohlgemuth
  Agglomeration Kernel Determination by Combining In-Process Image Analysis and Modeling
  Crystal Growth & Design 22 (9), 5363–5374 (2022)

- J. Vondran, AI. Seifert, K. Schäfer, A. Laudanski, T. Deysenroth, K. Wohlgemuth, T. Seidensticker
  Progressing the Crystal Way to Sustainability: Strategy for Developing an Integrated Recycling Process of Homogeneous Catalysts by Selective Product Crystallization
  Industrial & Engineering Chemistry Research 61 (27), 9621–9631 (2022)

- J. Sonnenschein, R. Heming, K. Wohlgemuth
  Archimedes Tube Crystallizer: Design and Operation of Continuous Cooling Crystallization Based on First-Principle Modeling
  Crystal Growth & Design 22 (9), 5272-5284 (2022)

- J. Lins, T. Harweg, F. Weichert, K. Wohlgemuth
  Potential of Deep Learning Methods for Deep Level Particle Characterization in Crystallization
  Applied Sciences 12 (5), 2465 (2022)

- C. Steenweg, J. Habicht, K. Wohlgemuth
  Continuous Isolation of Particles with Varying Aspect Ratios up to Thin Needles Achieving Free-Flowing Products
  Crystals 12 (2), 137 (2022)

- M. Peterwitz, S. Buchgeister, R. Meier, G. Schembecker
  Tracking raw material flow through a continuous direct compression line. Part II of II: Predicting dynamic changes in quality attributes of tablets due to disturbances in raw material properties using an independent residence time distribution model
  International Journal of Pharmaceutics 615, 121528 (2022)

- M. Peterwitz, J. Jodwirschat, R. Loll, G. Schembecker
  Tracking raw material flow through a continuous direct compression line Part I of II: Residence time distribution modeling and sensitivity analysis enabling increased process yield
  International Journal of Pharmaceutics 614, 121467 (2022)

2021

Peer-reviewed Journal Articles

- M Peterwitz, S Gerling, G Schembecker
  Challenges in tracing material flow passing a loss-in-weight feeder in continuous manufacturing processes
  International Journal of Pharmaceutics 612, 121304, (2021)

- M Termuehlen, B Strakeljahn, G Schembecker, K Wohlgemuth
  Quantification and evaluation of operating Parameters' effect on suspension behavior for slug flow crystallization
  Chemical Engineering Science 243, 116771 (2021)

- H Radatz, A Kragl, J Kampwerth, C Stark, N Herden, G Schembecker
  Application and evaluation of preselection approaches to decide on the use of equipment modules
  Chemical Engineering Research and Design 173, 89-107 (2021)

- M Schreiber, M Brunert, G Schembecker
  Extraction on a Robotic Platform–Autonomous Solvent Selection under Economic Evaluation Criteria
  Chemical Engineering & Technology 44 (9), 1578-1584 (2021)

- J Koop, J Merz, G Schembecker
  Hydrophobicity, amphilicity, and flexibility: Relation between molecular protein properties and the macroscopic effects of surface activity
  Journal of Biotechnology 334, 11-25 (2021)

- M Termühlen, MM Etmanski, I Kryschewski, AC Kufner, G Schembecker, K Wohlgemuth
  Continuous slug flow crystallization: Impact of design and operating parameters on product quality
  Chemical Engineering Research and Design 170, 290-303 (202

- M Peterwitz, G Schembecker
  Evaluating the potential for optimization of axial back-mixing in continuous pharmaceutical manufacturing
  Computers & Chemical Engineering 147, 107251 (2021)

- C Steenweg, AI Seifert, G Schembecker, K Wohlgemuth
  Characterization of a modular continuous vacuum screw filter for small-scale solid–liquid separation of suspensions
  Organic Process Research & Development 25 (4), 926-940 (2021)

- I Lukin, K Gładyszewski, M Skiborowski, A Górak, G Schembecker
Aroma absorption in a rotating packed bed with a tailor-made archimedean spiral packing
Chemical Engineering Science 231, 116334 (2021)

- I Lukin, L Pietzka, I Wingartz, G Schembecker
Aroma absorption in rapeseed oil using rotating packed bed
Flavour and Fragrance Journal 36 (1), 137-147 (2021)

- J Sonnenschein, K Wohlgemuth
Archimedes Tube Crystallizer: Design and Characterization for Small-Scale Continuous Crystallization
Chemical Engineering Research and Design 178, 488-501 (2021)

- C Steenweg, AC Kufner, J Habicht, K Wohlgemuth
Towards continuous primary manufacturing processes—Particle design through combined crystallization and particle isolation
Processes 9 (12), 2187 (2021)

- J Sonnenschein, P Friedrich, M Aghayarzadeh, O Mierka, S Turek, K Wohlgemuth
Flow Map for Hydrodynamics and Suspension Behavior in a Continuous Archimedes Tube Crystallizer
Crystals 11 (12), 1466 (2021)

- C Steenweg, AI Seifert, N Böttger, K Wohlgemuth
Process intensification enabling continuous manufacturing processes using modular continuous vacuum screw filter
Organic Process Research & Development 25 (11), 2525-2536 (2021)

- J Lins, S Heisel, K Wohlgemuth
Quantification of internal crystal defects using image analysis
Powder Technology 377, 733-738 (2021)

- A Fromme, C Fischer, K Keine, G Schembecker
Characterization and correlation of mobile phase dispersion of aqueous-organic solvent systems in centrifugal partition chromatography
Journal of Chromatography A 1620, 460990 (2020)

- L David, P Schwan, M Lobedann, SO Borchert, B Budde, M Temming
Side-by-side comparability of batch and continuous downstream for the production of monoclonal antibodies
Biotechnology and bioengineering 117 (4), 1024-1036 (2020)

- L David, MP Bayer, M Lobedann, G Schembecker
Simulation of continuous low pH viral inactivation inside a coiled flow inverter
Biotechnology and bioengineering 117 (4), 1048-1062 (2020)

- A Fromme, F Funke, J Merz, G Schembecker
Correlating physical properties of aqueous-organic solvent systems and stationary phase retention in a centrifugal partition chromatograph in descending mode
Journal of Chromatography A 1615, 460742 (2020)

- L David, LM Waldschmidt, M Lobedann, G Schembecker
Simulation of pH level distribution inside a coiled flow inverter for continuous low pH viral inactivation
Biotechnology and bioengineering 117 (2), 429-437 (2020)

- C Post, N Wentingmann, C Bramsiepe, G Schembecker
Using design spaces for more accurate cost estimation during early engineering phases
Chemical Engineering Research and Design 153, 592-602 (2020)

2020

Peer-reviewed Journal Articles

- J Koop, J Merz, C Pietzsch, G Schembecker
Contribution of Secondary Structure Changes to the Surface Activity of Proteins
Journal of Biotechnology 323, 208-220 (2020)

- I Lukin, I Wingartz, G Schembecker
Application of rotating packed bed for in- line aroma stripping from cell slurry
Journal of Chemical Technology & Biotechnology 95 (11), 2834-2841 (2020

- M Peterwitz, R Loll, J Jodwirschat, G Schembecker
Evaluating the potential of adjusting axial back mixing in continuous manufacturing of solid oral dosage forms
Chemie Ingenieur Technik 92 (9), 1162-1162 (2020)

- J Koop, J Merz, R Wilmshöfer, R Winter, G Schembecker
Influence of thermally induced structure changes in diluted ß-lactoglobulin solutions on their surface activity and behavior in foam fractionation
Journal of Biotechnology 319, 61-68 (2020)

- I Lukin, L Pietzka, K Groß, A Górak, G Schembecker
Economic evaluation of rotating packed bed use for aroma absorption from bioreactor off-gas
Chemical Engineering and Processing-Process Intensification 154, 108011 (2020)

- A Fromme, C Fischer, D Klump, G Schembecker
Correlating the phase settling behavior of aqueous-organic solvent systems in a centrifugal partition chromatograph
Journal of Chromatography A 1620, 461005 (2020)

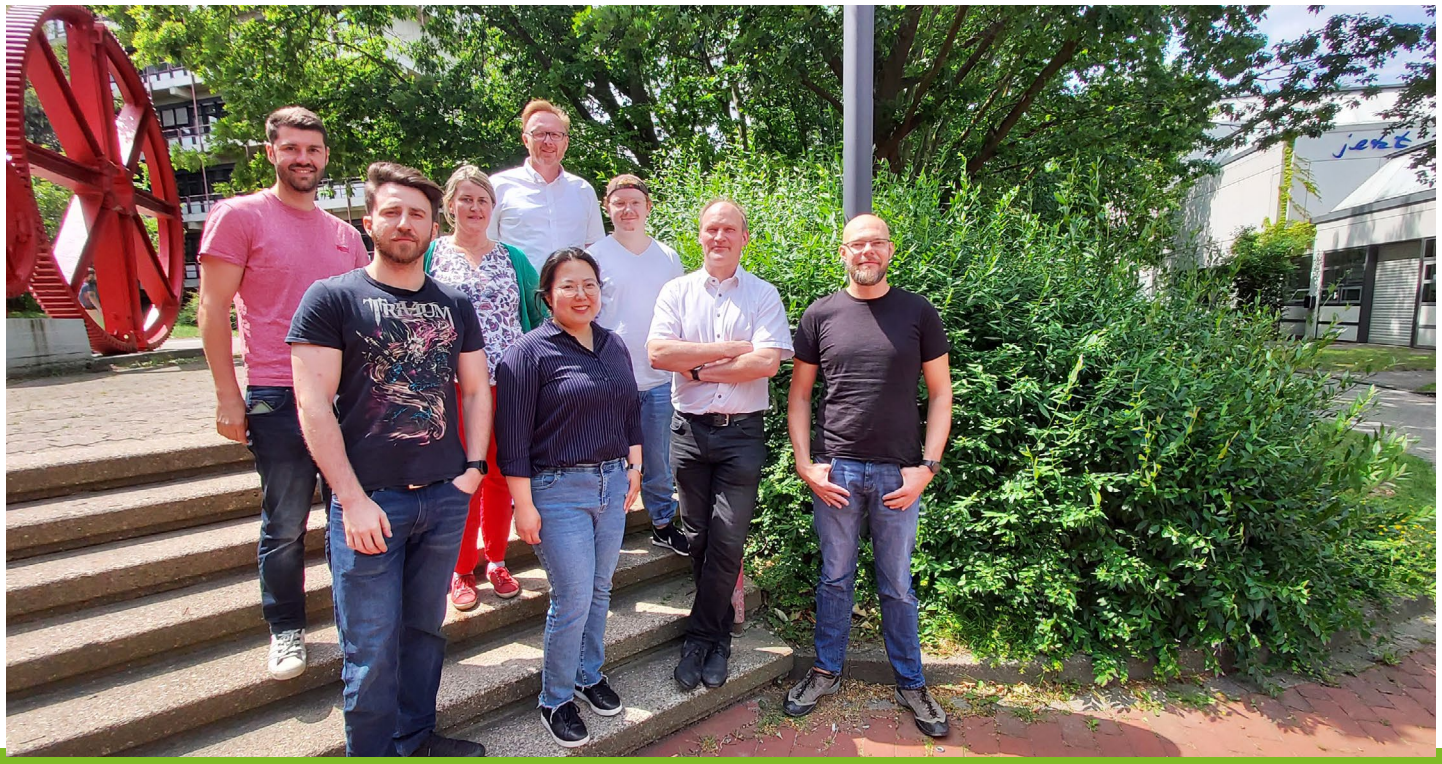

Biomaterials and Polymer Science (BMP)

New Insights into Strain-Induced Crystallization of Natural Rubber

How the amorphous phase takes influence on the stability of polymer crystals

Dominik Segiet, Sebastian Weckes, Juergen Austermuehl, Joerg C. Tiller, Frank Katzenberg

Crosslinked Natural Rubber (NR) has been used in countless products since its discovery until today. This is due to the fact that no other elastomer is capable of withstanding large stress up to 30 MPa at strains of many 100%. Strain-induced crystallization (SIC), the formation of crystals under strain and their disappearance once the stretching force is released, is thought to be responsible for this unique self-strengthening effect. SIC was explored in countless works, since it was first recognized in 1925. Nevertheless, it is not fully understood yet. Recently a shape memory effect was found for NR, when it is lowly crosslinked slightly above the borderline between thermoplastic and elastomer. Exploring the cause of this shape memory effect, the amorphous phase and stearic acid, a natural impurity in NR, were found to play a major role regarding the stability of the strain-induced polymer crystals. Thus, we proposed a new mechanism for SIC that possibly unveils the secret of NR

Wide- and small-angle X-ray scattering experiments (WAXS, SAXS) of NR and synthetic rubber (IR) samples additivated with stearic acid and stretched at room temperature as well as 80°C revealed that the melting temperature T_m of the strain-induced crystals deviates significantly up- as well downward from the crystal dimension-related, calculated melting temperature $T_{m,calc}$ Strain-induced crystallization of unadditivated NR at room temperature results in a $T_{m,meas}$ that is significantly smaller than $T_{m,calc}$ which approaches $T_{m,calc}$ when StA is added and is equivalent to $T_{m,calc}$ at a content of 9 wt% StA. Strain-induced crystallization at 80 °C of unadditivated NR initially causes a $T_{m,meas}$ nearly equal to $T_{m,calc}$ which increasingly exceeds $T_{m,calc}$ with increasing amount of added StA (see Fig. 1).

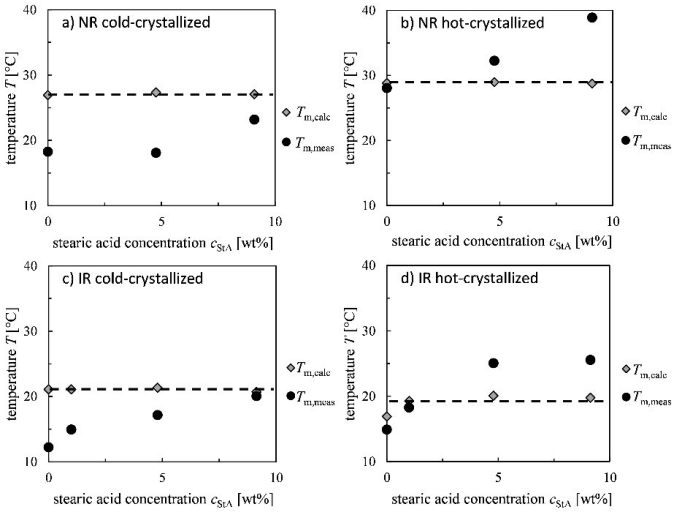

Figure 1: Comparison of measured melting temperature $T_{m,meas}$ and calculated melting temperature $T_{m,calc}$ of IR and NR samples in dependence on stearic acid concentration c_{StA} and kind of crystallization.

These results allow the hypothesis that the observed discrepancy between $T_{m,meas}$ and $T_{m,calc}$ is the result of internal stress, which is exerted by the surrounding amorphous phase onto the crystals. It is assumed that the direction and intensity of this internal stress depends on crystallization conditions and StA concentration, and can be influenced by the amount and the location of StA crystals in the amorphous phase as depicted in Fig. 2.

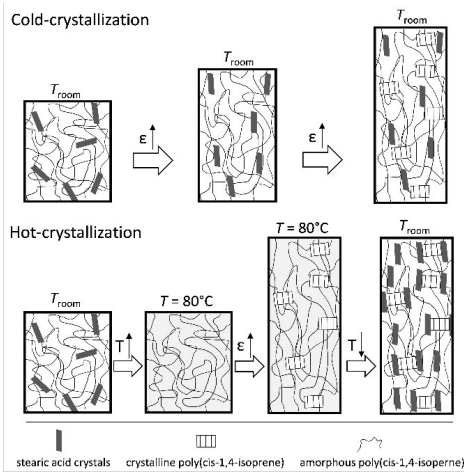

Figure 2: Assumed formation and arrangement of poly(cis-1,4-isoprene) and StA crystals during strain-induced crystallization of crosslinked NR and IR samples at room temperature and at 80°C.

This points out that T_m of polymer crystals does not only depend on surface-to-volume effects but can be also significantly influenced by internal stress that is exerted by the surrounding amorphous phase on the crystal. The transfer of these findings to other polymers and, especially, the hypothesized opportunity to increase the T_m of a polymer crystal above its so far known T_m will be focus of future works.

Contacts:
frank.katzenberg@tu-dortmund.de

Publications:
D. Segiet, S. Weckes, J. Austermuehl, J.C. Tiller, F. Katzenberg, Journal of Applied Polymer Science e53146 (2022)

Ultrastiff, Highly Permeable Separation Membranes

Enzyme-induced Mineralization of Hydrogels improves Stiffness and Permeability of Separation Membranes

Marko Milovanovic, Joerg C. Tiller

Separation membranes are considered as important tool towards sustainable chemical engineering processes. They are often designed by combining a fragile, soft separation membrane with a mechanically stable scaffold. This often limits permeability or separation performance of the membrane and makes it prone to fouling. In this study, we let a stiff inorganic scaffold grow within a soft separation membrane and can thus stabilize the latter and even improve the permeability without using an additional carrier membrane. Thus is demonstrated on the example of the challenging chiral separation of racemates.

A novel design of separation membranes was realized by formation of an inorganic framework (IF) within an organic polymer membrane (see Figure 1). This design greatly improves the stiffness and the strength of the membrane. Furthermore, the inorganic scaffold affords higher solute permeability. The new design is demonstrated on the example of a diffusion based separation membrane that consists of copolymerized and cross-linked acrylamide and (R/S)-N-(1-hydroxy-butan-2-yl) acrylamide (PAAm-co-(R/S)-HBA-l-MBAm). The IF was implemented by enzyme-induced mineralization (EIM) of calcium phosphate using alkaline phosphatase. Thereby, the stiffness and strength of the organic membrane could be improved from <1 and <0.2 MPa to 150 and 1.5 MPa, respectively, upon EIM. The composite material is suitable as a highly permeable membrane in swelling solvents, such as methanol, as well as in non-swelling solvents, such as toluene. It was demonstrated that the solutes naproxen, BINOL, and pseudoephedrine show varying solute permeability in a range of 1.3 to 35.9 x 10^{-11} m^2 s^{-1}, which indicates separation potential for small molecules.

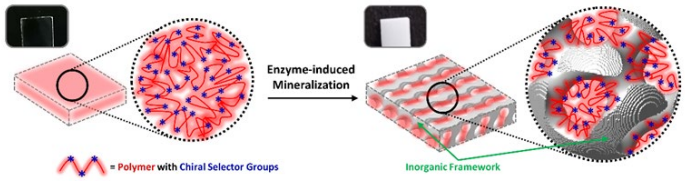

Figure 1: Illustration of the enzyme-induced mineralization-based scaffold growth within a separation membrane.

The pore size of the inorganic phase can be controlled by introducing charged monomers, like ethyl 2-[4-(dihydroxyphosphoryl)-2-oxabutyl] acrylate (EDPOA) and varying the nature of the neutral monomers from PAAm to poly(N,N-dimethylacrylamide) (PDMA). Figure 2 shows that the inorganic structure becomes significantly finer and more homogeneous in the presence of PDMA, most likely affording a smaller pore size. Thus, the scaffold structure can be controlled.

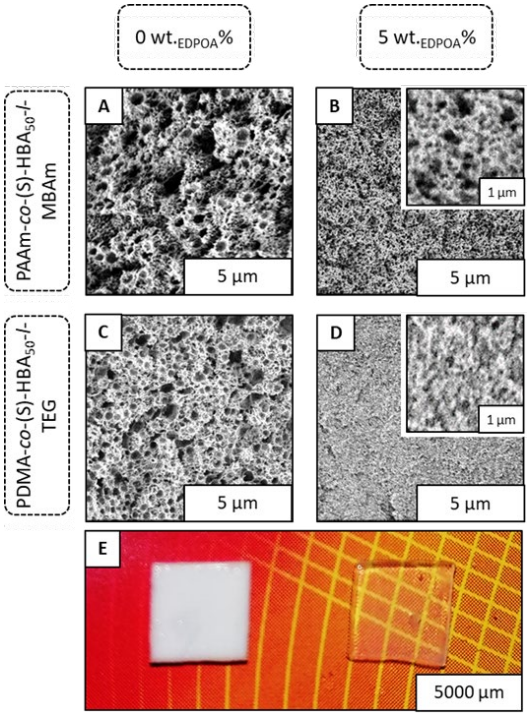

Figure 2: SEM-Images and photographs of mineralized PDMA-co-(S)-HBA50-l-TEG (E) without (left) and with 5 wt.EDPOA% (right).

In order to investigate the ability of the here studied chiral O-I-DN membranes to separate racemic mixtures, the diffusion of the racemate of (R/S)-naproxen in MeOH through a mineralized membrane with 75 wt.(S)-HBA% was examined. It could be shown that this membrane has potential for chiral separation (selectivity up to 1.7). Altogether, the high solute permeabilities in combination with solute selectivity and even enantioselectivity and excellent mechanical properties make these membranes an alternative to commonly reported separation membranes.

Publications:
Milovanovic, M.; Tabakoglu, F.; Saki, F.; Pohlkoetter, E.; Buga, D.; Brandt, V.; Tiller, J. C., Journal of Membrane Science 2023, 668, 121190

Contacts:
joerg.tiller@tu-dortmund.de

Hydrogels Stronger Than Cartilage

Double network hydrogels based on poly(2-oxazoline)s and poly(acrylic acid) show superior match mechanical characteristics of cartilage and are even more stable than the original

Paola Benitez-Duif, Montasser Hijazi, Joerg C. Tiller

The substitution of cartilage is a problem that is world-wide relevant to more than 500 million people with osteoarthritis, because cartilage cannot be regrown. Unfortunately, cartilage is a hydrogel that contains up to 70% of water and is as strong as concrete against compression. This and other challenges regarding mechanical and biological properties makes it highly difficult to substitute cartilage with an artificial material. One way to create a strong and stiff hydrogel is the formation of a double network hydrogel (DNH). So far, all such hydrogels are not shown to be working in their natural surroundings. We have created a new DNH based on poly(2-oxazoline)s and poly(acrylic acid) that meets the mechanical and biological requirements of cartilage and is even more resistant against compression than the natural Idol.

The present work has been made possible in a collaboration with the BG University Hospital Bergmannsheil, Bochum (Dr. Breisch) and the department for mechanical engineering, TU Dortmund (Prof. Tillmann). DNHs composed of cross-linked poly(2-oxazoline)s (POx) and poly(acrylic acid) (PAA) were synthesized by free radical polymerization in a two-step process as shown in Figure 1. The resulting DNHs are stabilized by hydrogen bridges even at pH 7.4 (physiological PBS buffer) due to the pKa-shifting effect of POx on PAA. DNHs based on poly(2-methyl-2-oxazoline), which have a water content of around 66 wt% and are not cytotoxic, show biomechanical properties that match those of cartilage in terms of water content, stiffness, toughness, coefficient of friction, compression in body relevant stress conditions and viscoelastic behavior. This material also has high strength in PBS pH 7.4 and in egg white as synovial liquid substitute.

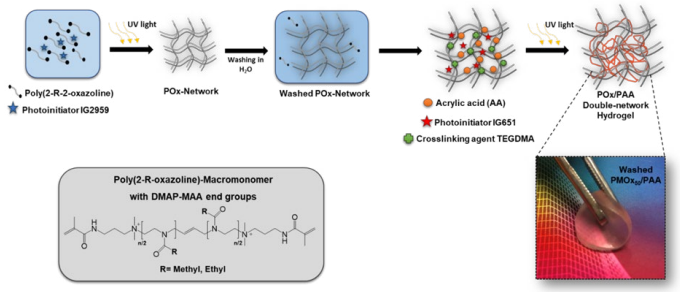

Figure 1: Steps of the synthesis of POx/PAA double-networks hydrogels.

The novel PMOx/PAA networks also use the pKa shifting effect of the combination of PAA and POx to obtain a non-ionic high performance double network hydrogel. The resulting material is shifting the pKa of PAA by almost three orders of magnitude, which makes the material a cartilage-like hydrogel, which does not react on environmental changes, such as salt concentration or pH changes up to 7.4. The hydrogel is taking up to 66 wt% of water- and has a two to three-fold higher compression strength than other cartilage-like materials.

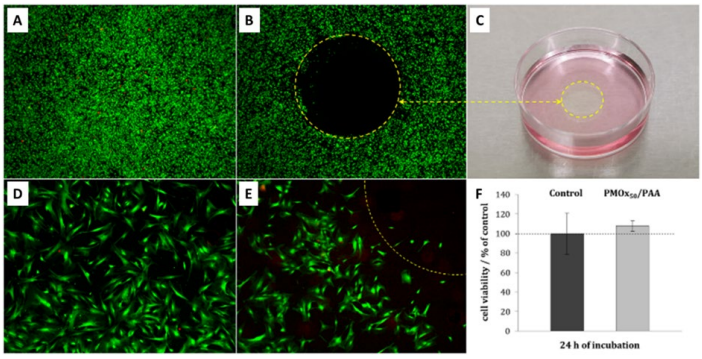

Figure 2: Cell morphology and viability of human mesenchymal stem cells (hMSC) in the presence of PMOx50/PAA DNH after 24 h of incubation.

As seen in Figure 2B and E, the stem cells did not grow on top of the hydrogel, which is a typical and desirable feature of cartilage-like materials due to their hydrogel character. However, the cells did attach and grow to the very proximity of the DNH indicating that the material does not leach toxic components. This is also shown by the spreading of the cells. Altogether, it can be stated the PMOx50/PAA is not cytotoxic and does not allow attachment and growth of human stem cells on its surface.
All these properties combine make the here shown DNH a very promising material for an artificial cartilage.

Contacts:
joerg.tiller@tu-dortmund.de

Publications:
Benitez-Duif, P. A.; Breisch, M.; Kurka, D.; Edel, K.; Gökcay, S.; Stangier, D.; Tillmann, W.; Hijazi, M.; Tiller, J. C., Advanced Functional Materials 2022, 32 (44), 2204837

Publications 2021– 2022

2022

Peer-reviewed Journal Articles

- Benitez-Duif, P. A.; Breisch, M.; Kurka, D.; Edel, K.; Gökcay, S.; Stangier, D.; Tillmann, W.; Hijazi, M.; Tiller, J. C.
  Ultrastrong Poly(2-Oxazoline)/Poly(Acrylic Acid) Double-Network Hydrogels with Cartilage-Like Mechanical Properties
  Advanced Functional Materials 32 (44), 2204837 (2022)

- Milovanovic, M.; Rauner, N.; Civelek, E.; Holtermann, T.; El Jid, O.; Meuris, M.; Brandt, V.; Tiller, J. C.
  Enzyme-Induced Ferrification of Hydrogels for Toughening of Functional Inorganic Compounds
  Macromol. Mater. Eng. 307 (8), 2200051 (2022)

- Segiet, D.; Weckes, S.; Austermuehl, J.; Tiller, J. C.; Katzenberg, F.
  On the influence of the amorphous phase on the stability of crystals in poly(cis-1,4-isoprene) networks
  J. Appl. Polym. Sci. 139 (46), e53146 (2022)

- Wilhelm, S. A.; Maricanov, M.; Brandt, V.; Katzenberg, F.; Tiller, J. C.
  Amphiphilic polymer conetworks with ideal and non-ideal swelling behavior demonstrated by small angle X-ray scattering
  Polymer 242, 124582 (2022)

2021

Peer-reviewed Journal Articles

- Benski, L.; Viran, I.; Katzenberg, F.; Tiller, J. C.
  Small-Angle X-Ray Scattering Measurements on Amphiphilic Polymer Conetworks Swollen in Orthogonal Solvents
  Macromolecular Chemistry and Physics, 222 (1), 2000292 (2021)

- Milovanovic, M.; Isselbaecher, N.; Brandt, V.; Tiller, J. C.
  Improving the Strength of Ultrastiff Organic–Inorganic Double-Network Hydrogels
  Chemistry of Materials, 33 (21), 8312-8322 (2021)

- Milovanovic, M.; Mihailowitsch, L.; Santhirasegaran, M.; Brandt, V.; Tiller, J. C.
  Enzyme-induced mineralization of hydrogels with amorphous calcium carbonate for fast synthesis of ultrastiff, strong and tough organic–inorganic double networks
  Journal of Materials Science, 56 (27), 15299-15312 (2021)

- Niedik, C. F.; Jenau, F.; Maricanov, M.; Segiet, D.; Tiller, J. C.; Katzenberg, F.
  Improvement of high voltage direct current material properties upon tailoring the morphology of crosslinked polyethylenes
  Polymer Crystallization, 4 (6), e10208 (2021)

- Romanovska, A.; Keil, J.; Tophoven, J.; Oruc, M. F.; Schmidt, M.; Breisch, M.; Sengstock, C.; Weidlich, D.; Klostermeier, D.; Tiller, J. C.
  Conjugates of Ciprofloxacin and Amphiphilic Block Copoly(2-alkyl-2-oxazolines)s Overcome Efflux Pumps and Are Active against CIP-Resistant Bacteria
  Molecular Pharmaceutics, 18 (9), 3532-3543 (2021)

- Segiet, D.; Stockmann, A.; Sadowski, J.; Katzenberg, F.; Tiller, J. C.
  Insights in the Thermal Volume Transition of Poly(2-oxazoline) Hydrogels
  Macromolecular Chemistry and Physics, 222 (18), 2100157 (2021)

2020

Peer-reviewed Journal Articles

- Milovanovic, M.; Unruh, M.T.; Brandt, V.; Tiller, J.C.
  Forming amorphous calcium carbonate within hydrogels by enzyme-induced mineralization in the presence of N-(phosphonomethyl) glycine
  Journal of Colloid and Interface Science 579,357-368 (2020)

- Hijazi, M.; Tuerkmen, E. ;Tiller, J. C.,
  Poly (2-oxazoline)s with a 2,2`-Iminodiacetate End Group Inhibit and Stabilize Laccase
  ChemBioChem 21, 874-882 (2020)

- Segiet, D.; Jerusalem, R.; Katzenberg, F.; Tiller, J. C.
  Investigation of the Swelling Behavior of Hydrogels Derived from High Molecular Weight Poly(2-Ethyl-2-Oxazoline)
  Journal Polymer Science, Part B: Polymer Physics 58, 747-755 (2020)

- Breisch, M: Loza, K.; Pappert, K.; Rostek, A.; Rurainsky, C.; Tschulik, K.; Heggen, M.; Epple, M.; Tiller, J. C.; Schildhauer, T. A.; Köller, M.; Sengstock, C.
  Enhanced dissolution of silver nanoparticles in a physical mixture with platinum nanoparticles based on sacrifcial anode effect
  Nanotechnology 31, 055703 (2020)

- Krumm, C.; Trump, S.; Benski, L.; Wilken, J.; Oberhaus, F.; Köller, M.; Tiller, J.C.
  Fast-Acting Antibacterial. Self-Deactivating Polyionene Esters
  ACS Applied Materials Interfaces 12, 21201-21209 (2020)

- Segiet, D.; Neunedorf, L.M.; Tiller, J.C.; Katzenberg, F.
  Realizing a shape-memory effect for synthetic rubber (IR)
  Polymer 203, 122788 (2020)

- Hijazi, M.; Tuerkmen, E.; Tiller, J. C.
  Full Thermal Switching of Enzymes by Thermoresponsive Poly(2-oxazoline)-Based Enzymes Inhibitors
  Chemistry A European Journal 26, 13367-13371 (2020)

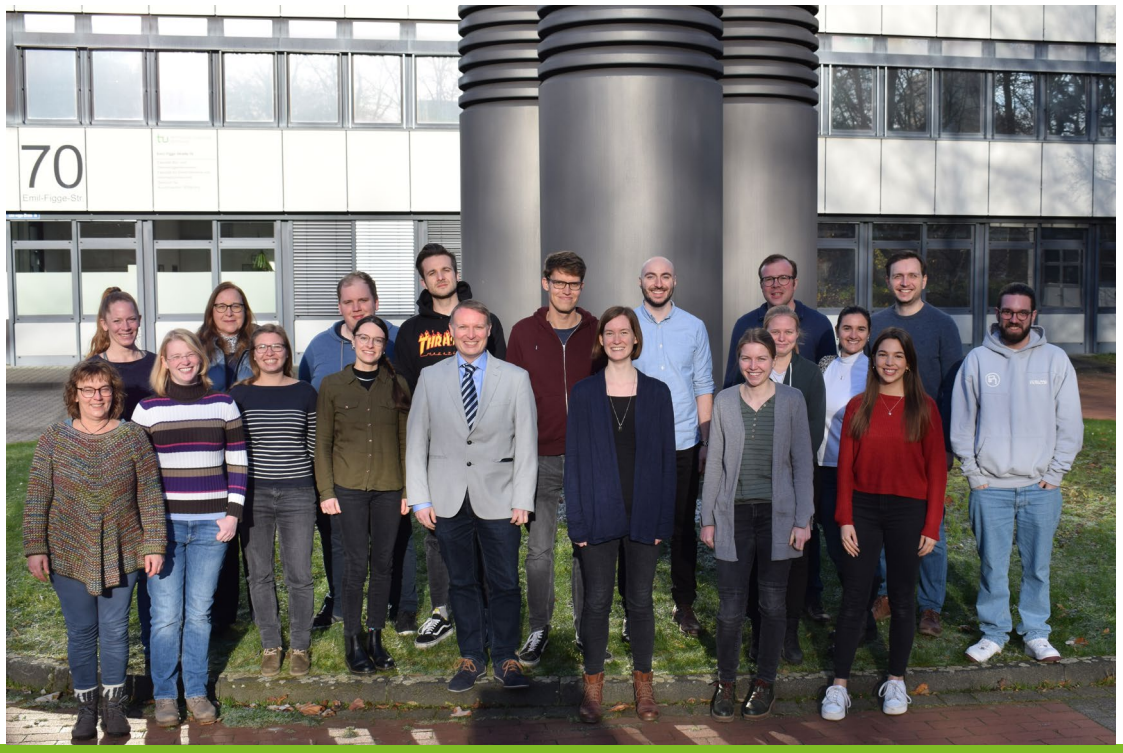

Bioprocess Engineering (BPT)

Comparative Life Cycle Assessment of Chemical and Biocatalytic 2'3' cGAMP Synthesis

The Green Route to Cyclic Dinucleotides

Martin Becker, Aleksandra Ziemińska-Stolarska, Dorota Markowska, Stephan Lütz, and Katrin Rosenthal

Life cycle assessments (LCAs) can provide insights into the environmental impact of production processes. In this study, a comparative LCA in an early development stage was performed for the synthesis of 2'3'-cyclic GMP-AMP (2'3'-cGAMP), which is of interest for pharmaceutical applications such as cancer immunotherapy. Cyclic dinucleotides (CDNs) can be synthesized either by enzymes or chemical catalysis. Both routes have their advantages and disadvantages, such as a poor yield for the chemical synthesis and low titers for the biocatalytic synthesis. The biocatalytic synthesis turned out to be superior to the chemical synthesis in all considered categories. This study demonstrates the value of assessment at an early development stage when the choice between different routes is still possible.

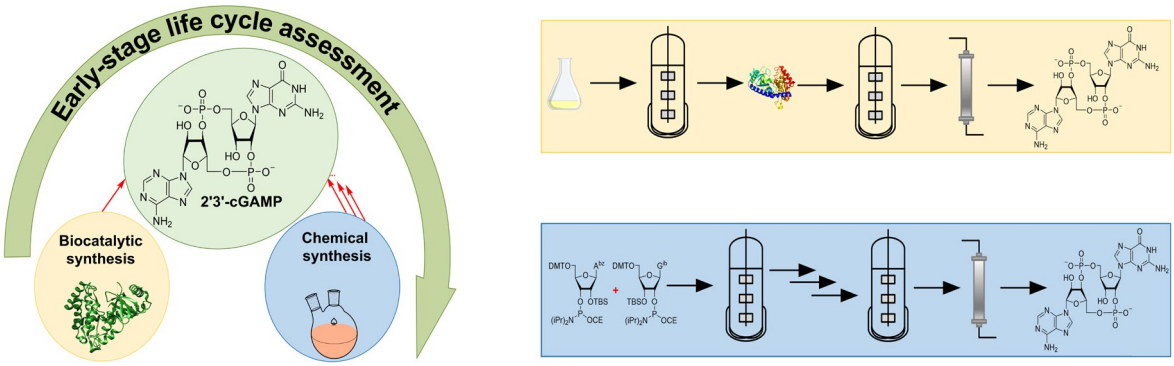

Figure 1: Scheme of the early-stage process for the production of 2'3'-cGAMP by biocatalytic or chemical synthesis.

The LCA was conducted for the chemical and biocatalytic production of 200 g 2'3'-cGAMP. With available laboratory data, literature, and rule of thumbs, both processes for production and purification were designed. The environmental assessment was performed with SimaPro and interpretated using the impact categories global warming potential (GWP 100), human health, resource scarcity, ecosystems and water use which are summarized in Table 1.

The obtained results show that the biocatalytic synthesis of 200 g 2'3'-cGAMP has a global warming potential of 3,055 kg CO_2 equiv. and the chemical synthesis 56,454 kg CO_2 equiv., which is 18 times higher. In the other impact categories, the results differ in a similar range. Main reasons for the harmful environmental impact of the chemical synthesis are the complex synthesis based on phosphoramidites within 8 steps with yield of 5% compared to 68% yield in the biocatalytic synthesis. In a sensitivity analysis, the effect of solvent recycling, scale-up, and reusing the enzyme were investigated, which revealed possible optimizations of both synthesis routes.

The results demonstrate that LCAs can provide valuable information for decisions at an early stage of development to optimize the production of 2'3'-cGAMP in an environmentally sustainable manner. In the case of 2'3'-cGAMP production, the biocatalytic synthesis route is clearly less harmful in the categories considered.

	GWP 100 [kg CO_2 eq.]	Human health [DALY]	Resource scarcity [USD2013]	Ecosystems [species.yr]	Water use [m3]
Biocatalytic synthesis	3,055.6	$5.9 \cdot 10^{-3}$	249.0	$1.4 \cdot 10^{-5}$	31.88
Chemical synthesis	56,454.0	1.1 · 10-1	4,250.1	2.7 · 10-4	482.39
fold-difference	18	19	17	19	15

Table 1: Contribution of environmental impact categories to the biocatalytic and chemical synthesis of 200 g 2'3'-cGAMP. GWP 100 is the 100 year time horizon global warming potential in kg CO_2 eq.. Human health indicates the disability-adjusted life years (DALYs). Resource scarcity considers the surplus cost of resource production. Ecosystems indicates the loss of species in a given period of time and in a certain area in years. Water use is given in m^3 water.

Contacts:
Martin4.Becker@tu-dortmund.de
stephan.luetz@tu-dortmund.de
KRosenthal@constructor.university

Publications:
M. Becker, A. Ziemińska-Stolarska, D. Markowska, S. Lütz, K. Rosenthal, ChemSusChem, e202201629 (2022)

Publications

2022

Peer-reviewed Journal Articles

- T. Bartsch, M. Becker, J. Rolf, K. Rosenthal, S. Lütz
  Biotechnological Production of Cyclic Dinucleotides–Challenges and Opportunities
  Biotechnology and Bioengineering, 119, 677-684 (2022)

- M. Becker, A. Ziemińska-Stolarska, D. Markowska, S. Lütz, K. Rosenthal
  Comparative life cycle assessment of chemical and biocatalytic 2'3'-cyclic GMP-AMP synthesis
  ChemSusChem, e202201629 (2022)

- J. Grühn, A. Behr, T. Eroglu, V. Trögel, K. Rosenthal, N. Kockmann
  From Coiled Flow Inverter to Stirred Tank Reactor – Bioprocess Development and Ontology Design
  Chemie Ingenieur Technik, 94(6), 1-13 (2022)

- A. Kinner, S. Lütz, K. Rosenthal
  Agar Plate-Based Screening Approach for the Identification of Enzyme-Catalyzed Oxidations
  Chemie Ingenieur Technik, 94(11) (2022)

- A. Kinner, P. Nerke, R. Siedentop, T. Steinmetz, T. Claassen, K. Rosenthal, M. Nett, J. Pietruszka, S. Lütz
  Recent Advances in Biocatalysis for Drug Synthesis
  Biomedicines, 10(5), 964C. Dowidat, M (2022)

- M. Menke, A. Behr, K. Rosenthal, N. Kockmann, U. Bornscheuer, M. Dörr
  Development of an ontology in Biocatalysis
  Chemie Ingenieur Technik, 94(11), 1827-1835 (2022)

- J. Rolf, A. Ngo, S. Lütz, D. Tischler, K. Rosenthal
  Cell-free protein synthesis for the screening of novel azoreductases and their preferred electron donor
  ChemBioChem, 23(15), e202200121 (2022)

- R. Siedentop, K. Rosenthal
  Industrially relevant enzyme cascades for drug synthesis and their ecological assessment
  International Journal of Molecular Science, 23(7), 3605 (2022)

- A. Steinmann, K. Schullehner, A. Kohl, C. Dickmeis, M. Finger, G. Hubmann, G. Jach, U. Commandeur, M. Girhard, V. B. Urlacher, S. Lütz
  A targeted metabolomics method for extra- and intracellular metabolite quantification covering the complete monolignol and lignan synthesis pathway
  Metabolic Engineering Communications 15, 1-12 (2022)

- A. Steinmann, M. Finger, C. Nowacki, D. Decembrino, G. Hubmann, M. Girhard, V. B. Urlacher, S. Lütz
  Heterologous Lignan Production in Stirred-Tank Reactors—Metabolomics-Assisted Bioprocess Development for an In Vivo Enzyme Cascade
  Catalysts 12, 1473 (2022)

- K. Rosenthal, UT. Bornscheuer, S. Lütz
  Cascades of Evolved Enzymes for the Synthesis of Complex Molecules
  Angewandte Chemie International Edition, e202208358 (2022)

- J. Vogt, K. Rosenthal
  Validation of easy fabrication methods for PDMS-based microfluidic (bio)reactors
  Sci, 4(4), 36 (2022)

2021

Peer-reviewed Journal Articles

- Siedentop R., Claaßen C., Rother D., Lütz S., Rosenthal K.
  Getting the Most Out of Enzyme Cascades: Strategies to Optimize In Vitro Multi-Enzymatic Reactions
  Catalysts 11, 1183 (2021)

- Rolf J., Nerke P., Britner A., Krick S., Lütz S., Rosenthal K.
  From Cell-Free Protein Synthesis to Whole-Cell Biotransformation: Screening and Identification of Novel - -Ketoglutarate-Dependent Dioxygenases for Preparative-Scale Synthesis of Hydroxy-L-Lysine
  Catalysts 11(9), 1038 (2021)

- Kinner A., Rosenthal K., Lütz S.
  Identification and Expression of New Unspecific Peroxygenases – Recent Advances, Challenges and Opportunities
  Frontiers in Bioengineering and Biotechnology 9:705630 (2021)

- Schmitz LM., Hageneier F., Rosenthal K., Busche T., Brandt D., Kalinowski J., Lütz S.
  Recombinant Expression and Characterization of Novel P450s from Actinosynnema mirum
  Bioorganic & Medicinal Chemistry 116241 (2021)

- Becker M., Nikel P., Andexer JN., Lütz S., Rosenthal K.
  A Multi-Enzyme Cascade Reaction for the Production of 2'3'-cGAMP
  Biomolecules 11(4), 590 (2021)

- Schmitz LM., Kinner A., Althoff K., Rosenthal K., Lütz S.
  Investigation of vitamin D2 and vitamin D3 hydroxylation by Kutzneria albida
  ChemBioChem 22, 1-10 (2021)

- Schwarz J., Hubmann G., Rosenthal K., and Lütz S.
  Triaging of Culture Conditions for Enhanced Secondary Metabolite Diversity from Different Bacteria
  Biomolecules 11(2), 193 (2021)

- Becker M., Lütz S., and Rosenthal K. (2021)
  Environmental Assessment of Enzyme Production and Purification
  Molecules 26(3), 573 (2021)

2020

Peer-reviewed Journal Articles

- K. Rosenthal, M. Becker, J. Rolf, R. Siedentop, M. Hillen, M. Nett, S. Lütz
  Catalytic promiscuity of cGAS: A facile enzymatic synthesis of 2'- 3' linked cyclic dinucleotides
  ChemBioChem, 21(22), 3225-3228 (2020)

- S. Lütz and A. Liese
  30 Jahre sichere Gentechnik in Deutschland
  Angewandte Chemie, 132, 2-4 (2020)

- J. Schwarz, K. Rosenthal, R. Snajdrova, M. Kittelmann, S. Lütz
  The Development of Biocatalysis as a Tool for Drug Discovery
  CHIMIA, 74(5), 368-377 (2020)

- J. Rolf, M. Julsing, K. Rosenthal, S. Lütz
  A Gram-Scale Limonene Production Process with Engineered Escherichia coli
  Molecules, 2020, 25(8), 1881 (2020)

• A. Sester, K. Stüer-Patowsky, W. Hiller, F. Kloss, S. Lütz, M. Nett
Biosynthetic Plasticity Enables Production of Fluorinated Aurachins
ChemBioChem 21(16), 2268-2273 (2020)

Computational Bioengineering (CBE)

PPI-Affinity: A Web Tool for Protein Engineering and Binding Affinity Predictions

Sandra Romero-Molina, Joel Mieres-Perez, Elsa Sanchez-Garcia

The accurate prediction of the binding affinity (BA) of protein–protein and protein–peptide complexes is highly relevant for the success of virtual screening in the early stages of the drug design process and for bioengineering applications. Several machine learning (ML)-based models have been introduced to predict the BA of protein-protein and protein-ligand complexes. However, with a scarce representation of protein-peptide samples on the training data, most tools underestimate the complexity of peptide compounds, which results in low accuracy when predicting the BA of protein-peptide complexes. We developed a web tool called PPI-Affinity that predicts the BA of protein-protein and protein-peptide complexes using two separate support vector machine (SVM) models. PPI-Affinity can generate and rank thousands of mutants of a given peptide or protein sequence to improve their affinity for a protein target. Notably, we introduced a protein engineering module that allows the automatic generation and evaluation of massive amounts of variants of protein complexes.

Protein-protein interactions (PPIs) are a topic of high interest to our research group since PPIs are relevant to most biological processes and their deregulation is related to severe disorders. For instance, the interaction between the serine protease HTRA1 and the cysteine protease calpain 2 (CAPN2) has important implications for allosteric processes and amyloidogenesis. In this context, we used docking techniques, molecular dynamics simulations, and free energy calculations to investigate the interactions between HTRA1 and peptides derived from CAPN2. However, although the fast and correct estimation of the binding affinity (BA) of protein–protein complexes can accelerate the discovery of therapeutic and industrially relevant compounds targeting PPIs, it remains a challenging task, especially by means of atomistic approaches.

As a complementary alternative to physics-based approaches, several ML methods have been introduced in the last decades to predict the BA of protein-protein and protein-ligand complexes. Peptides are an attractive target for the pharmaceutical industry, since they can be highly effective and have fewer side effects than small-molecule drugs. However, despite the strengths displayed by peptides, most ML-based methods contemplate peptides the same way as small molecules or large proteins and there are few representations of protein-peptide complexes among the training data. This consideration limits the applicability of many ML models.

To address this limitation, we developed machine learning (ML)-based predictors of protein-protein and protein-peptide binding affinity for three-dimensional structures. A peptide was defined as an amino acid sequence with less than 30 residues. We created the ML models by leveraging BA information annotated in publicly available databases and Support Vector Machines. We validated the generalization capabilities of PPI-Affinity on several external test sets.

Contacts:
sandra.romero-molina@tu-dortmund.de
joel.mieresperez@tu-dortmund.de
elsa.sanchez@tu-dortmund.de

The evaluation included a set of 26 wild-type and 151 mutants of protein-protein complexes taken from the SKEMPI dataset. There, the model delivered a Pearson's correlation coefficient (R) of 0.78 and a mean absolute error (MAE) of 1.4 kcal/mol between experimental and predicted BA. We assessed the protein-peptide model, among other test sets, on 56 derivatives of EPI-X4, an endogenous antagonist of the CXC chemokine receptor 4 (CXCR4) and on the interactions of peptides with the serine protease HTRA1. The output models were implemented as PPI-Affinity, a web tool which allows, in addition to BA predictions, the optimization of a protein sequence (Figure 1) with a three dimensional structure as template. Precisely, PPI-Affinity permits the generation of thousands of protein derivatives by applying substitutions and/or deletions on the residues found at the interface of contact of an input structure. These derivatives are then ranked by their BA values. Such functionalities are applicable in mutagenesis and protein design studies aimed to improve the binding affinity. Thus, PPI-Affinity can be leveraged in the design and optimization of peptides and in protein engineering applications.

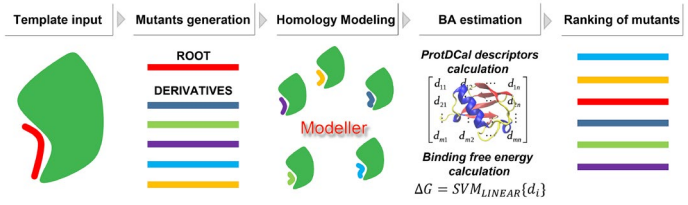

Figure 1: PPI-Affinity allows to generate and rank derivatives of protein-peptide and protein-protein complexes.

Publications:
J. Rey, M. Breiden, V. Lux, A. Bluemke, M. Steindel, K. Ripkens, B. Möllers, K. Bravo Rodriguez, P. Boisguerin, R. Volkmer, J. Mieres-Perez, T. Clausen, E. Sanchez-Garcia, M. Ehrmann, PNAS, 119 (14), e2113520119 (2022)
S. Romero-Molina, Y. B. Ruiz-Blanco, J. Mieres-Perez, M. Harms, J. Münch, M. Ehrmann, E. Sanchez-Garcia, J. Proteome Res., 21 (8), 1829–1841 (2022)

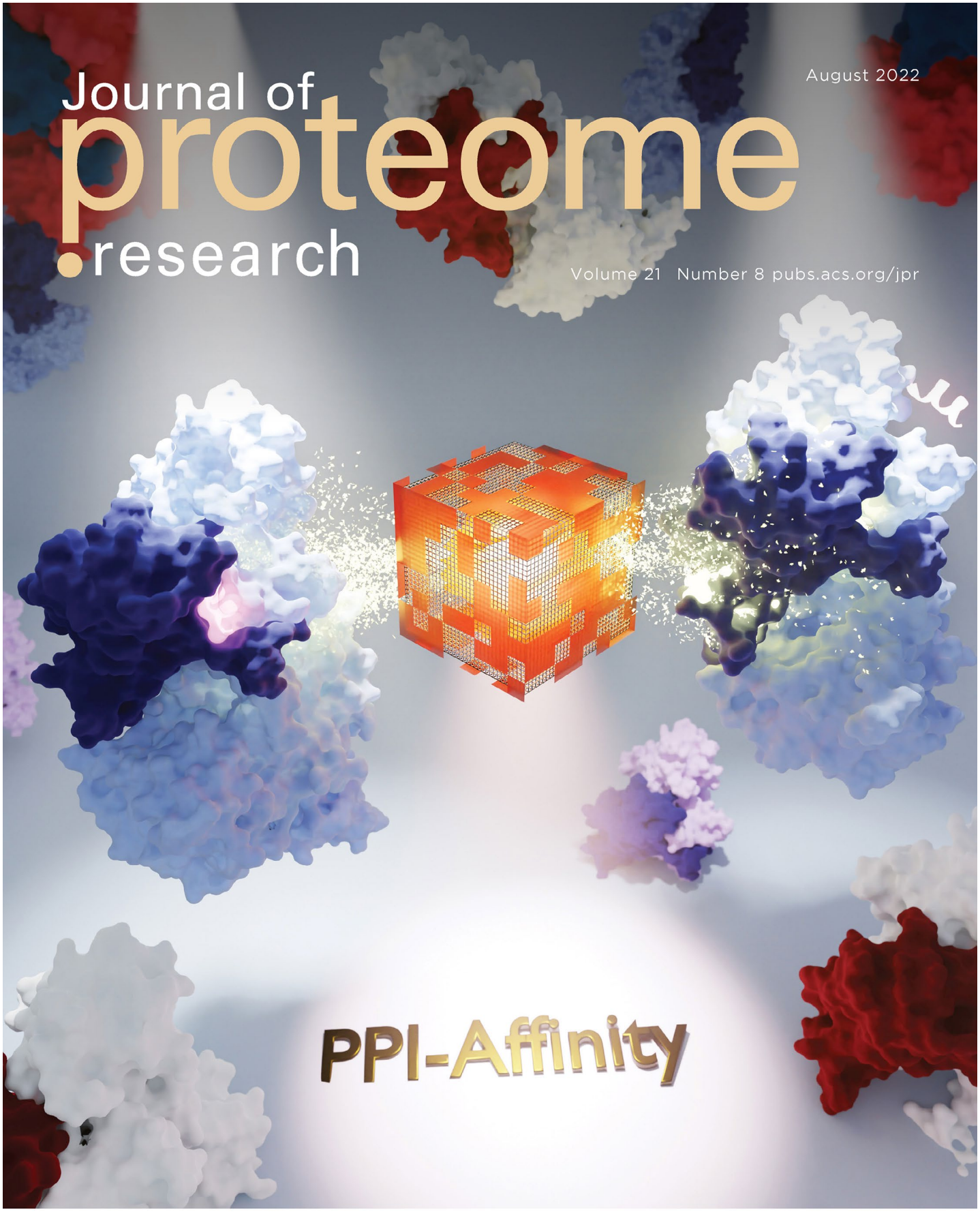
Journal of
proteome
research
August 2022
Volume 21 Number 8 pubs.acs.org/jpr
PPI-Affinity
ACS Publications
Most Trusted. Most Cited. Most Read.
www.acs.org

Mechanisms of supramolecular regulation: development of therapeutics and new strategies in biocatalysis

Joel Mieres-Perez and Elsa Sanchez-Garcia

Supramolecular chemistry finds many applications in the pharmaceutical industry, in the development of catalytic systems, and in materials technology, among others. However, the mechanistic understanding, design and optimization of supramolecular agents are challenging tasks due to the complexity of the structures and the dynamics of these systems. Our computational models allowed addressing these challenges towards the successful design and optimization of ligands with broad-spectrum antiviral activity as well as of nanostructures for the supramolecular modulation of catalytic activity.

Mechanisms of supramolecular inhibition of viral infectivity, new therapeutic alternatives: We established supramolecular tweezers as potential therapeutic alternatives against SARS-CoV-2 that act by destabilizing the envelope of viruses with the subsequent loss of viral infectivity. Our computational models delivered the mechanism of disruption of viral membranes by a new generation of advanced tweezers. These advanced tweezers were rationally modified with respect to the parent compounds to increase their antiviral activity. By means of extensive Gaussian accelerated Molecular Dynamics simulations (GaMD) on model systems of the supramolecular ligands with viral membranes, we demonstrated that the advanced tweezers (Figure 1) bind to the membrane lipid's head groups by incorporating the lipid's cationic ammonium moiety into the tweezers' cavity. This binding destabilizes the membrane by changing the orientation of the lipid's head group by nearly 90° with respect to its normal orientation in the membrane. Furthermore, we showed that these newly designed ligands are able to introduce their functionalized arms into the viral membrane thus increasing surface tension. In conjunction with the experimental results of our collaborators, our simulations lead to the discovery of novel molecular tweezers as broad-spectrum antiviral agents with potential therapeutic activity against SARS-CoV-2 and other pathogenic viruses.

Mechanisms of modulation of the catalytic efficiency of enzymes by DNA nanostructures: Large synthetic DNA structures complexed with proteins via spatially defined supramolecular interactions provide another perspective of supramolecular chemistry. However, the large size, dynamic behavior and structural complexity of these systems hinder the molecular mechanistic understanding of the role of these nanostructures in biocatalysis. We addressed these challenges by building novel models of a DNA origami encapsulating thrombin, an archetypical, allosterically regulated, serine protease and studying the dynamics of the complex (Figure 2). Our molecular dynamics simulations showed the structural changes undertaken by the DNA nanostructure. These changes lead to the enzyme being immersed in a potential "hole", which tunes the incorporation of peptide substrates. Furthermore, molecular dynamics simulations of reduced models of the DNA origami – enzyme complexes with peptide substrates of different charges indicated that the charge at the C-terminal position of the peptide greatly influences the dynamics of the substrate. Our work thus allowed elucidating the role of the substrate and confinement in enzymatic activity, and showed how spatial confinement with DNA nanostructures can be used for the regulation of allosteric processes.

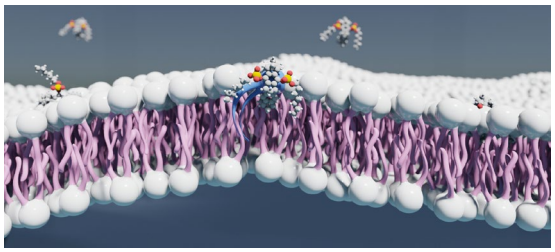

Figure 1: Representation of the mode of action of modified tweezers on membranes. The lipid head group (blue) complexed with the molecular tweezer is tilted with respect to the normal of the membrane.

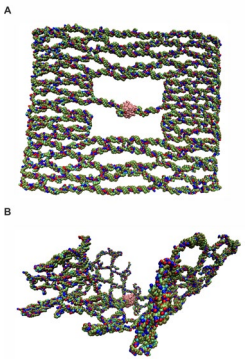

Figure 2: DNA origami model, including the protein thrombin (in light pink).

(A) Initial structure of the DNA origami with thrombin at the center.

(B) Structure of the DNA origami after GaMD simulations (120 ns).
The structure of the DNA origami is distorted and the enzyme is located in an electrostatic potential "hole" inside the nanostructure.

Contacts:
joel.mieres-perez@tu-dortmund.de
elsa.sanchez@tu-dortmund.de

Publications:
T. Weil, A. Kirupakaran, M.-H. Le, P. Rebmann, J. Mieres-Perez, L. Issmail, C. Conzelmann, J. A. Müller, L. Rauch, A. Gilg, L. Wettstein, R. Groß, C. Read, T. Bergner, S. A. Pålsson, N. Uhlig, V. Eberlein, H. Wöll, F.-G. Klärner, S. Stenger, B. M. Kümmerer, H. Streeck, G. Fois, M. Frick, P. Braubach, A. Spetz, T. Grunwald, J. Shorter, E. Sanchez-Garcia, T. Schrader, J. Münch, JACS Au, 2 (9), 2187-2202 (2022)
R. Kosinski, J. Mieres-Perez, E. Schöneweiß, Y.B Ruiz-Blanco, I. Ponzo, K. Bravo-Rodriguez, M. Erkelenz, S. Schlücker, G. Uhlenbrock, E. Sanchez-Garcia, B. Saccà, Sci. Adv., 8 (1), eabk0425 (2022)

Publications 2020 – 2022

2022

Peer-reviewed Journal Papers

- H. Shahpasand-Kroner, I. Siddique, R. Malik, G. Linares, M. Ivanova, J. Ichida, T. Weil, J. Münch, E. Sanchez-Garcia, F.-G. Klärner, T. Schrader, G. Bitan
Molecular tweezers – supramolecular hosts with broad-spectrum biological applications
Pharmacological Reviews, PHARMREV-AR-2022-000654 (2022)

- A. Rodríguez-Alfonso, A. Heck, Y. B Ruiz-Blanco, A. Gilg, L.Ständker, S. L. Kuan, T. Weil, E. Sanchez-Garcia, S. Wiese, J. Münch, M. Harms
Advanced EPI-X4 derivatives covalently bind human serum albumin resulting in prolonged plasma stability
International Journal of Molecular Sciences, 23(23), 15029 (2022)

- Y. B. Ruiz-Blanco, G. Agüero-Chapin, S. Romero-Molina, A. Antunes, L.-R. Olari, B. Spellerberg, J. Münch, E. Sanchez-Garcia
ABP-Finder: A Tool to Identify Antibacterial Peptides and the Gram-Staining Type of Targeted Bacteria
Antibiotics 11(12), 1708 (2022)

- N. Samanta, Y. B. Ruiz-Blanco, Z. Fetahaj, D. Gnutt, C. Lantz, J. A. Loo, E. Sanchez-Garcia, S. Ebbinghaus
Superoxide Dismutase Folding Stability as a Target for Molecular Tweezers in SOD1-related Amyotrophic Lateral Sclerosis
ChemBioChem 23 (21), e20220039 (2022)

- T. Weil, A. Kirupakaran, M.-H. Le, P. Rebmann, J. Mieres-Perez, L. Issmail, C. Conzelmann, J. A. Müller, L. Rauch, A. Gilg, L. Wettstein, R. Groß, C. Read, T. Bergner, S. A. Pålsson, N. Uhlig, V. Eberlein, H. Wöll, F.-G. Klärner, S. Stenger, B. M. Kümmerer, H. Streeck, G. Fois, M. Frick, P. Braubach, A.-L. Spetz, T. Grunwald, J. Shorter, E. Sanchez-Garcia, T. Schrader, J. Münch
Advanced Molecular Tweezers with Lipid Anchors against SARS-CoV-2 and Other Respiratory Viruses
JACS Au 2 (9), 2187-2202 (2022)

- L. Wettstein, P. Immenschuh, T. Weil, C. Conzelmann, Y. Almeida-Hernández, M. Hoffmann, A. Kempf, I. Nehlmeier, R. Lotke, M. Petersen, S. Stenger, F. Kirchhoff, D. Sauter, S. Pöhlmann, E. Sanchez-Garcia, J. Münch
Native and activated antithrombin inhibits TMPRSS2 activity and SARS-CoV-2 infection
Journal of Medical Virology 12 (1), 1726 (2022)

- A. Bera, S. Henkel, J. Mieres-Perez, Y. A. Tsegaw, E. Sanchez-Garcia, W. Sander, K. Morgenstern
Surface Diffusion Aided by a Chirality Change of Self-Assembled Oligomers under 2D Confinement
Angewandte Chemie 61 (43) e202212245 2022

- S. Romero-Molina, Y. B. Ruiz-Blanco, J. Mieres-Perez, M. Harms, J. Münch, M. Ehrmann, E. Sanchez-Garcia
PPI-Affinity: A web tool for the prediction and optimization of protein – peptide and protein – protein binding affinity
Journal of Proteome Research, 21 (8), 1829–1841 (2022)

- J. Rey, M. Breiden, V. Lux, A. Bluemke, M. Steindel, K. Ripkens, B. Möllers, K. Bravo Rodriguez, P. Boisguerin, R. Volkmer, J. Mieres-Perez, T. Clausen, E. Sanchez-Garcia, M. Ehrmann
An allosteric HTRA1-calpain 2 complex with restricted activation profile
Proceedings of the National Academy of Sciences, 119 (14) e2113520119. (2022)

- M. Harms, R. F. Hansson, S. Carmali, Y. Almeida-Hernández, E. Sanchez-Garcia, J. Münch, A. N. Zelikin.
Dimerization of the peptide CXCR4-antagonist on macromolecular and supramolecular protraction arms affords increased potency and enhanced plasma stability
Bioconjugate Chemistry 33 (4), 594-607 2022

- R. Kosinski, J. Mieres Perez, E.-C. Schöneweiß, Y. B. Ruiz-Blanco, I. Ponzo, K. Bravo-Rodriguez, M. Erkelenz, S. Schlücker, G. Uhlenbrock, E. Sanchez-Garcia, B. Saccà
The role of DNA nanostructures in the catalytic properties of an allosterically regulated protease
Science Advances 8 (1), eabk0425 (2022)

- D. Aschmann, C. Vallet, S. K. Tripathi, Y. B. Ruiz-Blanco, M. Brabender, C. Schmuck, E. Sanchez-Garcia, S. K. Knauer, M. Giese
Selective Disruption of Survivin's Protein-Protein Interactions: A Supramolecular Approach Based on Guanidiniocarbonylpyrrole
ChemBioChem, 23 (5), e202100618 (2022)

- K. N. Ingenbosch, J. C. Vieyto-Nuñez, Y. B. Ruiz-Blanco, C. Mayer, K. Hoffmann-Jacobsen, E. Sanchez-Garcia
Effect of Organic Solvents on the Structure and Activity of a Minimal Lipase
The Journal of Organic Chemistry 87 (3), 1669-1678 (2022)

Invited Lectures

- E. Sanchez-Garcia
Special Shimadzu lecture at the 9th Heron Island Conference: Reactive Intermediates and Unusual Molecules: Synthesis and Mechanism, Queensland, Australia

- E. Sanchez-Garcia
25th IUPAC International Conference on Physical Organic Chemistry, Hiroshima, Japan

- E. Sanchez-Garcia
Center of Molecular Immunology, Havana, Cuba

- E. Sanchez-Garcia
University of California Los Angeles (UCLA), California, United States

2021

- G. König, P. Sokkar, N. Pryk, S. Heinrich, D. Möller, G. Cimicata, D. Matzov, P. Dietze, W. Thiel, A. Bashan, J. E. Bandow, J. Zuegg, A. Yonath, F. Schulz, E. Sanchez-Garcia
  Rational prioritization strategy allows the design of macrolide derivatives that overcome antibiotic resistance
  Proceedings of the National Academy of Sciences 118 (46), e2113632118 (2021)

- P. Sokkar, M. Harms, C. Stürzel, A. Gilg, G. Kizilsavas, M. Raasholm, N. Preising, M. Wagner, F. Kirchhoff, L. Ständker, G. Weidinger, B. Mayer, J. Münch, E. Sanchez-Garcia
  Computational modeling and experimental validation of the EPI-X4/CXCR4 complex allows rational design of small peptide antagonists
  Communications Biology 4 (1), 1-13 (2021)

- T. Lohmiller, S. K. Sarkar, J. Tatchen, S. Henkel, T. Schleif, A. Savitsky, E. Sanchez-Garcia, W. Sander
  Sequential hydrogen tunneling in o-tolylmethylene
  Chemistry–A European Journal 27 (71), 17873-17879 (2021)

- R. Malishev, N.Salinas, J. Gibson, A. B. Eden, J. Mieres-Perez, Y. B. Ruiz-Blanco, O. Malka, S.Kolusheva, F.-G. Klarner, T. Schrader, E. Sanchez-Garcia, C. Wang, M. Landau, G. Bitan, R. Jelinek
  Inhibition of Staphylococcus aureus biofilm-forming functional amyloid by molecular tweezers
  Cell Chemical Biology 28, 1–11 (2021)

- M. Böhm, K. Killinger, A. Dudziak, P. Pant, K. Jänen, S. Hohoff, K. Mechtler, M.Örd, M.Loog, E. Sanchez-Garcia, S. Westermann
  Cdc4 phospho-degrons allow differential regulation of Ame1CENP-U protein stability across the cell cycle
  eLife 10, e67390 (2021)

- J. Mieres-Perez, K. Lucht, I. Trosien, W. Sander, E. Sanchez-Garcia, K. Morgenstern
  Controlling reactivity—real-space imaging of a surface metal carbene
  Journal of the American Chemical Society 143 (12), 4653–4660 (2021)

- L. Wettstein, T. Weil, C. Conzelmann, J. A. Müller, R. Groß, M. Hirschenberger, A. Seidel, S. Klute, F. Zech, C. P. Bozzo, N. Preising, G. Fois, R. Lochbaum, P. M. Knaff, V.Mailänder, L. Ständker, D. R. Thal, C. Schumann, S. Stenger, A. Kleger, G. Lochnit, B. Mayer, Y. B. Ruiz-Blanco, M. Hoffmann, K. M. J. Sparrer, S. Pöhlmann, E. Sanchez-Garcia, F. Kirchhoff, M. Frick & J. Münch
  Alpha-1 antitrypsin inhibits TMPRSS2 protease activity and SARS-CoV-2 infection
  Nature Communications 12, 1726 (2021)

- A. Meiners, S. Bäcker, I. Hadrović, C. Heid, C. Beuck, Y. B. Ruiz-Blanco, J. Mieres-Perez, M. Pörschke, J.-N. Grad, C. Vallet, D. Hoffmann, P. Bayer, E. Sánchez-García, T. Schrader & S. K. Knauer
  Specific inhibition of the Survivin–CRM1 interaction by peptide-modified molecular tweezers
  Nature Communications 12, 1505 (2021)

2020

- Y.B. Ruiz-Blanco, E. Sanchez-Garcia
  CL-FEP: An end-state free energy perturbation approach
  Journal of Chemical Theory and Computation 6 (3), 1396-1410 (2020)

- T. Weil, R. Groß, A. Röcker, K. Bravo-Rodriguez, C. Heid, A. Sowislok, M.-H. Le, N. Erwin, M. Dwivedi, S. M. Bart, P. Bates, L. Wettstein, J. A. Müller, M. Harms, K. Sparrer, Y. B. Ruiz-Blanco, C. M. Stürzel, J. v. Einem, S. Lippold, C. Read, P. Walther, M. Hebel, F. Kreppel, F.-G. Klärner, G. Bitan, M. Ehrmann, T. Weil, R. Winter, T. Schrader, J. Shorter, E. Sanchez-Garcia, J. Münch
  Supramolecular mechanism of viral envelope disruption by molecular tweezers
  Journal of American Chemical Society 142, 17024–17038. (2020)

- D. Schütz, Y. B. Ruiz-Blanco, J. Münch, F. Kirchhoff, E. Sanchez-Garcia, J. A. Müller
  Peptide and peptide-based inhibitors of SARS-CoV-2 entry
  Advanced Drug Delivery Reviews 167, 47-65 (2020)

- A. Kuusk, J. F. Neves, K. Bravo-Rodriguez, R. G. Doveston, A. Gunnarsson, M. Ehrmann, H. Chen, I. Landrieu, E. Sanchez-Garcia, H. Boyd, C. Ottmann
  Adoption of a turn conformation drives the binding affinity of p53 c-Terminal domain peptides to 14-3-3σ
  ACS Chemical Biology 15, 262-271 (2020)

- M. Harms, M. M.W. Habib, S. Nemska, A. Nicolò, A. Gilg, N. Preising, P. Sokkar, S. Carmignani, M. Raasholm, G. Weidinger, G. Kizilsavas, M. Wagner, L. Ständker, A. H. Abadi, H. Jumaa, F. Kirchhoff, N. Frossard, E. Sanchez-Garcia, J. Münch
  An optimized derivative of an endogenous CXCR4 antagonist prevents atopic dermatitis and airway inflammation
  Acta Pharmaceutica Sinica B 11, 2694-2708 (2020)

- A. Holch, R. Bauer, L.-R. Olari, A. A. Rodriguez, L. Ständker, N. Preising, M. Karacan, S. Wiese, P. Walther, Y. B. Ruiz-Blanco, E. Sanchez-Garcia, C. Schumann, J. Münch & B. Spellerberg
  Respiratory ß-2-Microglobulin exerts pH dependent antimicrobial activity
  Virulence 11 (1), 1402-1414 (2020)

- T. Schleif, J. Tatchen, J. F. Rowen, F. Beyer, E. Sanchez-Garcia, W. Sander
  Heavy atom tunneling in semibullvalenes: how driving force, substituents, and environment influence the tunneling rates
  Chemistry – A European Journal 26, 10452-10458 (2020)

- R. Groß, R. Bauer, F. Krüger, E. Rücker-Braun, L.-R. Olari, L. Ständker, N. Preising, A. A. Rodríguez, C. Conzelmann, F. Gerbl, D. Sauter, F. Kirchhoff, B. Hagemann, J. Gačanin, T. Weil, Y. B. Ruiz-Blanco, E. Sanchez-Garcia, W.-G. Forssmann, A. Mankertz, S. Santibanez, S. Stenger, P. Walther, S. Wiese, B. Spellerberg, J. Münch
  A placenta derived C-terminal fragment of ß-hemoglobin with combined antibacterial and antiviral activity
  Frontiers in Microbiology 11, 508. (2020)

Book Chapter

- Joel Mieres-Perez, Elsa Sanchez-Garcia
  Quantum mechanics/molecular mechanics multiscale modeling of biomolecules
  Advances in Physical Organic Chemistry 54, 143-183. 2020

Computational Systems Biology (CSB)

Publications 2020 – 2022

2022

Peer-reviewed Journal Articles

- T. Goßmann und D. Waxman
  Correcting bias in allele frequency estimates due to an observation threshold: a Markov chain analysis
  Genome Biology and Evolution 14 (4) (2022) DOI: 10.1093/gbe/evac047

- K. Mavreas, T. Goßmann, und D. Waxman
  Loss and fixation of strongly favoured new variants: Understanding and extending Haldane's result via the Wright–Fisher model
  Biosystems 211, 104759 (2022) DOI: 10.1016/j.biosystems.2022.104759

- J. Muenzner u. a.
  The natural diversity of the yeast proteome reveals chromosome-wide dosage compensation in aneuploids
  bioRxiv (2022) DOI: 10.1101/2022.04.06.487392

- D. L. J. Vendrami u. a.
  Signatures of selection on mitonuclear integrated genes uncover hidden mitogenomic variation in fur seals
  Genome Biology and Evolution 14 (7) (2022) DOI: 10.1093/gbe/evac104

2021

Peer-reviewed Journal Articles

- F. Hildebrand u. a.
  Dispersal strategies shape persistence and evolution of human gut bacteria
  Cell Host and Microbe 29 (7), 1167-1176 (2021) DOI: 10.1016/j.chom.2021.05.008

- N. Junker und T. Goßmann
  Adaptation-driven evolution of sirtuin 1 (SIRT1), a key regulator of metabolism and aging, in marmot species
  Frontiers in Ecology and Evolution 9, 666564 (2021) DOI: 10.3389/fevo.2021.666564

- Ø. Strømland u. a.
  Discovery of fungal surface NADases predominantly present in pathogenic species
  Nature Communications 12 (1), 1631 (2021) DOI: 10.1038/s41467-021-21307-z

- J. M. Waterman, T. Goßmann, O. Brandler, und J. L. Koprowski
  Editorial: Ecological, behavioral and genomic consequences in the rodent family sciuridae: Why are squirrels so diverse?
  Frontiers in Ecology and Evolution 9, 765558 (2021) DOI: 10.3389/fevo.2021.765558

2020

Peer-reviewed Journal Articles

- L. Yusuf, M. C. Heatley, J. P. G. Palmer, H. J. Barton, C. R. Cooney, und T. Goßmann
  Noncoding regions underpin avian bill shape diversification at macroevolutionary scales
  Genome research 30 (4), 553–565 (2020) DOI: 10.1101/gr.255752.119

- T. Goßmann und M. Ralser
  Marmota marmota
  Trends in Genetics 36 (5), 383–384 (2020) DOI: 10.1016/j.tig.2020.01.006

Fluid Mechanics (FM)

Experimental and Numerical Investigation of Emergency Pressure Relief

Michael-David Fischer, Simon Baier, Fabienne Ryll, Konrad Boettcher

The emergency pressure relief of gas-filled vessels is a fluid-mechanical problem with great relevance to the field of safety engineering. Prediction models for the description of such pressure reliefs were complex and not universal and therefore not very practical. Numerical simulations are very time and cost intensive due to the transient nature of the problem. Although it is a fundamental problem, the Reynolds number dependence of a free jet is still controversially discussed in the literature. The Reynolds number represents the ratio of inertial to frictional forces. However, understanding such free jet propagations is essential for the approval of new plants such as hydrogen electrolysers. Therefore, a self-similar model was derived to predict the subcritical pressure discharge of arbitrary vessels and systems within seconds.

Fischer and Boettcher derived a dimensionless number based on the Buckingham π theorem. This dimensionless number is already able to capture the variation in the molar mass of the outflowing gas, the temperature, the vessel volume and the orifice diameter and showed constant values for these. In a next step, Fischer et al. (a) managed to extend the dimensionless number by the heat capacity ratio in such a way that it provided a self-similar solution for arbitrary gases. Furthermore, the pressure ratio from the vessel to the environment could also be captured, so that there is a single curve for describing any subcritical, isentropic discharge (Figure 1). The self-similar model was validated in a parameter study with a large number of computational fluid dynamics (CFD) simulations. The mean deviation between the CFD simulations and the similarity-model is 1.94 %.

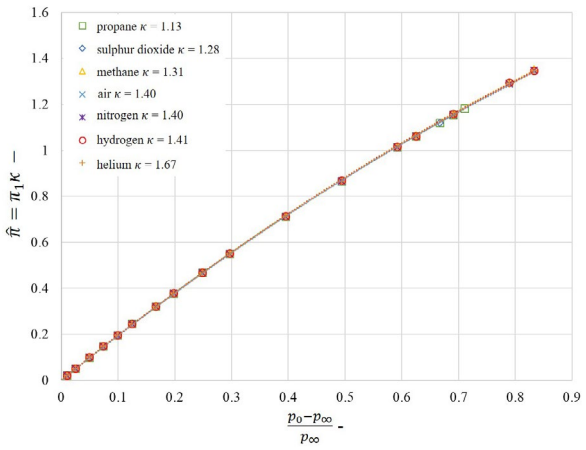

Figure 1: Similarity result of the parameter study with the similarity discharge model and CFD simulations.

Based on these findings, Fischer et al. (b) carried out experimental investigations into gas free jet propagation (Figure 2). Phase Doppler anemometry (PDA) was used, which can measure tracer velocity as well as tracer size. This provided an important contribution to the validation of the results and a cut-off size for perfect following tracers could be experimentally determined. This made it possible to equate the tracer velocity with the gas velocity. On the basis of a thorough statistical evaluation, a significant relationship (p-value < 1.703·10-4) between the propagation behaviour and the Reynolds number could be clearly verified.

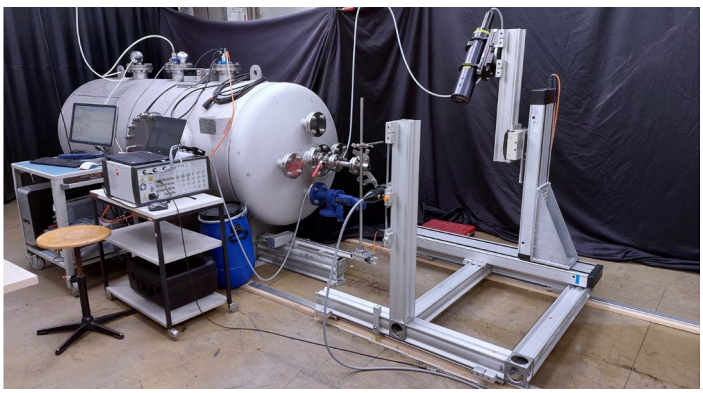

Figure 2: Experimental setup for phase Doppler anemometry measurements of transient emergency pressure reliefs from gas vessels.

Publications:
[1] M.-D. Fischer, K.E.R. Boettcher, A Fast Method to Predict the Transient, Subcritical Gas Discharge From a Pressure Vessel, Chemical Engineering Science, 117276, 2022, https://doi.org/10.1016/j.ces.2021.117276
[2] M.-D. Fischer, S. Baier, K.E.R. Boettcher, Similarity Solution of Subcritical Pressure Discharges From Vessels for Arbitrary Gases, Chemical Engineering Science, 118312, 2022 (a), https://doi.org/10.1016/j.ces.2022.118312
[3] M.-D. Fischer, F. Ryll, K.E.R. Boettcher, Measurement of the Reynolds Number Dependence of a Transient Air Jet from a Pressure Vessel, Pre-Print, 2022 (b), https://doi.org/10.21203/rs.3.rs-2311542/v1

Contacts:
michael-david.fischer@tu-dortmund.de
konrad.boettcher@tu-dortmund.de

Cross-Reality Laboratories for Learning and Working 4.0 in Engineering Education

Konrad Boettcher, Alexander Behr

The world of work is undergoing a transformation as a result of digitization. As a result, additional competencies are required, which are not limited to the use of certain technologies. In the context of the development of Industry 4.0 and, in particular, 5.0, autonomy, interface competence, ethical decision-making skills and the ability to develop one's personality are becoming crucial as future skills. These should therefore find their way into university teaching. Scenario-based laboratory experiments together with decision-making problems and guided reflection discussions are particularly suitable for this purpose. This is feasible as a simulated remote or VR laboratory, because physical laws and legal or ethical regulations can be bypassed here at will.

The joint project CrossLabs with the partner universities TU Bergakademie Freiberg, TU Ilmenau and NORDAKADEMIE gAG Hochschule der Wirtschaft and TU Dortmund University aims to make flexibly combinable laboratory objects available to teachers and learners. To this end, the aim is to combine laboratory types, laboratory elements, universities and disciplines in different experiments.

From a instructional perspective, a laboratory experiment is aligned with Feisel and Rosa's 13 fundamental laboratory learning objectives and iteratively designed and improved according to the Constructive Alignment framework. However, the 13 fundamental laboratory learning objectives do not yet relate to the requirements of Work 4.0. Initial research has been conducted to identify industry expectations of laboratory learning objectives in this context. In an explorative study, interviews were conducted in various companies of different sizes and engineering specializations at different job levels and analyzed qualitatively. In addition to conventional learning objectives, working mindset, thinking out of the box and technical knowledge, such as the organizational design principles of Industrie 4.0, were identified. To address these, emerging technologies such as AR and VR are suitable. For this purpose, procedures were developed on the basis of the professional 3D engine Unreal Engine 4, with which any data (analytical and experimental results, image sequences, numerical simulations, CAE simulations) can be displayed and influenced as vector fields with particle movement, scalar fields in 2D and even in 3D, field lines and explanatory fields in virtual reality on basic PCs (Figure 1). The basis for implementing the results of CFD simulations is the use of the fictitious domain method. In this, flow domains representing a solid are assigned an extremely high flow resistance and are thus impermeable. Statistical models for pressure drops in fiber filter media have also been developed using this method. The method can be used to calculate flows in different flow geometries without time-consuming remeshing, and to automate data preparation. This enables the embedding of information transparency, technical assistance and the use of cyberphysical systems such as digital twins in laboratory experiments as a teaching-learning activity.

In a university-wide competition, 10 cross-reality laboratories (VR, AR, remote or ultra-concurrent remote) are currently being developed. The developed VR and AR procedures enable e.g. laboratory experiments on AI-based process control of a column, on safety guidelines in chemistry laboratories, on reduction of concrete waste in civil engineering (Figure 2) and on completely new experiments in the quantum laboratory of physics. Existing lab experiments on flow visualization led to a increase in learning effect as the scores in specific tasks were doubled.

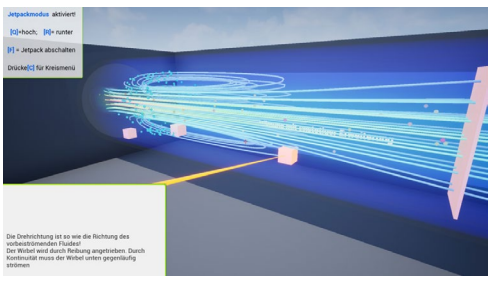

Figure 1: Representation of a pipe with a cross-sectional jump, streamlines and a 3d-scalar field.

Figure 2: (left) Experimental rig for anchor testing in concrete and (right) after pulling out with the whole concrete block as waste.

Publications:
[1] K. Boettcher, A. Behr, C. Terkowsky, Development Methodology for Immersive Home Laboratories in Virtual Reality – Visualizing Arbitrary Data in Virtual Reality, International Journal of Biomedical and Online Engineering – Special Issue: Online-Labs in Education, 18 (14), https://doi.org/10.3991/ijoe.v18i14.35099
[2] I. Aubel et al., 2022, Adaptable Digital Labs – Motivation and Vision of the CrossLab Project, 2022 IEEE German Education Conference (GeCon), 2022, https://doi.org/10.1109/GeCon55699.2022.9942759
[3] M. Soll, K. Boettcher, Expected Learning Outcomes for Laboratories at Universities by the Industry, 2022 IEEE German Education Conference (GeCon), pp. 1-6, 2022, https://doi.org/10.1109/GeCon55699.2022.9942762
[4] S. Behr, L. Neuendorf, P. Sakthithasan, K. Boettcher, N. Kockmann, Process control using AI on a digital twin of an extraction column in VR, 2022 IEEE German Education Conference (GeCon), 2022, https://doi.org/10.1109/GeCon55699.2022.9942788
[5] A. Frede, S. Höving, K. Boettcher, I. Aubel, N. Kockmann, Microcontroller-based Titration for Remote Lab, 2022 IEEE German Education Conference (GeCon), 2022, https://doi.org/10.1109/GeCon55699.2022.9942767

Contacts:
konrad.boettcher@tu-dortmund.de

Publications 2021 – 2022

2022

Journal contributions

- M.-D. Fischer, K.E.R. Boettcher
  A Fast Method to Predict the Transient, Subcritical Gas Discharge From a Pressure Vessel
  Chemical Engineering Science, 117276, 2022, https://doi.org/10.1016/j.ces.2021.117276

- M.-D. Fischer, S. Baier, K.E.R. Boettcher
  Similarity Solution of Subcritical Pressure Discharges From Vessels for Arbitrary Gases
  Chemical Engineering Science, 118312, 2022, https://doi.org/10.1016/j.ces.2022.118312

- M.-D. Fischer, F. Ryll, K.E.R. Boettcher
  Measurement of the Reynolds Number Dependence of a Transient Air Jet from a Pressure Vessel
  Pre-Print, 2022, https://doi.org/10.21203/rs.3.rs-2311542/v1

- K. Boettcher, A. Behr, C. Terkowsky
  Development Methodology for Immersive Home Laboratories in Virtual Reality – Visualizing Arbitrary Data in Virtual Reality
  International Journal of Biomedical and Online Engineering – Special Issue: Online-Labs in Education, 18 (14), https://doi.org/10.3991/ijoe.v18i14.35099

- K. E. R. Boettcher, M.-D. Fischer, T. Neumann, P. Ehrhard
  Experimental investigation into the pre-Darcy regime
  Experiments in Fluids, 63 (42)

- J. Chaudhuri, K. Boettcher, P. Ehrhard, 2022, https://doi.org/10.1007/s00348-022-03387-9
  Optical investigations into wetted commercial coalescence filter using 3D micro-computer tomography
  Chemical Engineering Science, 248 A, 117096, 2022, https://doi.org/10.1016/j.ces.2021.117096

Peer-reviewed Conference Papers

- A. Frede, S. Höving, K. Boettcher, I. Aubel, N. Kockmann
  Microcontroller-based Titration for Remote Lab
  2022 IEEE German Education Conference (GeCon), 2022 https://doi.org/10.1109/GeCon55699.2022.9942767

- S. Behr, L. Neuendorf, P. Sakthithasan, K. Boettcher, N. Kockmann
  Process control using AI on a digital twin of an extraction column in VR
  2022 IEEE German Education Conference (GeCon), 2022, https://doi.org/10.1109/GeCon55699.2022.9942788

- M. Soll, K. Boettcher
  Expected Learning Outcomes for Laboratories at Universities by the Industry, 2022
  IEEE German Education Conference (GeCon), pp. 1-6, 2022, https://doi.org/10.1109/GeCon55699.2022.9942762

- I. Aubel et al., 2022
  Adaptable Digital Labs – Motivation and Vision of the CrossLab Project, 2022
  IEEE German Education Conference (GeCon), 2022, https://doi.org/10.1109/GeCon55699.2022.9942759

2021

Presentations

- Th. B. Goudoulas, S. Vanderhaeghen, and N. Germann
  Micro-dispersed essential oils loaded gelatin hydrogels with antibacterial activity
  LWT-Food Science and Technology, 154:112797, 2022. DOI: https://doi.org/10.1016/j.lwt.2021.112797 [Impact factor: 4.79]

- N. Germann
  Perspectives of experiment-based OpenFOAM simulation in food process design and optimization
  EFFOST, Lausanne, Switzerland, November 1-4, 2021, Spain. Invited Plenary

- A. Moeini, S. Mayer, M. Tallawi, I. De Luca, A. Calarco, N. Reinhardt, L.A. Gray, K. Drechsler, and N. Germann.
  Antimicrobial and physicochemical characterization of 2,3 dialdehyde cellulose-based wound dressing systems International online conference on Macromolecules: Synthesis, Morphology, Processing, Structure, Properties and Applications
  Kottayam, India, September 10-12, 2021. Invited Talk

- L. Abu-Farah, and N. Germann
  Thermal phase change and bacterial inactivation in a superheated steam application using CFD simulations
  74th Annual Meeting of the APS Division of Fluid Dynamics, Phoenix, Arizona, USA, November 21-24, 2021

Solids Process Engineering (FSV)

Semi-Mechanistic Modelling of Droplet-Size Distribution

from Two-Fluid Atomizers via Maximization of Entropy Generation

Leander Mehlis, Jens Bartsch, Patrick Kranz, Werner Hoheisel, Markus Thommes

The use of superheated steam in dishwashers as a means of reducing water consumption and cleaning time without the use of chemical cleaning agents has great future potential for the restaurants, hotels, and hospitals. In these sectors in particular, hygienic safety is an important concern in addition to the removal of food residues. The present study demonstrates how superheated steam effectively kills bacterial cells in a dishwasher.

During spray formation of a two-fluid nozzle the spray liquid is accelerated by a surrounding gas jet, which causes instabilities on the liquid surface. These are responsible for its dissipation. A semi mechanistic model for the instability of the liquid is presented by Aliseda et al. and is used for the prediction of Sauter-Mean diameter. The general idea as well as the relevant input variables of the Aliseda model are shown in Figure 1.

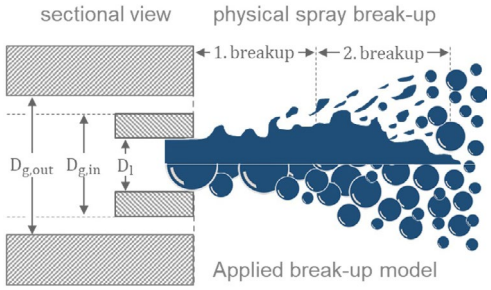

Figure 1: Two-fluid nozzle design spray instability modelling.

Information on spray distribution is lost in the application of instability analysis. However, the most probable droplet-size distribution can be deduced by combination of a predictive model for Sauter Mean diameter, an entropy balance, and a probability distribution. Log-normal distributions are widely used for droplet-size distributions.
The developed model predicts the droplet-size distribution close to the spray nozzle. In addition to three fitting parameters, the droplet-size distribution depends on critical process parameters (CPPs), critical material attributes (CMAs) and the nozzle geometry. Laser diffraction measurements in combination with a central composite experimental design were applied for model validation. Atomization pressure and liquid volumetric flow rate were varied between 0.5 - 2.4 bar and 15 - 35 mL/min, respectively. Water was used as liquid.
To determine the predictive power of the developed model, the 25% and 75% percentile of the volumetric distribution were evaluated. As shown in Figure 2, the maximum relative deviation of the model is 15%. Larger droplets, which are conterminous with low atomization pressures, show a greater relative deviation. However, the developed model is suitable to predict the droplet size distribution for the tested design space.

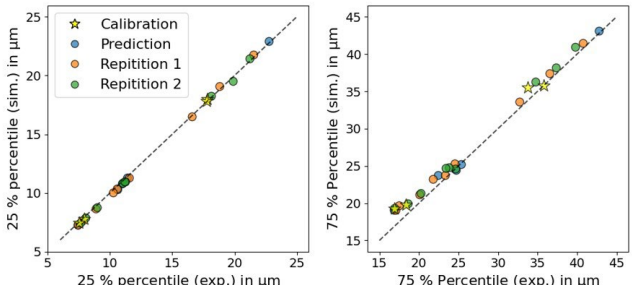

Figure 2: Comparison of experimental data and model predictions.

Contacts:
leander.mehlis@tu-dortmund.de
jens.bartsch@tu-dortmund.de
hoheisel@invite-research.com
markus.thommes@tu-dortmund.de

Categorization of Sprays by Image Analysis with Convolutional Neuronal Networks

Damian Pieloth, Matthias Rodeck, Gerhard Schaldach, Markus Thommes

Medical spray pumps for pharmaceutical applications are widely used to administer drugs into the lungs, the throat or the nose. These nebulizers are employed to deliver drug solutions to the mucosa, and their performance depends on the droplet size and velocity. Therefore, the droplet size and the spray-cone geometry are frequently measured for each unit as part of process control during the production of pharmaceutical nebulizers. However, conventional methods like laser diffraction and phase Doppler anemometer analysis are insufficient to keep up with the high production rates of spray pumps at this time. Image analysis with convolutional neuronal networks (CNNs) has been successfully applied in fields such as facial recognition, autonomous driving, and cancer detection. Based on this, CNNs should be suitable for spray characterization by images.

The median droplet size ($d_{50,3}$) and the droplet size distribution were generated by a nozzle from a medical spray pump at five different spray conditions were measured via laser diffraction.
Additionally images of the spray cones (Fig. 1) were acquired using a digital camera, so data sets of 2500 images (500 repetitions of five different spray conditions) were generated. Each image were labeled with a corresponding $d_{50,3}$ as well as the drop size distribution were determined by laser diffraction. During the training of a convolutional neuronal network CNN, the weights of the individual neurons of the convolutional neuronal network are adjusted iteratively until the predicted value, the reference value or "label" converge.

Figure 1: Representative raw image of the spray ($d_{50,3}$ = 86µm).

Heat maps indicate the relevance of certain parts of the spray image for correlation with the label value. These heat maps were super-imposed on the spray image (Fig. 2) for easy interpretation. Some relevant areas are close to the nozzle orifice, which might be related to the deviation in the spray angle. Moreover, there is also a relevant region on the left-hand side of the image, about 100–150mm from the orifice. In this region distinctive droplet clusters can be identified visually, which are reasonably believed to affect the categorization with respect to size.
As a first result 500 spray images (from 5 different categories) were labeled by their $d_{50,3}$ and not used for training interpreted by the CNN correctly, given an accuracy of more than 99.8 %. In a second step, the CNN were trained to categorize images of sprays by the drop size distribution measured by laser diffraction.

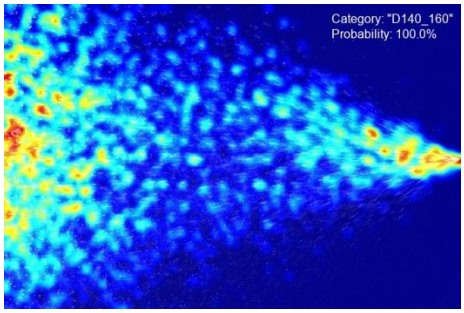

Figure 2: Heat map for the CNN ($d_{50,3}$ = 86µm.) Red indicates relevant and blue less relevant regions in the image for CNN training.

As shown in Figure 3 the droplet size distribution categorized by CNN is comparable to those of the reference measurement since no relevant differences were observed between the methods. The error bars are the standard deviations of the measurement repetitions for laser diffraction (n = 20) and CNN determination (n = 100).
Overall, spray categorization by CNN is a versatile and powerful technique and even suitable for an in-line production environment for process or product control applications since cheap equipment like single-board computers and digital cameras provide fast and reliable results.

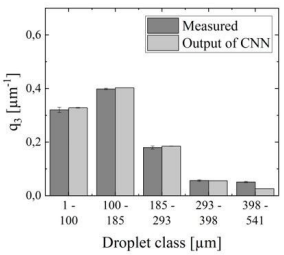

Figure 3: Representative droplet size distribution obtained by laser diffraction measurements (reference, av±s, n = 20) and CNN determination (av± s, n = 100).

Contacts:
damian.pieloth@tu-dortmund.de
gerhard.schaldach@tu-dortmund.de
markus.thommes@tu-dortmund.de

Publications:
Damian Pieloth, Matthias Rodeck, Gerhard Schaldach, Markus Thommes, Chem. Eng. Technol. 45, 1–7 (2022)

Investigations Concerning the Melt Viscosity of ASD Formulations as Key Factor in Process Design

Vincent Kimmel, Judith Winck, Markus Thommes

Amorphization is a promising concept to overcome the low bioavailability of poorly soluble drugs. In order to stabilize the amorphous state, the formulation as Amorphous Solid Dispersions (ASD) is favored, in which the drug is molecularly dispersed in a polymer matrix. In the context of fusion methods, the melt viscosity is a key factor in process design. Therefore, the viscosity of drug/polymer mixtures above the glass transition temperature was studied. Finally, a model based on molecular interactions was developed to predict the drug dependent melt viscosity.

Amorphization is a promising concept to overcome the low bioavailability of poorly soluble drugs. In order to stabilize the amorphous state, the formulation as Amorphous Solid Dispersions (ASD) is favored, in which the drug is molecularly dispersed in a polymer matrix. In the context of fusion methods, the melt viscosity is a key factor in process design. Therefore, the viscosity of drug/polymer mixtures above the glass transition temperature was studied. Finally, a model based on molecular interactions was developed to predict the drug dependent melt viscosity.

The investigation of melt viscosity was performed with the model drugs Itraconazole (ITR), Acetaminophen (ACE) and Griseofulvin (GRI), which were dispersed in the polymer Eudragit (bBMA). Prior to the viscosity measurements the drug/polymer mixtures were processed by vacuum compression molding (VCM) to generate a homogeneous and air bubble free sample (Figure 1). The film with 20 wt% ITR appears transparent, thus this ASD forms a single-phase system. In comparison, the system with 20 wt% GRI forms a two-phase system which is confirmed by the opaque appearance.

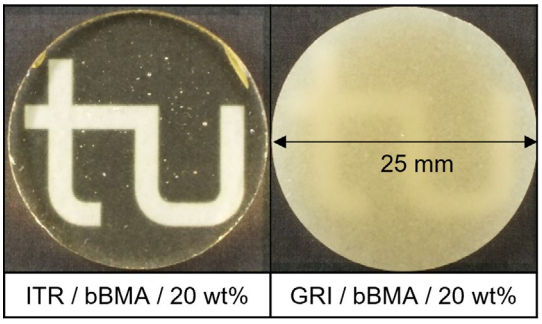

Figure 1: ASD films performed by VCM for 20 wt% ITR with bBMA (left) and 20 wt% GRI with bBMA (right).

Afterwards, the viscosity was determined using small amplitude oscillation measurements for various frequencies and temperatures. The viscosity data was shifted to a master curve using the Arrhenius temperature-time superposition and modeled with the Carreau approach (Figure 2, left). The pure polymer bBMA shows the typical shear-thinning behavior. The formulation ITR and ACE with bBMA shows a decrease of viscosity by increasing the drug content which demonstrates a plasticizing effect of the drug. The formulation GRI with bBMA shows an increase of viscosity by increasing the drug content so that the drug behaves here as a filler. Afterwards, a model was developed, which is based on a shift factor a_{drug} like in the temperature time superposition, where the zero-shear viscosity of the drug/polymer mixture is referred to that of the pure polymer. For single phase drug/polymer formulations containing the drugs ITR and ACE, a linear correlation was detected in logarithmic scale (Figure 2, right). The respective course of the shift factors over the drug weight fractions is explained by individual drug/polymer interactions. This relation is considered by introducing the interaction factor E_{drug}.

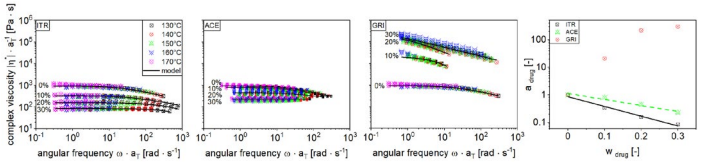

Figure 2: Master curves of viscosity for the substance systems ITR, ACE and GRI with bBMA (left) and drug shift model (right).

In conclusion, the melt viscosity of drug/polymer mixtures was evaluated. The plasticizing or filler effect of the drug was attributed to molecular interactions. Finally, a model was developed to describe the drug dependent melt viscosity based on these drug/polymer interactions, which is of great importance in process design.

Contacts:
vincent.kimmel@tu-dortmund.de
judith.winck@tu-dortmund.de
markus.thommes@tu-dortmund.de

Publications 2020 – 2022

2022

Publications:

- M. Evers, D. Weis, S. Antonyuk, M. Thommes
  Particle movement in the spheronizer – Experimental investigations with respect to the toroidal and poloidal direction
  Powder Technology, 404, 117452 (2022)

- M. Zimmermann, C. Raffel, J. Bartsch, M. Thommes
  Simulation of Powder Flow Behavior in an Artificial Feed Frame Using an Euler-Euler Model
  Chemical Engineering and Technology, 45, 5, 853–859 (2022)

- F. Wolbert, I.-K. Fahrig, T. Gottschalk, C. Luebbert, M. Thommes, G. Sadowski
  Factors Influencing the Crystallization-Onset Time of Metastable ASDs
  Pharmaceutics, 14, 2, 269 (2022)

- C. Lauscher, G. Schaldach, M. Thommes
  An Approach for Small Droplet Production: Nebulization by Expansion of Water/Liquid Carbon Dioxide Emulsion
  Atomization and Sprays, 32, 4, 77–93 (2022)

- T. Gottschalk, B. Grönniger, E. Ludwig, F. Wolbert, T. Feuerbach, G. Sadowski, M. Thommes
  Influence of process temperature and residence time on the manufacturing of amorphous solid dispersions in hot melt extrusion
  Pharmaceutical Development and Technology, 27, 3, 313–318

- P. da Igreja, D. Klump, J. Bartsch, M. Thommes
  Reduction of submicron particle agglomeration via melt foaming in solid crystalline suspension
  Journal of Dispersion Science and Technology, Doi 10.1080/01932691.2022.2146707 (2022)

- J. Winck, M. Daalmann, A. Berghaus, M. Thommes
  In-line-monitoring of solid dispersion preparation in smale scale extrusion based on UV-vis spectroscopy
  Pharmaceutical Development and Technology, 27,10, 1009-1015 (2022)

- D. Pieloth, M. Rodeck, G. Schaldach, M. Thommes
  Categorization of Sprays by Image Analysis with Convolutional Neuronal Networks
  Chemical Engineering Technology, 46, 2, 264-269 (2023), DOI: 10.1002/ceat.202200356 (2022)

Books & Book Chapters

- A. Bauer-Brandl, W. A. Ritschel, M. Thommes, G. Warnke
  Die Tablette, Handbuch der Entwicklung, Herstellung und Qualitätssicherung, Editio Cantor Verlag,
  ISBN 978-3-87193-487-2, 4. Auflage (2022)

2021

Publications:

- A. Mansuri, P. Münzner, T. Feuerbach, A. W. P. Vermeer, W. Hoheisel, R. Böhmer, M. Thommes, C. Gainaru
  The relaxation behavior of supercooled and glassy imidacloprid
  Journal of Chemical Physics 155, 174502 (2021)

- M. Evers, A. Mattusch, D. Weis, E. Garcia, S. Antonyuk, M. Thommes
  Elucidation of mass transfer mechanisms in pellet formation by spheronization
  European Journal of Pharmaceutics and Biopharmaceutics 160, 92-99 (2021)

- K. Flügel, K. Schmidt, L. Mareczek, M. Gäbe, R. Hennig, M. Thommes
  Impact of incorporated drugs on material properties of amorphous solid dispersions
  European Journal of Pharmaceutics and Biopharmaceutics 159, 88-98 (2021)

- T. Feuerbach, M. Thommes
  Design and Characterization of a Screw Extrusion Hot-End for Fused Deposition Modeling
  Molecules 26, 3, 590 (2021)

- D. Weis, P. Grohn, M. Evers, M. Thommes, E. García, S. Antonyuk
  Implementation of formation mechanisms in DEM simulation of the spheronization process of pharmaceutical pellets
  Powder Technology 378, Part A, 667-679 (2021)

- P. da Igreja, A. Erve, M. Thommes
  Melt milling as manufacturing method for solid crystalline suspensions
  European Journal of Pharmaceutics and Biopharmaceutics 158, 245-253 (2021)

- D. Sleziona, A. Mattusch, G. Schaldach, D.R. Ely, G. Sadowski, M. Thommes
  Determination of Inherent Dissolution Performance of Drug Substances
  Pharmaceutics 13, 146 (2021)Publications 2020 – 2022

2020

Publications:

- R. Schneider, J. Kerkhoff, A. Danzer, A. Mattusch, A. Ohmann, M. Thommes, G. Sadowski
  The interplay of dissolution, solution crystallization and solid-state transformation of amorphous indomethacin in aqueous solution
  International Journal of Pharmaceutics X 2, 100063 (2020)

- K. Flügel, R. Hennig, M. Thommes
  Impact of structural relaxation on mechanical properties of amorphous polymers
  European Journal of Pharmaceutics and Biopharmaceutics 154, 214-221 (2020)

- R. Strob, T. Babaria, M. Rodeck, G. Schaldach, P. Walzel, M. Thommes
  Evaluation of spray impact on a sphere with a two-fluid nozzle
  Journal of Aerosol Science 140, 105483 (2020)

- T. Feuerbach, S. Kock, M. Thommes
  Slicing parameter optimization for 3D printing of biodegradable drug-eluting tracheal stents
  Pharmaceutical Development and Technology, 25, 6, 650-658 (2020)

- P. Grohn, D. Weis, M. Thommes, S. Heinrich, S. Antonyuk
  Contact Behavior of Microcrystalline Cellulose Pellets Depending on their Water Content
  Chem. Eng. Technol. 43, 5, 887-895 (2020)

- K. Hoppe, M. Maricanov, G. Schaldach, R. Zielke, D. Renschen, W. Tillmann, M. Thommes, D. Pieloth
  Modeling the separation performance of depth filter considering tomographic data
  Environmental Progress and Sustainable Energy Vol. 39, Issue 5, e13423 DOI: 10.1002/ep.13423 (2020)

- K. Fluegel, R. Hennig, M. Thommes
  Impact of structural relaxation on mechanical properties of amorphous polymers
  Eur J Pharm Biopharm 154, 214-221 (2020)

Fluid Separations (FVT)

Recent Developments in Rotating Packed Bed Technology

Rouven Loll, Tobias Pyka, Gerhard Schembecker, Christoph Held

Separation processes are an essential part of the process industry and depend largely on mass transfer in the respective equipment. While mass transport in conventional gas-liquid separation columns are limited to gravitational force, rotating packed beds (RPBs) enable centrifugally assisted contacting of the phases which are 10 to 1000 times stronger than the gravitational force. One recent design concept for the internal structure of an RPB, which is particularly promising for mass transfer, is the Zickzack packing developed at TU Dortmund University. In our recent work, the design of this 3D-printed packing was modified so that the fluid and gas flows through the rotor of the RPB can be controlled more precisely and the mass transfer in the Zickzack packing is further enhanced. On top, increased mass transfer is also achieved by using several rotors in series in the RPB. For the first time, we characterized the hydrodynamics of a two-rotor RPB.

In conventional columns, wall effects of fluid streams affect the mass transfer of the equipment. This is usually compensated by wall wipers. In this study, a modified design of the Zickzack packing for RPBs was developed, which contains a seal structure (cf. Figure 1, dark gray) with O-ring seals (cf. Figure 1, black) and thereby prevents any liquid (cf. Figure 1, blue) or gas (cf. Figure 1, red) bypass flows around the packing structure within the rotor. The effect of the prevented gas and liquid bypasses on the mass transfer, quantified as the volumetric liquid-side mass transfer coefficient k_La, and the pressure drop Δp have been investigated in deaeration experiments with counter-current contacting of oxygen-rich water with pure nitrogen at ambient pressure and temperature. For comparison, sealed and unsealed Zickzack packings have been manufactured in our lab. With increasing rotational speed, liquid phase bypasses around the unsealed Zickzack packing occurred due to the increasing centrifugal force driving the liquid flow in radial direction. By adding seals to the Zickzack packing (SZP) and therefore avoiding bypasses, mass transfer in the RPB increased by 50% while pressure drop stayed nearly unchanged compared to the unsealed (ZP) Zickzack packing (cf. Figure 2).

Besides the packing, also putting rotors in series is an efficient means to increase the separation performance for demanding purification tasks. Fundamentally important operational parameters of multi-rotor RPBs are not yet fully understood. For example, pressure drop Δp is crucial for operational as well as capital expenses. Therefore, Δp of a two-rotor RPB (2R-RPB) was compared to a one-rotor RPB (1R-RPB) in order to elaborate the different contributions to Δp. The comparison of Δp of 2R-RPB and 1R-RPB showed that Δp of a 2R-RPB is scalable by knowing Δp of 1R-RPB. These results suggest that Δp of RPBs with more than two rotors might also be scalable.

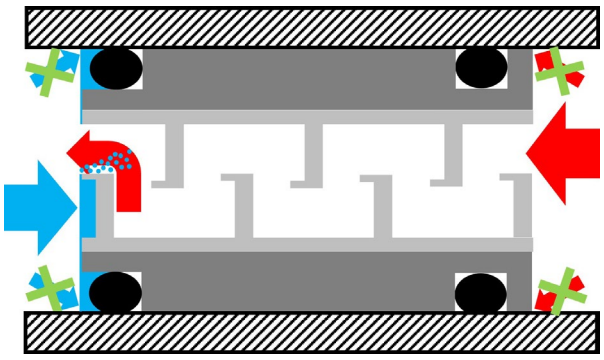

Figure 1: Sealed Zickzack packing cross section.

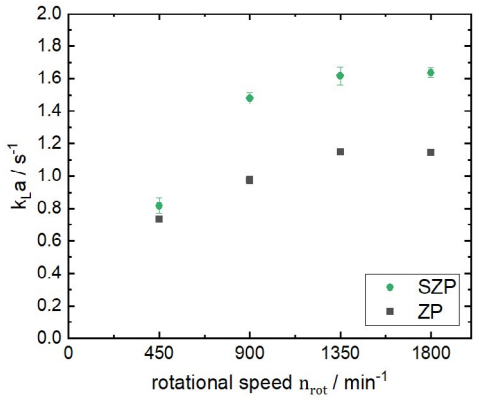

Figure 2: Mass transfer in a sealed (SZP) and unsealed (ZP) Zickzack packing at a liquid flow rate of 0.96 m^3h^{-1} and a gas flow rate of 1 m^3h^{-1}.

Contact:
christoph.held@tu-dortmund.de

Publications:
R. Loll, L. Runge, J. Koop, C. Held, G. Schembecker, Ind. Eng. Chem. Res. 61, 11934–11946 (2022)

Algorithmic synthesis of separation processes for azeotropic multicomponent mixtures

Thulasi Rolland, Mirko Skiborowski

The development of distillation processes for azeotropic systems is a challenging task due to the presence of distillation boundaries. Extractive distillation is a well-established alternative for the separation of azeotropic mixtures. While the application of extractive distillation has been extensively explored, little emphasis has been given to the generation of flowsheets containing extractive distillation columns. For this purpose, a novel algorithmic approach is developed that aims at an automatic synthesis of distillation-based separation processes for azeotropic mixtures using extractive distillation. Thereby, a computationally efficient and reliable process synthesis including suitable recycle streams is enabled, which further provides initial estimates of the minimum energy requirement.

The demand for more energy efficient separation processes in the chemical industry is growing rapidly. Given the high energy consumption of downstream processing the synthesis of separation processes is a key aspect of conceptual design. Especially the separation of azeotropic mixtures is a challenging task for multicomponent mixtures. While azeotropic mixtures may be separated in processes composed of simple distillation columns by exploiting the curvature of distillation boundaries and dedicated recycles, hybrid separation processes such as extractive distillation are more frequently applied. Extractive distillation involves the addition of a suitable entrainer that alters the relative volatility of the mixture such that the azeotrope can be overcome. Separations using extractive distillation columns has often relied on heuristics since they exhibit unusual performance and make conventional methods ineffective for design. Additionally, the choice and amount of entrainer add additional degrees of freedom, thus compounding the complexity of the design problem. The determination of the limiting parameters is crucial to obtain feasible extractive distillation column designs. Therefore, the majority of research has focused on entrainer screening. However, for the separation of multicomponent mixtures using extractive distillation, it is necessary to develop an algorithmic method to generate process alternatives.

The proposed approach aims at a fully algorithmic synthesis of distillation-based separation processes employing extractive distillation, building solely on a thermodynamic model of the multicomponent mixture. For this purpose, a general framework for the algorithmic identification of process alternatives for the separation of azeotropic multicomponent mixtures is extended to include extractive distillation with heavy boiling entrainers (Figure 1).The assessment of feasibility for extractive distillation includes a topological analysis of the mixture and determining the achievable products using univolatility lines. The limiting parameters, minimum entrainer flow and the corresponding window of feasible reflux ratios for a feasible column design, are computed mathematically using a bifurcation approach. A subsequent verification of the feasibility and the estimation of the minimum energy demand by means of the rectification body method is incorporated. Thus, the fully algorithmic approach enables a completely automatic generation of process variants without the need for a graphical illustration, along with a possible screening of the process alternatives. This ultimately helps to further develop fluid separations towards higher efficiencies even for difficult separation tasks – which did not exist before.

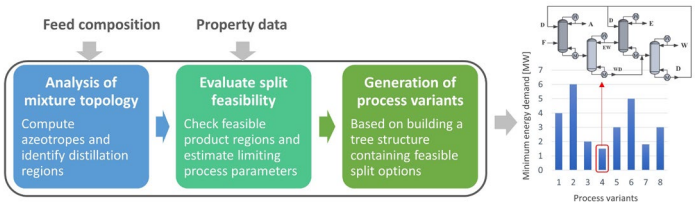

Figure 1: Schematic overview of the synthesis methodology for extractive distillation processes.

Publications:
T. Sasi, M. Skiborowski, Computer Aided Chemical Engineering 51, 751-756 (2022).

Contact:
thulasi.rolland@tu-dortmund.de
mirko.skiborowski@tuhh.de

Publications 2020 –2022

2022

Peer-reviewed Journal Articles

- D. Zawadzki, M. Blatkiewicz, M. Jaskulski, M. Piątkowski, J. Koop, R. Loll, A. Górak
  Design and Optimisation of Structural Packings for Rotating Bed Absorbers Using Computational Fluid Dynamics Simulation
  Chem. Eng. Sci. (2022) DOI: 10.2139/ssrn.4222640

- M. Peterwitz, J. Jodwirschat, R. Loll, G. Schembecker
  Tracking raw material flow through a continuous direct compression line Part I of II: Residence time distribution modeling and sensitivity analysis enabling increased process yield.
  Int. J. Pharm. 614, 121467 (2022)

- S. Schlüter, F. Huxoll, K. Grenningloh, G. Sadowski, M. Petzold, L. Böhm, M. Kraume, M. Skiborowski
  Unraveling the influence of dissolved gases on permeate flux in organic solvent nanofiltration – Experimental analysis
  Separation and Purification Technology 295, 121265 (2022)

- T. Pyka, J. Koop, C. Held, G. Schembecker
  Dry Pressure Drop in Two-Rotor Rotating Packed Bed
  Ind. Eng. Chem. Res. 61, 17156–17165 (2022)

- R. Loll, L. Runge, J. Koop, C. Held, G. Schembecker
  Zickzack Packings for Deaeration in Rotating Packed Beds - Improved Rotor Design to Counter Bypass Flows
  Ind. Eng. Chem. Res. 61, 11934–11946 (2022)

- M. Ascani, C. Held
  Thermodynamics for reactive separations
  Book Chapter in "Process Intensification by By Reactive and Membrane-assisted Separations" by Skiborowski and Górak Berlin, Boston: De Gruyter (2022)

- S. Schlüter, P. Franke
  OSN-assisted reaction and separation processes
  Book Chapter in "Process Intensification by By Reactive and Membrane-assisted Separations" by Skiborowski and Górak Berlin, Boston: De Gruyter (2022)

- J. Holtbrügge, J.R. Pela
  Pervaporation and vapor permeation– assisted reactive separation processes
  Book Chapter in "Process Intensification by By Reactive and Membrane-assisted Separations" by Skiborowski and Górak Berlin, Boston: De Gruyter (2022)

- T. Pyka, J. Koop
  Rotating packed beds in distillation: rotor configurations
  Book Chapter in "Process Intensification by By Rotating Packed Beds" by Skiborowski and Górak Berlin, Boston: De Gruyter (2022)

- R. Loll, J. Koop
  3D printed packings for rotating packed beds
  Book Chapter in "Process Intensification by By Rotating Packed Beds" by Skiborowski and Górak Berlin, Boston: De Gruyter (2022)

2021

Peer-reviewed Journal Articles

- J. Vondran, J. Pela, D. Palczewski, M. Skiborowski, T. Seidensticker
  Curse and Blessing–The Role of Water in the Homogeneously Ru-Catalyzed Epoxidation of Technical Grade Methyl Oleate
  ACS Sustainable Chem. Eng., 34, 11469 (2021)

- S. Schlüter, K. Künnemann, M. Freis, T. Roth, D. Vogt, J. Dreimann, M. Skiborowski
  Continuous co-product separation by organic solvent nanofiltration for the hydroaminomethylation in a thermomorphic multiphase system
  Chem. Eng. Journal 409, 128219 (2021)

- F. Huxoll, S. Schlüter, R. Budde, M. Skiborowski, M. Petzold, L. Böhm, M. Kraume, G. Sadowski
  Phase Equilibria for the Hydroaminomethylation of 1-Decene
  Journal of Chem. & Eng. Data, 66, 4484 (2021)

- B. Scharzec, D. Merschhoff, J. Henrichs, E.J. Kappert, M. Skiborowski
  Evaluation of membrane-assisted hybrid processes for the separation of a tetrahydrofuran-methanol-water mixture
  Chem Eng Proc 167, 108545 (2021)

- K.F. Kruber, T. Grueters, M. Skiborowski
  Advanced hybrid optimization methods for the design of complex separation processes Computers & Chemical Engineering 147, 107257 (2021)

- I. Lukin, K. Gładyszewski, M. Skiborowski, A. Górak, G. Schembecker
  Aroma absorption in a rotating packed bed with a tailor-made archimedean spiral packing Chemical Engineering Science 231, 116334 (2021)
  K. Gładyszewski, K. Groβ, A. Bieberle, M. Schubert, M. Hild, A. Górak, M. Skiborowski Evaluation of performance improvements through application of anisotropic foam packings in rotating packed beds Chemical Engineering Science 230, 116176 (2021)

- B. Scharzec, K.F. Kruber, M. Skiborowski
  Model-based evaluation of a membrane-assisted hybrid extraction-distillation process for energy and cost-efficient purification of diluted aqueous streams
  Chem Eng Sci, 116650 (2021)

2020

Peer-reviewed Journal Articles

- Goebel, R.; Skiborowski, M.
  Machine-based learning of predictive models in organic solvent nanofiltration: Pure and mixed solvent flux
  Separation and Purification Technology 237 (2020), 116363

- Hampel, U.; Schubert, M.; Döß, A.; Sohr, J.; Vishwakarma, V.; Repke, J.- U.; Gerke, S.; Leuner, H.; Rädle, M.; Kapoustina, V.; Schmitt, L.; Grünewald, M.; Brinkmann, J.; Plate, D.; Kenig, E.; Lutters, N.; Bolenz, L.; Buckmann, F.; Toye, D.; Arlt, W.; Linder, T.; Hoffmann, R.; Klein, H.; Rehfeldt, S.; Winkler, T.; Bart, H.- J.; Wirz, D.; Schulz, J.; Scholl, S.; Augustin, W.; Jasch, K.; Schlüter, F.; Schwerdtfeger, N.; Jahnke, S.; Jupke, A.; Kabatnik, C.; Braeuer, A.; D'Auria, M.; Runowski, T.; Casal, M.; Becker, K.; David, A.- L.; Górak, A.; Skiborowski, M.; Groß, K.; Qammar, H.
  Recent Advances in Experimental Techniques for Flow and Mass Transfer Analyses in Thermal Separation Systems
  Chemie Ingenieur Technik 92 (7) (2020), 926–948

- Waltermann, T.; Schlueter, S.; Benfer, R.; Knoesche, C.; Górak, A.; Skiborowski, M.
  Model Discrimination for Multicomponent Distillation – A Geometrical Approach for Total Reflux
  Chemie Ingenieur Technik 92 (7) (2020), 890–906

- Riese, J.; Hoff, A.; Stock, J.; Górak, A.; Grünewald, M.
  Separation Units 4.0 – Trennapparate heute und morgen
  Chemie Ingenieur Technik 92 (7) (2020), 818–830

- Jaworska, M.; Antos, D.; Górak, A.
  Review on the application of chitin and chitosan in chromatography
  Reactive and Functional Polymers 152 (5) (2020), 104606

- Lukin, I.; Pietzka, L.; Groß, K.; Górak, A.; Schembecker, G.
  Economic evaluation of rotating packed bed use for aroma absorption from bioreactor off-gas
  Chemical Engineering and Processing: Process Intensification 154 (5), (2020), p. 108011

- Groß, K.; Beer, M. de; Dohrn, S.; Skiborowski, M.
  Scale-Up of the Radial Packing Length in Rotating Packed Beds for Deaeration Processes
  Industrial & Engineering Chemisty Research 59 (23) (2020), 11042–11053

- Sasi, T.; Skiborowski, M.
  Automatic Synthesis of Distillation Processes for the Separation of Homogeneous Azeotropic Multicomponent Systems
  Industrial & Engineering Chemistry Research 59 (47), (2020), pp. 20816–20835

Process Automation Systems (PAS)

Exploiting monotonicity properties to enable robust model predictive control of systems with many uncertainties

Moritz Heinlein, Sankaranarayanan Subramanian, Marco Molnar, Sergio Lucia

Model predictive control (MPC) has become a standard approach for advanced process control because of its ability to directly consider multi-variable processes with constraints by solving an optimization problem online to compute optimal signals. One of the main challenges of MPC is that an accurate model is necessary. Many approaches have been proposed to robustify the MPC against model uncertainties and other disturbances. However, most of these approaches suffer from the curse of dimensionality, which means that computing the optimal solution becomes exponentially more demanding the more uncertainties are present. It is currently not possible to solve problems where many uncertainties are present. In this work, we exploit the properties of monotone systems, which are present in many areas of engineering, to formulate robust MPC approaches that are computationally feasible even when many uncertainties are present.

Model predictive control (MPC) is a widely used control scheme, because of its capabilities to handle nonlinear systems with multiple inputs, outputs and constraints, as well as the ability to take known future influences into account. One main drawback of MPC algorithms is the dependency on accurate models, which can influence performance and stability. To make sure that important quality or safety process constraints are not violated during operation despite of the uncertain model, it is necessary to compute all possible future trajectories that the system might be in. This computation is intractable when for systems of relevant size, especially when affected by many possible uncertainties. If a dynamic system is monotone, however, just by simulating the model with the largest and smallest uncertainties gives already a description of all possible states that the system might encounter in the future, making the design of robust MPC schemes tractable even in high dimensions. A monotone system is a dynamic system for which the effect of states and uncertainties affects monotonically the system dynamics. For example, when describing the temperature evolution inside of a room, the external temperature acts monotonically on the system, because a higher external temperature always leads to a higher internal temperature. There are engineering systems that are monotonic such as biochemical reaction networks traffic networks as well as temperature control in buildings.

We present two different robust MPC approaches for monotone systems which exploit this property. The first one, the open-loop robust monotone MPC optimizes a single input trajectory which needs to be robust for all possible future uncertainty realizations. This can be done by propagating the two worst-case scenarios of the uncertainty, leading to an approach that is just twice as complex as the nominal MPC problem while still guaranteeing robustness.

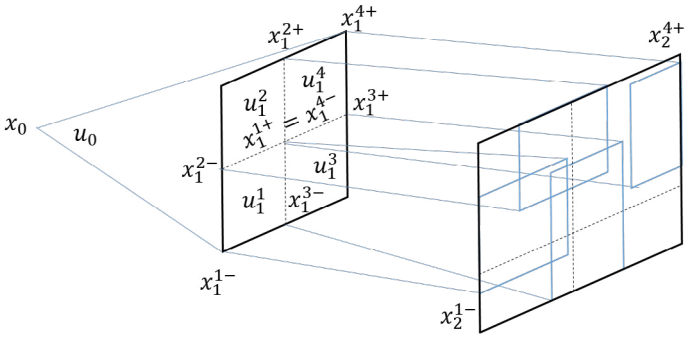

Figure 1: Schematic representation of the closed-loop robust monotone MPC. The exponential growth with the prediction horizon is circumvented via bounding the reachable sets by a rectangle spanned by two points, here x_2^{1-} and x_2^{4+}

The main drawback of this approach is its conservativeness. As we choose just one input trajectory in each future time step for all realizations of the uncertainty, we neglect that new measurement information will be obtained in the future, which can be used to counteract the effect of the uncertainty.

The closed-loop robust monotone MPC takes explicitly into account the fact that future measurements will be available, by dividing the possible regions of the space where the system might be in the future into multiple smaller regions and assigning individual inputs for each smaller region. To avoid an explosion of the complexity with larger prediction horizons, the propagation of the smaller regions is bounded in each time step by just one rectangle. This bounding rectangle is then divided again into smaller rectangles. This scheme is displayed in Figure 1. Under some usual assumptions, it is also possible to prove that safety of the closed-loop will be guaranteed and that a feasible control input will always be found.

The main advantage of the proposed approach is that it can be used to compute robust optimization-based controllers of large systems with many uncertainties.

Contacts:
moritz.heinlein@tu-dortmund.de
sergio.lucia@tu-dortmund.de

Publication: M. Heinlein, S. Subramanian, M. Molnar, and S. Lucia, "Robust MPC approaches for monotone systems," in 2022 IEEE 61st Conference on Decision and Control (CDC), Dec. 2022, pp. 2354–2360. doi: 10.1109/CDC51059.2022.9992502

Exploiting monotonicity properties to enable robust model predictive control of systems with many uncertainties

Moritz Heinlein, Sankaranarayanan Subramanian, Marco Molnar, Sergio Lucia

Figure 2 shows simulation results for nominal MPC and the closed-loop robust monotone for operating the heating and ventilation unit of a building with 4 rooms affected by uncertain parameters, such as solar radiation or external temperature. The goal is to keep the temperature in predefined 2-degree regions, while minimizing the energy for heating and cooling. When a nominal MPC with mean values of the uncertainty is employed, the temperature constraints in each room are violated, while the proposed robust approach achieves to control the system without constraint violations. Computing the optimal robust control inputs with a system with 12 dynamic states and 6 uncertain parameters took only 16 seconds on a standard computer.

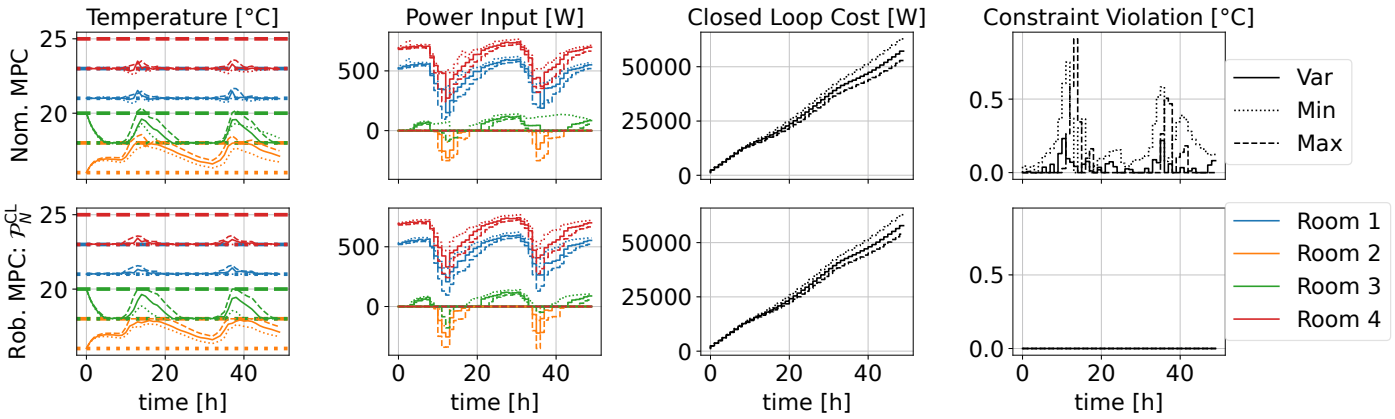

Figure 2: Closed-loop comparison of nominal MPC with closed-loop robust monotone MPC. In each of their respective rows the first column shows the four room temperatures and their respective constraints. Each trajectory is plotted for the maximum (dashed), minimum (dotted) and a time varying (solid) realization of the uncertainty. The second column shows the heating and the cooling inputs (plotted negative).

Publications 2020 – 2022

2022

Peer-reviewed Journal Articles

- N Krausch, JW Kim, T Barz, S Lucia, S Groß, MC Huber, SM Schiller, P Neubauer, MN Cruz Bournazou
  High - throughput screening of optimal process conditions using model predictive control
  Biotechnology and Bioengineering 119 (12), 3584-3595 (2022)

- C Döpmann, F Fiedler, S Lucia, F Tschorsch
  Optimization-Based Predictive Congestion Control for the Tor Network: Opportunities and Challenges
  ACM Transactions on Internet Technology 22 (4), 1-30 (2022)

- J Xu, M Kovatsch, D Mattern, F Mazza, M Harasic, A Paschke, S Lucia
  A Review on AI for Smart Manufacturing: Deep Learning Challenges and Solutions
  Applied Sciences 12 (16), 8239 (2022)

- S Braun, S Albrecht, S Lucia
  Adaptively robust nonlinear model predictive control based on attack identification
  at-Automatisierungstechnik 70 (4), 367-377 (2022)

- Y Wan, DE Shen, S Lucia, R Findeisen, RD Braatz
  A Polynomial Chaos Approach to Robust Static Output-Feedback Control With Bounded Truncation Error
  IEEE Transactions on Automatic Control 68 (1), 470-477 (2022)

- P Guillén, F Fiedler, H Sarnago, S Lucía, O Lucía
  Deep Learning Implementation of Model Predictive Control for Multioutput Resonant Converters
  IEEE Access 10, 65228-65237 (2022)

Peer-reviewed Conference Papers

- B Karg, S Lucia
  Guaranteed safe control of systems with parametric uncertainties via neural network controllers
  2022 IEEE 61st Conference on Decision and Control (CDC), 7302-7308 (2022)

- M Heinlein, S Subramanian, M Molnar, S Lucia
  Robust MPC approaches for monotone systemsIEEE 61st Conference on Decision and Control (CDC),
  2354-2360 (2022)

- C Utama, B Karg, C Meske, S Lucia
  Explainable artificial intelligence for deep learning-based model predictive controllers
  26th International Conference on System Theory, Control and Computing (ICSTCC), 464-471 (2022)

- F Fiedler, S Lucia
  Model predictive control with neural network system model and Bayesian last layer trust regions
  IEEE 17th International Conference on Control & Automation (ICCA), 141-147 (2022)

- A Mesbah, KP Wabersich, AP Schoellig, MN Zeilinger, S Lucia, TA Badgwell, JA Paulson
  Fusion of Machine Learning and MPC under Uncertainty: What Advances Are on the Horizon?
  American Control Conference (ACC), 342-357 (2022)

- S Braun, S Albrecht, S Lucia
  Resilient Control of Interconnected Microgrids Under Attack by Robust Nonlinear MPC
  Conference on Informatics in Control, Automation and Robotics, 58-66 (2022)

- S Subramanian, Y Abdelsalam, S Lucia, S Engell
  On the Practical Design of Tube-enhanced Multi-stage Nonlinear Model Predictive Control
  IFAC-PapersOnLine 55 (7), 477-482 (2022)

- Model predictive control guided with optimal experimental design for pulse-based parallel cultivation
  JW Kim, N Krausch, J Aizpuru, T Barz, S Lucia, EC Martínez, P Neubauer, MN Cruz Bournazou
  IFAC-PapersOnLine, 934-939 (2022)

- N Krausch, JW Kim, S Lucia, S Groß, T Barz, P Neubauer, MN Cruz Bournazou
  Optimal operation of parallel mini-bioreactors in bioprocess development using multi-stage MPC
  Computer Aided Chemical Engineering, 1069-1074 (2022)

2021

Peer-reviewed Journal Articles

- B Karg, S Lucia
  Approximate moving horizon estimation and robust nonlinear model predictive control via deep learning
  Computers & Chemical Engineering 148, 107266 (2021)

- S Braun, S Albrecht, S Lucia
  Attack Identification for Nonlinear Systems Based on Sparse Optimization
  IEEE Transactions on Automatic Control, in Press (2021)

- S Subramanian, S Lucia, R Paulen, S Engell
  Tube-enhanced multi-stage model predictive control for flexible robust control of constrained linear systems with additive and parametric uncertainties
  International Journal of Robust and Nonlinear Control 31 (9), 4458-4487

- S Subramanian, Y Abdelsalam, S Lucia, S Engell
  Robust Tube-Enhanced Multi-Stage NMPC With Stability Guarantees
  IEEE Control Systems Letters 6, 1112-1117 (2021)

- B Karg, T Alamo, S Lucia
  Probabilistic performance validation of deep learning- based robust NMPC controllers
  International Journal of Robust and Nonlinear Control 31 (18), 8855-8876 (2021)

- Y Wan, DE Shen, S Lucia, R Findeisen, RD Braatz
  Polynomial chaos-based H2 output-feedback control of systems with probabilistic parametric uncertainties
  Automatica 131, 109743 (2021)

- B Karg, S Lucia
  Model Predictive Control for the Internet of Things
  Recent Advances in Model Predictive Control, 165-189 (2021)

Peer-reviewed Conference Papers

- T Faulwasser, S Lucia, MS Darup, M Mönnigmann
  Teaching MPC: Which Way to the Promised Land?
  IFAC-PapersOnLine 54 (6), 238-243 (2021)

- Y Yang, S Lucia
  Multi-step Greedy Reinforcement Learning Based on Model Predictive Control
  IFAC-PapersOnLine 54 (3), 699-705 (2021) (Keynote paper)

- B Karg, S Lucia
  Reinforced approximate robust nonlinear model predictive control

- 23rd International Conference on Process Control, 149-156 (2021)
  (Best Paper by Young Author Award)

- F Fiedler, S Lucia
  On the relationship between data-enabled predictive control and subspace predictive control
  European Control Conference (ECC), 222-229 (2021)

- J Xu, M Kovatsch, S Lucia
  Open Set Recognition for Machinery Fault Diagnosis
  IEEE 19th International Conference on Industrial Informatics (INDIN), 1-7 (2021)

- Towards Optimization-Based Predictive Congestion Control for the Tor Network
  C Döpmann, F Fiedler, S Lucia, F Tschorsch
  Electronic Communications of the EASST 80 (2021)

- D Bermbach, S Lucia, V Handziski, A Wolisz
  Towards grassroots peering at the edge
  Proc. of the 8th International Workshop on Middleware and Applications for the Internet of Things, 14-17 (2021)

2020

Peer-reviewed Journal Articles

- S. Lucia, S. Subramanian, D.Limon, S. Engell
  Stability properties of multi-stage nonlinear model predictive control
  Systems & Control Letters 143, 104743 (2020)

- B. Karg, S. Lucia,
  Efficient representation and approximation of model predictive control laws via deep learning
  IEEE Transactions of Cybernetics 50 (9), 3866-3878 (2020)

- M. H. Ghasemi, O. Lucia, S. Lucia
  Computing in the blink of an eye: Current possibilities for edge computing and hardware –agnostic programming
  IEEE Access 8, 41626-41636 (2020)

- S. Lucia, D. Navarro, B. Karg, H. Sarnago, O. Lucia
  Deep learning based model predictive control for resonant power converters
  IEEE Transactions of Industrial Informatics 17 (1), 409-420 (2020)

Peer-reviewed Conference Papers

- N. Krausch, S. Hans, F. Fiedler, S. Lucia, P. Neubauer, M.N.C. Bournazou
  From Screening to Production: a Holistic Approach of Highthroughput Model-based Screening for Recombinant Protein Production
  Computer Aided Chemical Engineering 48, 1723-1728 (2020)

- S. Braun, S. Albrecht, S. Lucia
  Hierachical Attack Identification for Distributed Robust Nonlinear Control
  Proc. of the 21st IFAC World Congress, in Press (2020)

- F. Fiedler, A. Cominola, S. Lucia
  Economic nonlinear predictive control of water distribution networks based on surrogate modeling and automatic clustering
  Proc. of the 21st IFAC World Congress, in Press (2020)

- K. Eckhoff, M. Kok, S. Lucia, T. Seel
  Sparse Magnetometer-free Inertial Motion Tracking – A Condition for Observability in Double Hinge Joint Systems
  Proc. of the 21st IFAC World Congress, in Press (2020)

- M. Mammarella, T. Alamo, S. Lucia, F. Dabbene
  A probabilistic validation approach for penalty function design in Stochastic Model Predictive Control
  Proc. of the 21st IFAC World Congress, in Press (2020)

- F. Fiedler, D. Baumbach, A. Börner, S. Lucia
  A Probabilistic Moving Horizon Estimation Framework Applied to the Visual-Inertial Sensor Fusion Problem
  Proc. of the European Control Conference (ECC), 1009-1016 (2020)

- S. Braun, S. Albrecht, S. Lucia
  Identifying Attacks on Nonlinear Cyber-Physical Systems in a Robust Model Predictive Control Setup
  Proc. of the European Control Conference (ECC), 513-520 (2020)

- F. Fiedler, C. Döpmann, F. Tschorsch, S. Lucia
  PredicTor: Predictive Congestion Control of the Tor Network
  Proc. of the IEEE Conference on Control Technology and Applications (CCTA), 863-870 (2020)

- B. Karg, S. Lucia
  Stability and feasibility of neural network-based controllers via output range analysis
  Proc. of the 59th IEEE Conference on Decision and Control (CDC), 4947-4957 (2020)

- S. Braun, S. Albrecht, S. Lucia
  A Hierachical Attack Identification Method for Nonlinear Systems
  Proc. of the 59th IEEE Conference on Decision and Control (CDC), 5035-5042 (2020)

Reaction Engineering and Catalysis (REC)

Dynamically operated Power-to-X processes

Development of a methodology for microkinetic model reduction and semi-mechanistic approach on the example of the CO_2 methanation

Moritz Langer, David Kellermann, Hannsjörg Freund

The production of green hydrogen from fluctuating renewable energy resources and its utilization as a sustainable feedstock for the production of chemical energy carriers and platform chemicals are key processes for the ongoing transition of the energy and chemical industry sector. The conversion of hydrogen to value added chemicals by Power-to-X processes requires technical implementations that take the fluctuating character of energy and hydrogen supply into account. To allow for a robust and efficient dynamic operation, detailed understanding of the behavior of catalytic reactors is required under such conditions. In this work, we have developed a methodology for the description of the dynamic kinetic behavior on the example of CO_2 methanation.

In view of the ongoing energy transition, the prediction of transient reactor behavior by reaction kinetic models (Fig. 1) is of growing interest. Microkinetic elementary step models are able to describe the dynamic behavior of reaction kinetics in heterogeneous catalysis. However, these models are laborious to derive, parameterize and result in comparably high computational effort. Semi-mechanistic models represent a good trade-off between accuracy and computational effort, but are generally derived using steady-state data and assumptions that are questionable for transient operation since sorption processes, changes in reaction mechanisms and alterations in the catalyst structure are not considered.

In this work, a methodology for reduction of a literature elementary step microkinetic model for CO_2 methanation based on so-called rate-affecting steps (RAS) is demonstrated. Based on detailed analysis of the elementary step model, the main reaction pathway, the RAS and the most abundant surface intermediates (MASI) are identified. The RAS reflect possible changes in the rate-determining step within the transient catalyst state. Additionally, surface dynamics are captured by time dependent description of surface coverages. The RAS approach results in a reduced model considering seven rate-affecting steps (RAS 7-step) based on simulated (steady-state and transient) data using the elementary step model. Furthermore, the applicability of the RAS approach in kinetic modeling from steady-state data is investigated and compared to a LHHW-type (Langmuir-Hinshelwood-Hougen-Watson) model with similar degree of detail (RAS 3-step).

Results show a high fidelity prediction of the dynamic catalyst behavior by the RAS models with significantly better performance compared to the LHHW-type model (Fig. 2). By considerable reduction of the kinetic parameters (here: 18 vs. 137) the computational effort is reduced by up to 80 % in comparison to the elementary step model. Ongoing investigations aim to additionally include potential catalyst deactivation over time.

In conclusion, the RAS approach is suitable to describe the storage capacity of the catalyst surface with adsorbed species and dynamic kinetic effects while preserving a higher degree of mechanistic characteristics than single RDS models. Kinetic model reduction for dynamically operated reactors, such as in Power-to-X applications, benefits particularly computationally demanding tasks, such as, e.g., model-based reactor optimization and scale-resolving CFD simulations.

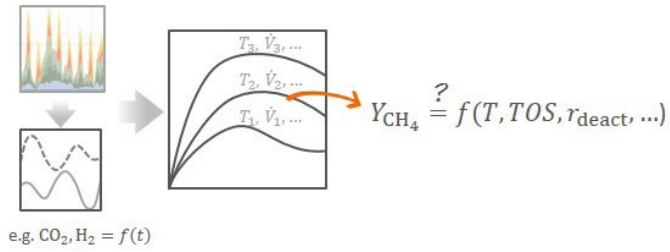

Figure 1: Schematic of the integration of the fluctuating behavior of renewable energy resources, which result in variations of feed composition and reactor temperature profile, into reaction kinetics.

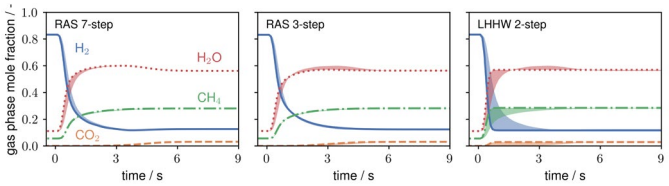

Figure 2: Effect of inlet composition step change from a ratio CO_2/H_2 = 1/19 to CO_2/H_2 = 1/4 on outlet gas phase compositions at a temperature of 310°C. Deviations between the simulations using the reduced models and the elementary step model are indicated by the shaded areas.

Contact:
hannsjoerg.freund@tu-dortmund.de

Publications:
M. Langer, H. Freund, Annual Meeting on Reaction Engineering, Würzburg, Germany (2022).
M. Langer, H. Freund, ProcessNet-Jahrestagung, Aachen, Germany (2022)
M. Langer, H. Freund, 758th WE-Heraeus Seminar "From Wind and Solar Energy to Chemical Energy Storage: Understanding and Engineering Catalysis under Dynamic Conditions", Web Conference, Germany (2022)

Additively manufactured structured catalyst supports as possibility to selectively adjust mass and heat transfer in heterogeneous catalysis

Auxetic POCS offer the advantage of enormous design flexibility

Dominik Rudolf, Lisa Eckendörfer, Hannsjörg Freund

Periodic open cellular structures (POCS) are additively manufactured lattice-like structures that can be used as catalyst supports in heterogeneous catalysis. They represent a promising alternative to the commonly used randomly packed beds consisting of a large number of individual catalyst pellets, where the latter approach comes with a few drawbacks for the operation of a chemical reactor. The relatively low porosities result in a high pressure drop. Furthermore, the pellets in the bed are interconnected by point contact only, which leads to a low radial heat transfer. POCS, on the other hand, are characterized by a continuous solid matrix in combination with large cavities between the solid struts, and therefore exhibit good heat conduction and radial heat and mass transfer in combination with low pressure drop. Due to the high design flexibility associated with additive manufacturing methods, the properties of the structures can be systematically adjusted according to the required demands in a chemical reactor. For a systematic adjustment and optimization of the geometry and the resulting properties, a fundamental understanding is required. In our group, numerical CFD and FEM simulations are used to gain deep insight into the interaction of structural geometry, hydrodynamics and transport characteristics.

A special focus in recent investigations was placed on the diamond unit cell, which has been identified as the most promising structure in several investigations, e.g. for heat transfer. It was demonstrated that the strut diameter of the diamond unit cell influences the fluid flow as well as the effective heat conduction. In Figure 1, the influence of the strut diameter on the flow field in a diamond unit cell-based POCS is exemplified. Entering the structure on the left side, the fluid is deflected characteristically in the cell. Lateral mass transfer is improved for thicker struts.

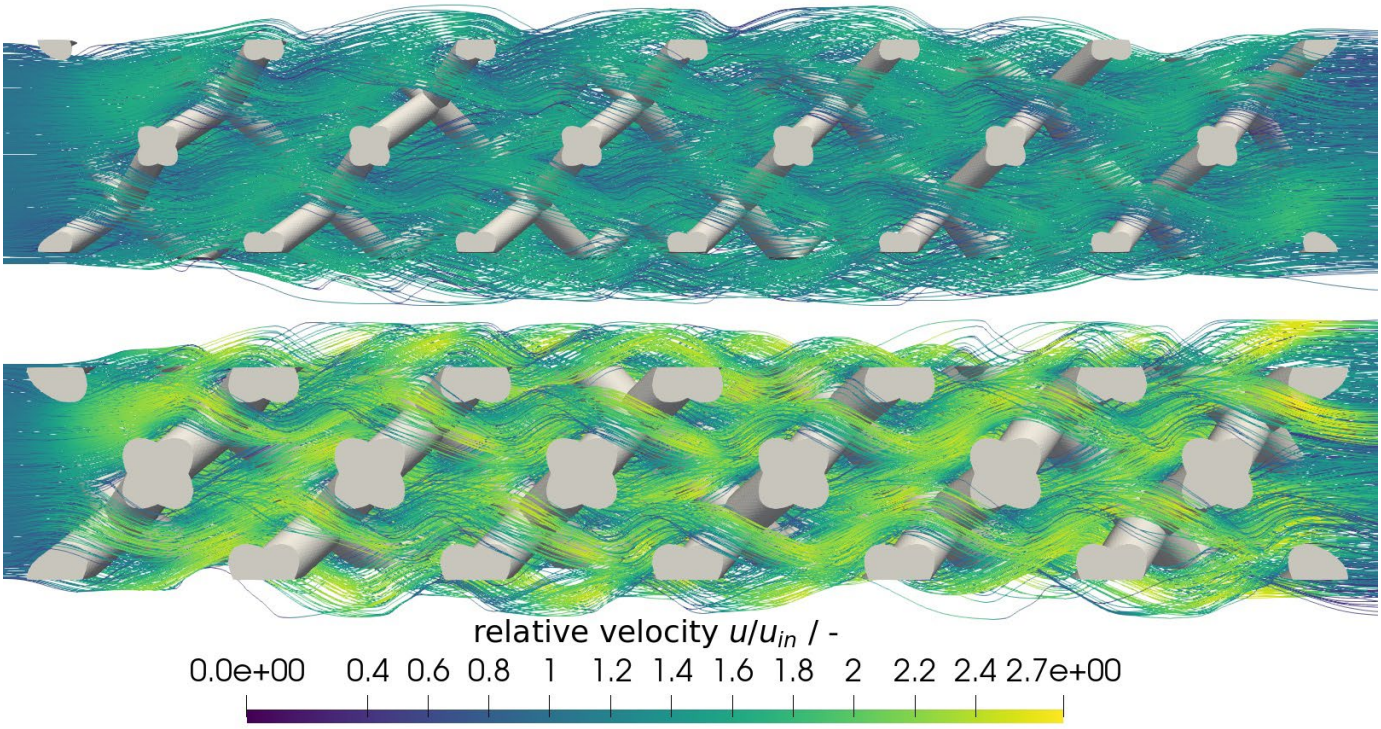

Figure 1: The effect of the strut diameter on the flow field. Streamlines in two different diamond POCS with varying strut diameter colored by the local velocity relative to the inlet velocity. The fluid is entering the structure on the left side.

Applied in a tubular reactor, one of the main challenges in the technical implementation of POCS is to realize a good wall contact of tube wall and the structure, where the latter needs to be reversibly insertable. This requires an intelligent catalyst support design, which is developed in this work. Anisotropic auxetic structures show special mechanical properties. Struts designed with arcs allow a negative Poisson's ratio, i.e., they are contracting in perpendicular direction of pressure loading. In combination with a shape memory alloy, the structures can be compressed, inserted into the tube and then expanded again.

This functionality enables an improved wall contact during reactor operation, while still allowing for a replacement of the catalyst support structure in case of deactivation. FEM simulations were carried out to investigate the resulting effective heat conduction and the mechanical properties for different geometries of the auxetic structures. In Figure 2, the dimensionless effective heat conduction $\hat{k}_{eff}$ is shown in dependency of the solid fraction (1-ε) and in comparison to various literature correlations that were developed for other unit cell types.

A clear dependency of the heat conduction on the amplitude of the arc a and the strut diameter d_s is demonstrated. Low amplitudes and high strut diameters favor the thermal properties. In contrast, the mechanical properties behave the reverse way. To account for this trade-off, the objective of further studies is to match mechanical and thermal properties of this novel structure. Both, CFD and FEM simulations represent powerful tools in quantifying transport properties of POCS, which leads to a preselection of potent prototypes. For these most promising structures, the experimental validation on a laboratory and technical scale is an essential next step. In ongoing research and often in collaboration with research partners from material sciences, we apply various additive manufacturing techniques to realize the next generation of structured catalysts.

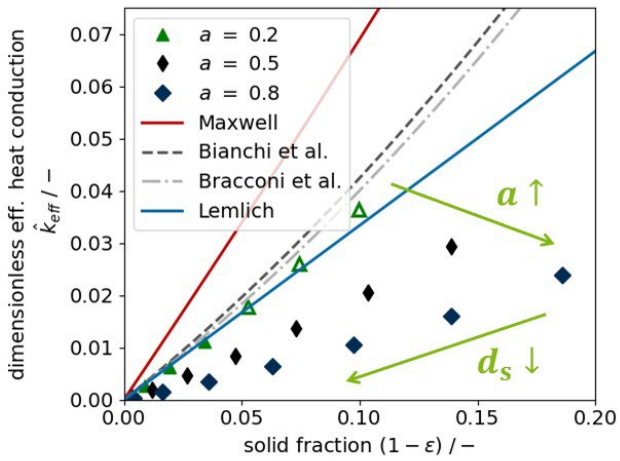

Figure 2: Thermal properties of different auxetic POCS. The dimensionless effective heat conduction against the solid fraction are shown. The solid fraction is a function of the amplitude of the arc a and the strut diameter d_s Additionally, literature correlations according to Maxwell, Bianchi et al., Bracconi et al. and Lemlich are shown.

Contacts:
dominik.rudolf@tu-dortmund.de
lisa.eckendoerfer@tu-dortmund.de
hannsjoerg.freund@tu-dortmund.de

markus.thommes@tu-dortmund.de

Publications:
D. Rudolf, G. Littwin, H. Freund, 2nd International Conference on Unconventional Catalysis UCRA (2022)
A. Fink, D. Rudolf, Z. Fu, H. Freund, C. Körner, 7th International Conference on Cellular Materials CellMAT (2022)

Publications 2020 – 2022

2022

Peer-reviewed Journal Articles

- G. D. Wehinger, M. Ambrosetti, R. Cheula, Z. Ding, M. Isoz, B. Kreitz, K. Kuhlmann, M. Kutscherauer, K. Niyogi, J. Poissonnier, R. Réocreux, D. Rudolf, J. Wagner, R. Zimmermann, M. Bracconi, H. Freund, U. Krewer, M. Maestri
  Quo Vadis Multiscale Modeling in Reaction Engineering? – A Perspective
  Chemical Engineering Research and Design 184, 39-58 (2022)

- B. Worgul, A. F. Aguilera, C. Vergat-Lemercier, K. Eränen, O. Simakova, H. Held, H. Freund, D. Y. Murzin, T. Salmi
  Sugar Acid Production on Gold Nanoparticles in Slurry Reactor: Kinetics, Solubility and Modelling
  Chemical Engineering Science 260, 117948 (2022)

- H. Freund, J. Sauer, O. Wachsen
  Wie verändert sich die Reaktions- und Reaktortechnik durch die Elektrifizierung chemischer Prozesse?
  Editorial, Chemie Ingenier Technik 94(5), 615 (2022)

2021

Peer-reviewed Journal Articles

- K. L. Fischer, H. Freund
  Intensification of Load Flexible Fixed Bed Reactors by Optimal Design of Staged Reactor Setups
  Chemical Engineering and Processing 159, 108183 (2021)

- G. Littwin, S. Röder, H. Freund
  Systematic Experimental Investigations and Modeling of the Heat Transfer in Additively Manufactured Periodic Open Cellular Structures with Diamond Unit Cell
  Industrial & Engineering Chemistry Research 60(18), 6753-6766 (2021)

- E. Moioli, L. Schmid, P. Wasserscheid, H. Freund
  Kinetic Modelling of Reactions for the Synthesis of 2-Methyl-5-Ethyl-Pyridine
  Reaction Chemistry & Engineering 6, 1254-1264 (2021)

- S. Trunk, A. Brix, H. Freund
  Development and Evaluation of a New Particle Tracking Solver for Hydrodynamic and Mass Transport Characterization of Porous Media – A Case Study on Periodic Open Cellular Structures
  Chemical Engineering Science 244, 116768 (2021)

- G. Littwin, M. von Beyer, H. Freund
  Detailed Investigation of Liquid Distribution and Holdup in Periodic Open Cellular Structures Using Computed Tomography
  Chemical Engineering and Processing 168, 108579 (2021)

- H. Freund, J. Sauer, O. Wachsen
  "Circular Economy" – ein neues und zugleich altes Arbeitsgebiet der Reaktionstechnik
  Editorial, Chemie Ingenieur Technik 93(5), 735 (2021)

2020

Peer-reviewed Journal Articles

- J. Maußner, H. Freund
  Multi-Objective Reactor Design Under Uncertainty: A Decomposition Approach Based on Cubature Rules
  Chemical Engineering Science 212, 115304 (2020)

- A. Pietschak, J. Maußner, A. G. Dixon, H. Freund
  Comparative Evaluation of Heat Transfer Correlations with Different Fluid Property Considerations for Fixed-Bed Reactor Modeling
  Internationa Journal of Heat and Mass Transfer 148, 119099 (2020)

- G. Do, M. Geisselbrecht, W. Schwieger, H. Freund
  Additive Manufacturing of Interpenetrating Periodic Open Cellular Structures (interPOCS) with in Operando Adjustable Flow Characteristics
  Chemical Engineering and Processing 148, 107786 (2020)

- G. Ganzer, H. Freund
  Influence of Statistical Activity Variations in Diluted Catalyst Beds on the Thermal Reactor Behavior: Derivation of an A Priori Criterion
  Chemical Engineering Science 220, 115607 (2020)

- A. Pietschak, A. G. Dixon, H. Freund
  A New Heat Transfer Correlation Suited for the Design of Fixed-Bed Reactors via Numerical Optimization
  Chemical Engineering Science 220, 115614 (2020)

- K. L. Fischer, H. Freund
  On the Optimal Design of Load Flexible Fixed Bed Reactors: Integration of Dynamics into the Design Problem
  Chemical Engineering Journal 393, 124722 (2020)

- N. Delgado Otalvaro, M. Kaiser, K. Herrera Delgado, S. Wild, J. Sauer, H. Freund
  Optimization of the Direct Synthesis of Dimethyl Ether from CO_2 Rich Synthesis Gas: Closing the Loop between Experimental Investigations and Model-Based Reactor Design
  Reaction Chemistry & Engineering Journal 5, 949-960 (2020)

- H. Freund, R. Güttel, R. Horn, U. Krewer, J. Sauer
  Trendberichte Technische Chemie
  Nachrichten aus der Chemie 68(6), 46-53 (2020)

- F. Warnecke, L. Lin, S. Haag, H. Freund
  Identification of Reaction Pathways and Kinetic Modeling of Olefin Interconversion over an H-ZSM-5 Catalyst
  Industrial & Engineering Chemistry Research 59(28), 12696-12709 (2020)

- M. Ambrosetti, G. Groppi, W. Schwieger, E. Tronconi, H. Freund
  Packed Periodic Open Cellular Structures – An Option for the Intensification of Non-Adiabatic Catalytic Processes
  Chemical Engineering and Processing 155, 108057 (2020)

Technical Biochemistry (TB)

Publications 2020 – 2022

2022

- Nguyen, G.-N., Jordan, E.N., and Kayser, O.
  Protecting-group-free synthesis of novel cannabinoid-like 2,5-dihydrobenzoxepines
  Synthesis 2022, 54, A-K. DOI:10.1055/s-0042-1751361

- Nguyen, G.-N., Jordan, E.N., and Kayser, O.
  Synthetic strategies for rare cannabinoids derived from Cannabis sativa
  J Nat Products 2022, DOI: 10.1021/acs.jnatprod.2c00155.

- Jordan, E., Nguyen, G.-N., Piechot, A., and Kayser, O.
  Cannabinoids as new drug candidates for the treatment of glaucoma
  Planta Med 2022, 88: 1-18. DOI: 10.1055/a-1665-3100.

- Thomas, F. and Kayser, O.
  Natural deep eutectic solvents enhance cannabinoid biotransformation
  Biochem Engin J, DOI: 10.1016/j.bej.2022.108380.

- Pitakbut, T., Spiteller, M., and Kayser, O.
  Genome mining and gene expression reveal maytansine biosythetic genes from endophytic communities living inside Gymnosporia heterophylla (Eckl. and Zeyh.) Loes. and the relationship with the plant biosynthetic gene, Friedelin Synthase
  Plants 2022, 11:321

2021

Peer-reviewed Journal Articles

- Riga, R., Happyana, N., Quentmeier, A., Zamarelli, C., Kayser, O. and Hakim, E.H.
  Secondary metabolites from Diaporthe lithocarpus islated from Artocarpus heterophyllus
  Nat Prod Res. 2021, 35:2324-2328

- Pitakbut, T., Nguyen, G.-N., and Kayser, O.
  Activity of THC, CBD, and CBN on human ACE2 and SARS-CoV1/2 main protease to understand antiviral defense mechanism
  Planta Med 2021, DOI: 10.1055/a-1581-3707.

- Hussain, T., Jeena, G., Pitakbut, T., Vasilev, N., and Kayser, O.
  Cannabis sativa research trends, challenges and new-age perspectives
  ISCIENCE 2021, 24, DOI: https://doi.org/10.1016/j.isci.2021.103391.

- Daoud, F., Zühlke, S., Spiteller, M., and Kayser, O.
  Elimination of diethylenetriaminepentaacetic acid from effluents from pharmaceutical production by ozonation
  Ozone: Science & Engineering, DOI: 10.1080/01919512.2021.1983409.

- Hillebrands, L., Lamshoeft, M., Lagojda, A., Stork, A. and Kayser, O.
  In vitro metabolism of tebuconazole, flurtamone, fenhexamid, metalaxyl-M and spirodiclofen in Cannabis sativa L. (hemp) callus cultures
  Pest Manag Sci 2021, DOI: 10.1002/ps.6575.

- Pitakbut, T., Spiteller, M., and Kayser, O. In vitro production and exudation of 20-hydroxymaytenin from Gymnosporia heterophylla (Eckl. and Zeyh.) Loes. cell culture.
  Plants 2021, 10, 1493. https://doi.org/10.3390/plants100781493.

2020

Peer-reviewed Journal Articles

- Thomas, F., Schmidt, C., and Kayser, O.
  Bioengineering studies and pathway modeling of the heterologous biosynthesis of tetrahydrocannabinolic acid in yeast
  Appl Microbiol Biotechnol 2020, DOI: 10.1007/s00253-020-10798-3.

- Nguyen, G.-N., and Kayser, O.
  Biosynthesis and chemical modifications of minor cannabinoids. In: eLS. John Wiley & Sons, LTD: Chichester
  May 2020. DOI: 10.1002/9780470015902.a0028875

- Hensel, A., Bauer, R., Heinrich, M., Spiegler, V., Kayser, O., Hempel, G., Kraft, K.
  Challenges at the time of Covid-19: Opportunities and innovations in antivirals from nature
  Planta Med 2020, 86: 659-664.

- Averesch, N.J.H. and Kayser, O.
  Editorial: Biotechnological Production and Conversion of Aromatic Compounds and Natural Products
  Front. Bioeng. Biotechnol. doi: 10.3389/fbioe.2020.00646

- Rodziewicz, P. and Kayser, O.
  Cultivation and breeding of Cannabis sativa L. for medicinal use
  In: Handbook of Plant Breeding - Medicinal, aromatic and stiumlant plants.Vol. 12. Eds.: Novak, J., and Blüthner, J.-W. Springer International Publishing, Springer Nature Switzerland AG, ISBN 987-3-030-38791-4, 2020.

Technical Biology (TBL)

Biocatalytic Production of the Antibiotic Aurachin D

Engineering *Escherichia coli* for High-Level Expression of a Membrane-bound Enzyme

Sebastian Kruth, Lina Schibajew and Markus Nett

The quinolone antibiotic aurachin D is a potent inhibitor of cytochrome bd oxidases, which exclusively occur in bacteria and hence represent promising targets in the treatment of infectious diseases. It is therefore not surprising that the chemical synthesis of aurachin D has attracted considerable attention over the years. Up to now, the installation of the characteristic farnesyl moiety in aurachin D has not been satisfactorily solved, thus diminishing the achievable yields. In this study, we constructed a recombinant Escherichia coli *strain that is capable of executing this transformation with high efficiency.*

Aurachin D is an isoprenoid quinolone alkaloid, which was first isolated from cultures of the myxobacterium ***Stigmatella aurantica.*** Biosynthetic studies revealed that the quinolone core of aurachin D originates from anthranilate and two acetate units. After its assembly by a polyketide synthase enzyme complex, a membrane-bound protein named AuaA regioselectively introduces a farnesyl side-chain to give aurachin D (Figure 1).

The recovery of aurachin D from native producers is not very efficient due to low titers and several structurally related byproducts, which must be separated from the target molecule. To circumvent an extensive downstream processing, it seemed advisable to conduct the biosynthesis in an appropriate heterologous host. We decided to devise a whole-cell biotransformation process, in which a customized, AuaA-expressing microbe converts a synthetically prepared quinolone into aurachin D. ***Escherichia coli*** was selected as host, because AuaA had already been functionally expressed in this bacterium. Furthermore, ***E. coli*** possesses several favorable traits, such as fast growth and its ease of genetic manipulation.

In order to achieve a high-level production of the membrane-bound enzyme, the expression of the ***auaA*** gene was translationally coupled to an upstream cistron in accordance with a bicistronic design (BCD) strategy. Screening of various BCD elements led to the identification of expression cassettes, which increased the production of aurachin D by a factor up to 29 (Figure 2). The production level could be further raised by codon optimization of ***auaA*** and by introducing the mevalonate pathway into the production strain. The latter measure was intended to enhance the availability of farnesyl pyrophosphate (FPP), which is needed as a cosubstrate for the AuaA-catalyzed reaction. In sum, the described efforts resulted in a strain producing aurachin D with a titer that is 424 times higher than that obtained with the original, non-optimized expression host.

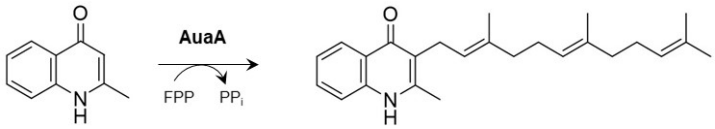

Figure 1: Biosynthetic conversion of 2-methyl-1H-quinolin-4-one into aurachin D by the membrane-bound farnesyltransferase AuaA.

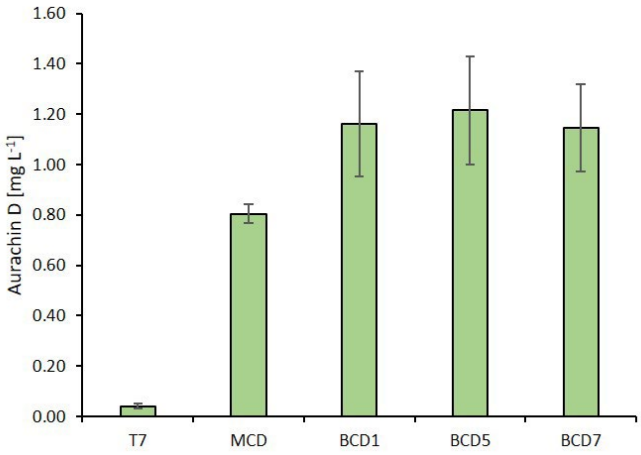

Figure 2: Production of aurachin D in *E. coli* cultures supplemented with 2-methyl-1H-quinolin-4-one. The cultures expressed *auaA* under control of the T7 promoter or, alternatively, the *trc** promoter using mono- and bicistronic design (MCD, BCD1, BCD5, BCD7).

Contacts:
sebastian.kruth@tu-dortmund.de
markus.nett@tu-dortmund.de

Publications:
S. Kruth, L. Schibajew, M. Nett, AMB Express, 12, 138 (2022)

A Biotechnological Route to Heterocyclic Compounds

Myxococcus xanthus as Host for the Production of Benzoxazoles

Lea Winand, Lucia Lernoud, Katharina Kuhr and Markus Nett

The chemical synthesis of heterocycles typically requires elevated temperature and acid or base addition to form the desired product. Moreover, these reactions often involve hazardous reagents, which is why biocatalytic routes for heterocycle formation have received increasing attention in pharmaceutical industry. In recent years, several heterocycle-forming enzymes have been identified in the amidohydrolase superfamily. We now report the reconstruction of benzoxazole biosynthesis in the myxobacterium Myxococcus xanthus *based upon the heterologous expression of an ATP-dependent ligase and an amidohydrolase. The* M. xanthus *expression strain achieved a benzoxazole titer of 114.6 ± 7.4 mg L^{-1} upon precursor supplementation, which is superior to other bacterial production systems. Crosstalk between the heterologously expressed pathway and a house-keeping enzyme led to the combinatorial biosynthesis of benzoxazoles.*

Benzoxazoles are important structural motifs in pharmaceutical drugs. Previously, the amidohydrolase NatAM from the nataxazole biosynthetic pathway was demonstrated to convert substituted 2-aminophenyl benzoates into benzoxazoles via a hemiorthoamide intermediate. In nature, the substrates for this reaction derive from the enzymatic linkage of 3-hydroxyanthranilic acid (3-HAA) with another aryl carboxylic acid, which is catalyzed by the ATP-dependent ligase NatL2 (Figure 1).

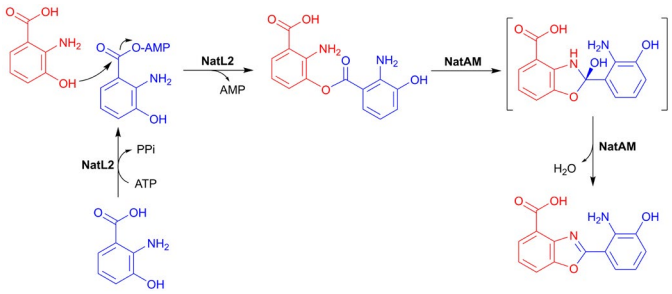

Figure 1: Amidohydrolase-mediated benzoxazole biosynthesis.

In order to synthesize benzoxazoles in *M. xanthus*, we recombinantly produced the enzymes NatL2 and NatAM in this myxobacterium using the plasmid-based expression system that had been developed in our group. Since *M. xanthus* can synthesize 3-HAA from L-tryptophan via the kynurenine pathway, the uptake of the expression plasmid was sufficient to induce benzoxazole formation in the myxobacterium, albeit only a low titer of 10.7 ± 1.8 mg L^{-1} was achieved in shake flasks. The supplementation of exogenous 3-HAA positively affected the benzoxazole titer in a concentration-dependent manner. The highest product titer (114.6 ± 7.4 mg L^{-1}) was obtained after the feeding of 320 mg L^{-1} 3-HAA, corresponding to a molar yield coefficient of 40.6 ± 2.6% and a space-time yield of 38.2 mg L^{-1} d^{-1}. These values indicate that *M. xanthus* is a promising host for recombinant benzoxazole production.

Chemical analyses revealed that *M. xanthus* is even capable to convert aryl carboxylic acids into benzoxazoles, which cannot be activated by NatL2. Follow-up studies confirmed that this feature is promoted by a house-keeping adenylating enzyme from *M. xanthus*. This finding has important implications for the biotechnological production of benzoxazoles, as it shows that the accessible product spectrum is not limited by the substrate tolerance of NatL2. Rather, it can be expanded by recruiting adenylating enzymes from other pathways.

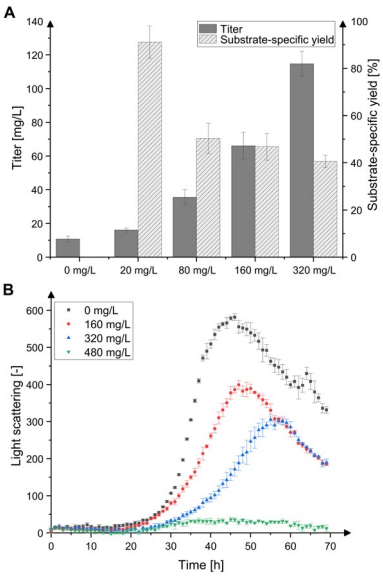

Figure 2: Influence of feeding *M. xanthus* NM: pMEX14 with 3-HAA. A) Benzoxazole production level and molar substrate-specific yield. Product titers were determined after extraction of 50 mL cultures from shake flasks. B) Growth curves recorded in a microbioreactor system (BioLector, m2p-labs).

Publications:
L. Winand, L. Lernoud, S. A. Meyners, K. Kuhr, W. Hiller, M. Nett, ChemBioChem, 23, e202200635

VIP: The paper was judged to be very important by three referees. The paper was selected by the editor for a cover feature of the journal.

Contacts:
lea.winand@tu-dortmund.de
markus.nett@tu-dortmund.de

Publications 2020 –2022

2022

Peer-reviewed Journal Articles

- L. Winand, L. Lernoud, S. A. Meyners, K. Kuhr, W. Hiller, M. Nett
  Myxococcus xanthus as Host for the Production of Benzoxazoles
  ChemBioChem, 23, e202200635 (2022)

- S. Kruth, L. Schibajew, M. Nett
  Biocatalytic Production of the Antibiotic Aurachin D in _Escherichia coli_
  AMB Express, 12, 138 (2022)

- B. K. Lombe, L. Winand, J. Diettrich, M. Töbermann, W. Hiller, M. Kaiser, M. Nett
  Discovery, Biosynthetic Origin, and Heterologous Production of Massinidine, an Antiplasmodial Alkaloid
  Organic Letters, 24, 2935-2939 (2022)

- T. Steinmetz, W. Hiller, M. Nett
  Amamistatins Isolated from _Nocardia altamirensis_
  Beilstein Journal of Organic Chemistry, 18, 360-367 (2022)

- A. Kinner, P. Nerke, R. Siedentop, T. Steinmetz, T. Classen, K. Rosenthal, M. Nett, J. Pietruszka, S. Lütz
  Recent Advances in Biocatalysis for Drug Synthesis
  Biomedicines, 10, 964 (2022)

- D. J. Vollmann, L. Winand, M. Nett
  Emerging Concepts in the Semisynthetic and Mutasynthetic Production of Natural Products
  Current Opinion in Biotechnology, 77, 102761 (2022)

2021

Peer-reviewed Journal Articles

- A. Tippelt, M. Nett
  Saccharomyces cerevisiae as Host for the Recombinant Production of Polyketides and Nonribosomal Peptides
  Microbial Cell Factories, 20, 161 (2021)

- D. J. Vollmann, T. Busche, C. Rückert, M. Nett
  Complete Genome Sequence of the Nonmotile _Myxococcus xanthus_ Strain NM
  Microbiology Resource Announcements, 10, e00989-21 (2021)

- L. Winand, P. Schneider, S. Kruth, N.-J. Greven, W. Hiller, M. Kaiser, J. Pietruszka, M. Nett
  Mutasynthesis of Physostigmines in _Myxococcus xanthus_
  Organic Letters, 23, 6563–6567 (2021)

- L. Winand, D. J. Vollmann, J. Hentschel, M. Nett
  Characterization of a Solvent-Tolerant Amidohydrolase Involved in Natural Product Heterocycle Formation
  Catalysts, 11, 892 (2021)

- L. Winand, A. Sester, M. Nett
  Bioengineering of anti-inflammatory natural products
  ChemMedChem, 16, 767-776 (2021)

2020

Peer-reviewed Journal Articles

- A. Sester, J. Korp, M. Nett
  Secondary metabolism of predatory bacteria
  The Ecology of Predation at the Microscale, edited by E. Jurkevitch, R. J. Mitchell, pp. 127-154, Springer Nature Switzerland (2020)

- A. Sester, K. Stüer-Patowsky, W. Hiller, F. Kloss, S. Lütz, M. Nett
  Biosynthetic plasticity enables production of fluorinated aurachins
  ChemBioChem 21, 2268-2273 (2020)

- A. Tippelt, T. Busche, C. Rückert, M. Nett
  Complete genome sequence of the cryptophycin-producing cyanobacterium Nostoc sp. strain ATCC 53789
  Microbiology Resource Announcements 9, e00040-20 (2020)

- A. Tippelt, M. Nett, M. S. Vela Gurovic
  Catalytic promiscuity of cGAS: a facile enzymatic synthesis of 2'-3'-linked cyclic dinucleotides
  Microbiology Resource Announcements 9, e00227-20 (2020)

- K. Rosenthal, M. Becker, J. Rolf, R. Siedentop, M. Hillen, M. Nett, S. Lütz
  Genomics-inspired discovery of massiliachelin, an agrochelin epimer from Massilia sp. NR 4-1
  ChemBioChem 21, 3225-3228 (2020)

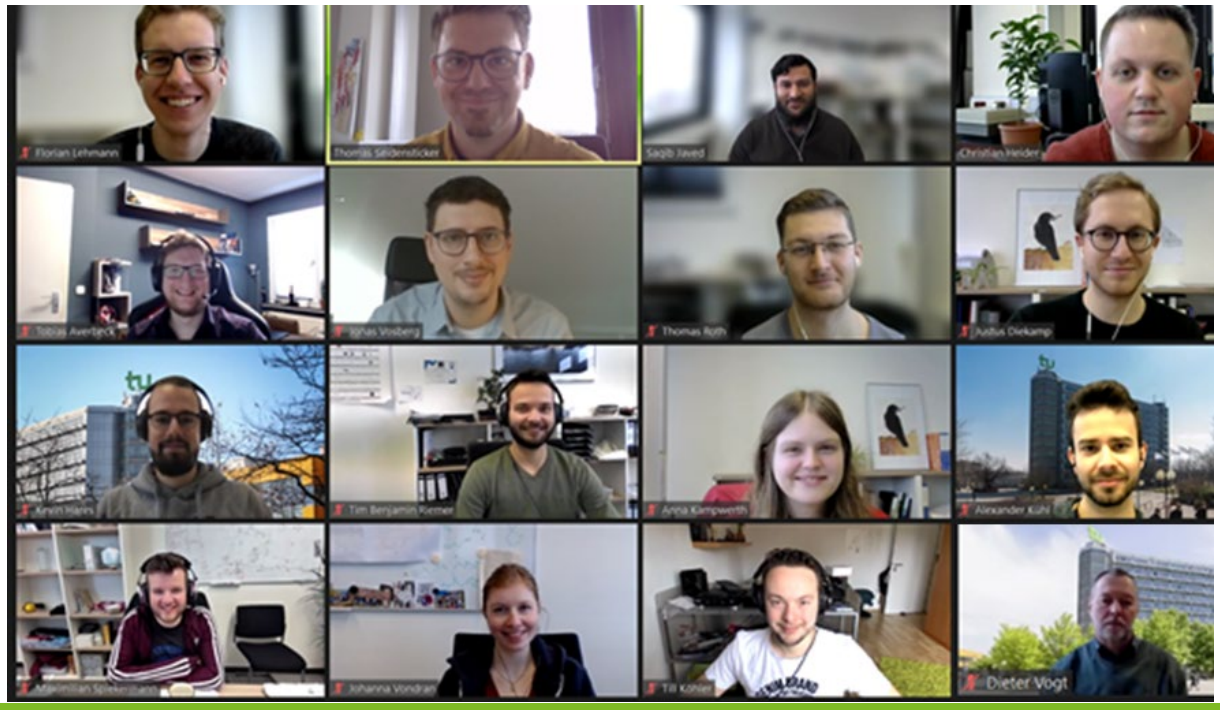

Industrial Chemistry (TC)

Controlling selectivity by catalyst and pH adjustment

Oxidative cleavage of a renewable based diol

Johanna Vondran, Marc Peters, Alexander Schnettger, Christian Sichelschmidt, Thomas Seidensticker

Renewable resources offer enormous potential to protect our planet by means of the reduction of CO_2-emissions. Additionally, fossil resources such as crude oil and natural gas are limited, whilst renewable resources such as fats and oils are obtained from plants that grow back. Assuming that the energy supply for chemical processes comes from renewable energy, chemical processes can be classified as "green" considering the usage of substrates from renewable resources. To further improve such processes, usage of catalysts results in a lower energy demand. Finally, by choosing the catalyst, selectivity is significantly influenced. Herein, a higher selectivity results in a low amount of waste contributing to a more sustainable chemistry. For a sustainable integrated process, the separation of the product from the catalyst must also be implemented to obtain a pure value product.

Methyl oleate is obtained from special breedings of the sunflower. Upon oxidative cleavage, the bio-based value products pelargonic acid and mono methyl azelate are obtained. They find application in plasticizers, lubricants or generally polymers.

The oxidative cleavage can be carried out as a green process, regarding usage of hydrogen peroxide as a green oxidant, since water is the only by-product. Herein, a homogeneously solved transition metal catalyst allows for activation. However, the oxidative cleavage of methyl oleate is complex, as several intermediate steps are required, and side-products occur. In contrast, the first two intermediate steps can be controlled easily, so that the intermediate diol methyl 9,10-dihydroxystearate is obtained selectively. Starting from this compound, the oxidative cleavage is carried out in the presence of phosphotungstic acid as the catalyst. Herein, the pH plays a crucial role for selectivity: The catalyst (Figure 1) is acidic, enhancing the oxidative cleavage. However, under highly acidic conditions, side-reactions occur, resulting in undesired high-molecular oligomer products. Through the addition of a low amount of sodium hydroxide as a base, this undesired side-reaction is inhibited, resulting in a total selectivity of up to 90%.

The same catalyst system is also investigated for the oxidative cleavage of methyl oleate directly. However, the pH adjustment to less acidic conditions inhibits a prior intermediate step towards the formation of the diol. Thus, the process benefits from a stepwise synthesis, (Figure 2) meaning the diol is synthesized first, ready for oxidative cleavage afterwards.

For a whole, sustainable process the reaction and product purification/separation both must be considered from the beginning of planning. Phosphotungstic acid exhibits a molecular weight of 2880 Da, which is by far higher than the molecular weight of all other compounds (such as substrate, oxidant and products). Thus, this is made use of regarding separation, as organic solvent nanofiltration is applied to selectively retain the catalyst, whilst all other compounds permeate through a membrane. From first experiments, a catalyst retention of 94% was reached. In future works, this concept could be extended to recycle the catalyst and increase the process economy.

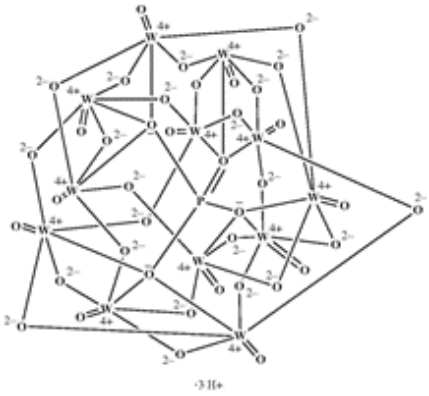

Figure 1: Chemical structure of phosphotungstic acid

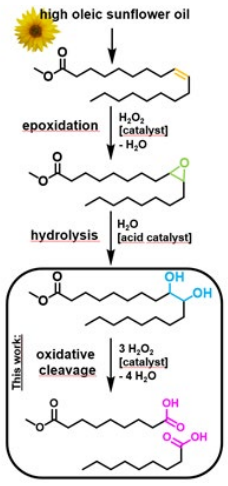

Figure 2: Stepwise oxidative cleavage of methyl oleate.

Contact:
Thomas.seidensticker@tu-dortmund.de

Publications:
J. Vondran, M. Peters, A. Schnettger, C. Sichelschmidt, T. Seidensticker, Catal. Sci. Technol. 12, 3622-3633 (2022)

Palladium-Catalyzed Synthesis of Mixed Anhydrides via Carbonylative Telomerization

Kevin Hares, Dennis Vogelsang, Charlotte S. Wernsdörfer, Dennis Panke, Dieter Vogt and Thomas Seidensticker

Developing resource-efficient transformations to functional intermediates and products is a cornerstone of sustainability. Especially highly active intermediates for synthesizing complex molecules are in high demand. However, their production often involves waste-intensive procedures. An elegant way to reduce waste is the use of efficient catalytic reactions with a high atom economy. A remarkable example is the Pd-catalyzed carbonylative telomerization (Figure 1). Four basic feedstock molecules are combined in a single multi-component transformation by a Pd catalyst. The nucleophile "H-Nu" can be an alcohol or amine until now.

For the first time, mixed carboxylic anhydrides were accessed directly via homogeneous palladium catalysis from 1,3-butadiene and carboxylic acids. Under carbonylative telomerization conditions, the respective mixed 3,8-nonadienoic anhydrides are formed in a single reaction step with yields of up to 82% (Figure 2). These very reactive mixed anhydrides can then be used for consecutive reactions in a one-pot manner and selectively transfer the newly formed unsaturated C_9 unit. Possible changes in the proposed mechanism were discussed, and in the first example, the mixed anhydrides were utilized to form amides. Our carbonylative telomerization path allows the reduction of synthetic steps necessary for adding a carbonyl group to the molecule, thus increasing the overall atom economy and reducing waste production.

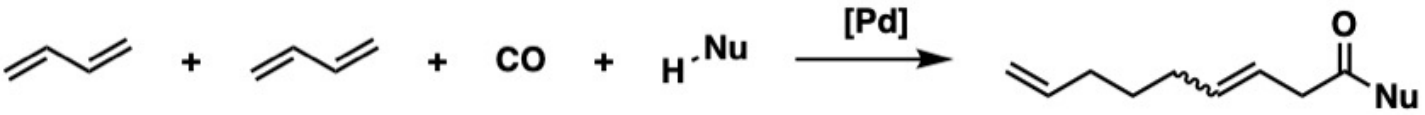

Figure 1: General carbonylative telomerization of butadiene.

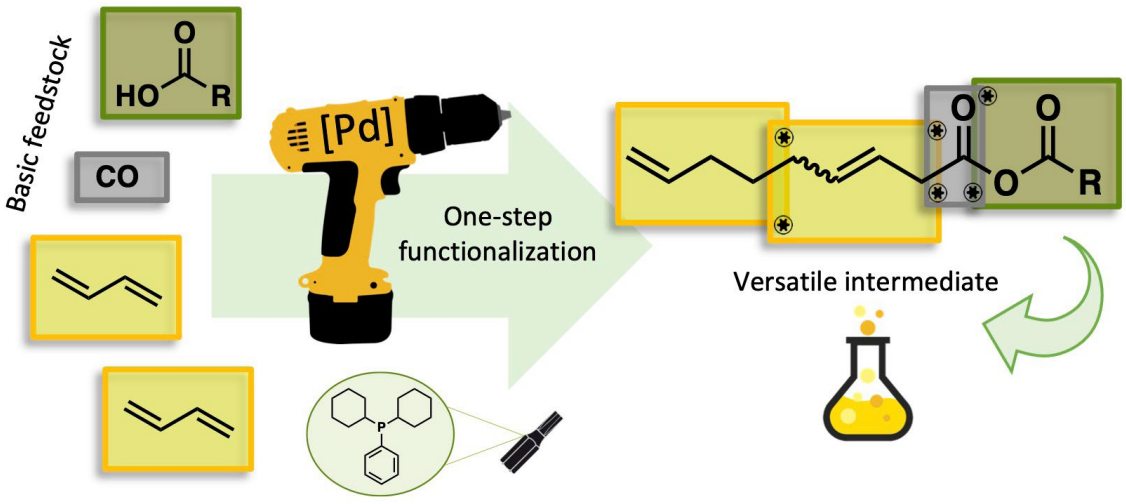

Figure 2: Application of carbonylative telomerization with carboxylic acids for synthesizing active mixed anhydrides.

Publication:
K. Hares, D. Vogelsang, C. S. Wernsdörfer, D. Panke, D. Vogt and T. Seidensticker, Catal. Sci. Technol., 2044-4761 (2022)

Contact:
thomas.seidensticker@tu-dortmund.de

Selective Synthesis of Primary Amines by Kinetic-based Optimization of the Ruthenium-Xantphos Catalysed Amination of Alcohols with Ammonia

Christian Heider, Dominik Pietschmann, Dieter Vogt, Thomas Seidensticker

Amines are used in a wide variety in the chemical industry, for instance, to produce fine chemicals, dyes, agrochemicals, pharmaceuticals, and polymers. Different catalytic amine syntheses have thus been established. Especially primary, terminal amines are important intermediates due to their high reactivity. However, this reactivity poses challenges to their synthesis, particularly on a large scale. For the synthesis of primary amines, a direct and selective reaction of ammonia with different bulk chemicals would be beneficial. But this higher reactivity of primary amines compared to ammonia favors the formation of secondary or even tertiary amines in consecutive reactions, thereby lowering overall selectivity. Nevertheless, using commercially available and robust catalyst systems, up to now, only secondary alcohols like cyclohexanol have been converted into primary amines with preparatively satisfying selectivities exceeding 90 %. The direct amination of primary alcohols with ammonia yielding primary amines in high selectivities is still complicated and often limited to:

- *poor catalyst activity/productivity*
- *huge ammonia excesses*
- *high selectivities only at low conversion*

The selective synthesis of primary amines directly from several alcohols and ammonia (Figure 1) using a homogeneous catalyst based on $HRuCl(CO)(PPh_3)_3$ and Xantphos is presented. The key to success was the detailed understanding of all mutually influencing parameters such as temperature, ammonia excess, and substrate concentration. These studies were supported by the determination of the kinetics, which allowed the reaction order to be calculated as 0.7. Furthermore, the kinetic model derived from the mechanism was confirmed. After measuring reaction profiles for all influencing parameters, optimized conditions were obtained, which finally allowed the amination of aliphatic, cyclic, as well as primary and secondary alcohols with selectivities to the desired primary amine exceeding 90 % at quantitative alcohol conversion with only minimal formation of the undesired secondary amines. Furthermore, the catalytic activity of the commercially available and robust Xantphos system was drastically improved, corresponding to a turnover frequency (TOF)>60 h^{-1} after 30 minutes and a turnover number (TON) of 120.

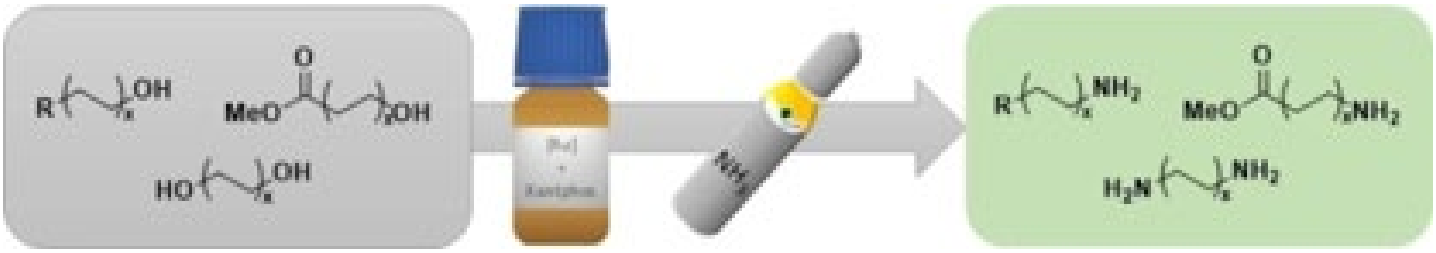

Figure 1: Amination of several alcohols using a Ru-based catalyst and ammonia.

Contact:
thomas.seidensticker@tu-dortmund.de

Publication:
C. Heider, D. Pietschmann, D. Vogt, T. Seidensticker, ChemCatChem. 14, e202200788 (2022)

Publications 2020 – 2022

2022

Peer-reviewed Journal Articles

- Huxoll, F., Kampwerth, A., Seidensticker, T., Vogt, D., Sadowski, G., (2022)
  Predicting Solvent Effects on Homogeneity and Kinetics of the Hydroaminomethylation: A Thermodynamic Approach Using PC-SAFT
  Ind. Eng. Chem. Res., 61, 2323-2332. DOI: 10.1021/acs.iecr.1c03891

- Vondran, J., Peters, M., Schnettger, A., Sichelschmidt, C., Seidensticker, T., (2022)
  From tandem to catalysis – organic solvent nanofiltration for catalyst separation in the homogeneously W-catalyzed oxidative cleavage of renewable methyl 9,10-dihydroxystearate
  Catal. Sci. Techn., 12, 3622-3633. DOI: 10.1039/D1CY02317A

- Vondran, J., Benninghoff, T., Emminghaus, A., Seidensticker, T. (2022)
  Catalytic Synthesis of Methyl 9,10-dihydroxystearate from Technical Feedstocks in Continuous Flow via Epoxidation and Hydrolysis
  Eur. J. Lipid Sci. Technol, 124, 2200041. DOI: 10.1002/ejlt.202200041

- Hares, K., Vogelsang, D., Wernsdörfer, C. S., Panke, D., Vogt, D., Seidensticker, T. (2022)
  Palladium-Catalyzed Synthesis of Mixed Anhydrides via Carbonylative Telomerization
  Catal. Sci. Techn., 12, 3992-4000. DOI: 10.1039/D2CY00486K

- Vondran, J., Seifert, A. I., Schäfer, K., Laudanski, A., Deysenroth, T., Wohlgemuth, K., Seidensticker, T. (2022)
  Progressing the Crystal Way to Sustainability: Strategy for Developing an Integrated Recycling Process of Homogeneous Catalysts by Selective Product Crystallization
  Ind. Eng. Chem. Res. 61, 9621–9631. DOI: 10.1021/acs.iecr.2c00476

- Heider, C., Pietschmann, D., Vogt, D., Seidensticker, T. (2022)
  Selective Synthesis of Primary Amines by kinetic-based Optimization of the Ruthenium-Xantphos Catalysed Amination of Alcohols with Ammonia
  ChemCatChem, 14, e202200788. DOI: 10.1002/cctc.202200788

2021

Peer-reviewed Journal Articles

- Huxoll, F., Jameel, F., Bianga, J., Seidensticker, T., Stein, M., Sadowski, G., Vogt, D. (2021)
  Solvent Selection in Homogeneous Catalysis—Optimization of Kinetics and Reaction Performance
  ACS Catal., 11, 590–594, DOI: 10.1021/acscatal.0c04431 .

- Künnemann, K. U., Weber, D., Becquet, C., Tilloy, S., Monflier, E., Seidensticker, T., Vogt, D. (2021).
  Aqueous Biphasic Hydroaminomethylation Enabled by Methylated Cyclodextrins: Sensitivity Analysis for Transfer into a Continuous Process
  ACS Sustainable Chem. Eng., 9, 273–283, DOI: 10.1021/acssuschemeng.0c07125 .

- Schlü¬ter, S., Künnemann, K. U., Freis, M., Roth, T., Vogt, D. , Dreimann, J. M. , and Skiborowski, M. (2021)
  Continuous co-product separation by organic solvent nanofiltration for the hydroaminomethylation in a thermomorphic multiphase system
  Chemical engineering journal, 409, 128219, DOI: 10.1016/j.cej.2020.128219

- Söderholm, V., Esteban, J., Vogt, D. (2021).
  Synthesis of a H-Sulfo-POSS catalyst and application in the acetalization of glycerol with 2-butanone to a biofuel additive
  Catal. Sci. Technol., 11, 4529-4538, DOI: 10.1039/D1CY00344E

- Vondran, J., Pela, J., Palczewski, D., Skiborowski, M., Seidensticker, T. (2021).
  Curse and Blessing – The Role of Water in the Homogeneously Ru-Catalyzed Epoxidation of Technical Grade Methyl Oleate
  ACS Sustainable Chem. Eng. 9 (34), 11469–11478, DOI: 10.1021/acssuschemeng.1c03573 .

- Vondran, J., Furst, M. R. L., Eastham, G. R., Seidensticker, T., Cole-Hamilton, D. J. (2021)
  Magic of Alpha: The chemistry of a remarkable bidentate phosphine, 1,2-bis(di-tert-butylphosphinomethyl)benzene
  Chem. Rev. 121 (11), 6610-6653, DOI: 10.1021/acs.chemrev.0c01254

2020

Peer-reviewed Journal Articles

- M. Terhorst, C. Plass, A. Hinzmann, A. Guntermann, T. Jolmes, J. Rösler, D. Panke, H. Gröger, D. Vogt, A. J. Vorholt, T. Seidensticker
  One-Pot Synthesis of Aldoximes from Alkenes via Rh-catalyzed Hydroformylation in an Aqueous Solvent System
  Green Chem. 22, 7974-7982 (2020) DOI:10.1039/D0GC03141K

- J. Bianga, N. Kopplin, J. Hülsmann, D. Vogt, T. Seidensticker
  Rhodium-Catalyzed Reductive Amination for the Synthesis of Tertiary Amines
  Adv. Synth. Catal. 362, 4415-4424 (2020). DOI: 10.1002/adsc.202000746

- M. Terhorst, C. Heider, A. J. Vorholt, D. Vogt, T. Seidensticker
  Productivity leap in the homogeneous ruthenium-catalysed alcohol amination through catalyst recycling avoiding volatile organic solvents
  ACS Sust. Chem.Eng. 8, 9962-9967 (2020) DOI:10.1021/acssuschemeng.0c03413

- R. Savela, D. Vogt, R. Leino
  Ruthenium Catalyzed N-Alkylation of Cyclic Amines with Primary Alcohols
  Eur JOC 3030-3040 (2020) DOI:10.1002/ejoc.202000167

- J. Bianga, K. U. Künnemann, L. Goclik, L. Schurm, D. Vogt, T. Seidensticker,
  Tandem Catalytic Amine Synthesis from Alkenes in Continuous Flow Enabled by Integrated Catalyst Recycling
  ACS Catal. 10, 6463-6472 (2020) DOI:10.1021/acscatal.0c01465

- K. U. Künnemann, N. Gumbiowski, P. Müller, Y. Jirmann, J. M. Dreimann, D. Vogt,
  Chemometrics in the Homogeneously Catalyzed Reductive Amination: Combing in-situ FT-IR & Band-Target Entropy Minimization
  Ind. Eng. Chem. Res. 59, 9055-9065 (2020) DOI:10.1021/acs.iecr.0c01527

- K. U. Künnemann, L. Schurm, D. Lange, S. Seidensticker, S. Tilloy, E. Monflier, D. Vogt, J. M. Dreimann,
  Continuous Hydroformylation of 1-Decene in an Aqueous Biphasic System using Methylated Cyclodextrins
  Green Chem. 22, 3809-3819 (2020) DOI:10.1039/d0gc00820f

- B. Scharzec, J. Holtkötter, J. Bianga, J. Dreimann, D. Vogt, M. Skiborowski
  Membrane-based separation of co-products from catalyst-rich recycle streams in thermomorphic multiphase systems
  Chem. Eng. Res. Design 157, 65-76 (2020) DOI: 10.1016/j.cherd.2020.02.028

- M. Terhorst, A. Kampwerth, A. Marschand, D. Vogt, A. J. Vorholt, T. Seidensticker
  Facile Catalyst Recycling by Thermomorphic Behavior Avoiding Organic Solvents: A Reactive Ionic Liquid in the Homogeneous Pd-Catalysed Telomerization of the Renewable - -Myrcene
  Catal. Sci. Technol. 10, 1827-1834 (2020) DOI: 10.1039/C9CY02569C

- K. U. Künnemann, J. Bianga, R. Scheel, T. Seidensticker, J. M. Dreimann, D. Vogt
  Process Development for the Rhodium-Catalyzed Reductive Amination in a Thermomorphic Multiphase System
  Org. Proc. Res. Dev. 24, 41-49 (2020) DOI: 10.1021/acs.oprd.9b00409

- N. Herrmann, J. Bianga, M. Palten, T. Riemer, D. Vogt, J. M. Dreimann, T. Seidensticker
  Improving Aqueous Biphasic Hydroformylation of Unsaturated Oleochemicals Using a Jet- Loop- Reactor
  Eur. J. Lipid Sci. Technol. 122, 1900166 (2020) DOI: 10.1002/ejlt.201900166

- J. Bianga, N. Herrmann, L. Schurm, T. Gaide, J. Dreimann, D. Vogt, T. Seidensticker
  Improvement of Productivity for Aqueous Biphasic Hydroformylation of Methyl 10-Undecenoate – A Detailed Phase Investigation
  Eur. J. Lipid Sci. Technol. 122, 1900317 (2020) DOI: 10.1002/ejlt.201900317

- N. Herrmann, K. Köhnke, T. Seidensticker
  Selective Product Crystallization for Concurrent Product Separation and Catalyst Recycling in the Isomerizing Methoxycarbonylation of Methyl Oleate
  ACS Sust. Chem. Eng. 8, 29, 10633–10638 (2020) DOI: 10.1021/acssuschemeng.0c03432

- D. Vogelsang, J. Vondran, K. Hares, K. Schäfer, T. Seidensticker, A. J. Vorholt
  Palladium Catalysed Acid- Free Carboxytelomerisation of 1,3-Butadiene with Alcohols Accessing Pelargonic Acid Derivatives Including Triglycerides under Selectivity Control
  Adv. Synth. Catal 362, 679-687 (2020) DOI: 10.1002/adsc.201901383

Thermodynamics (TH)

Predictive parametrization of thermodynamic models using Machine Learning

Accessing PC-SAFT pure-component parameters with neural network ensembles

Jonas Habicht, Christoph Brandenbusch, Gabriele Sadowski

Simulation of chemical or biotechnological processes is a key concept to efficiently design and optimize industrial processes or production plants. Thereby, thermodynamic phase equilibria of complex systems have to be available using advanced models, such as PC-SAFT. PC-SAFT requires the parametrization of each component, which is usually performed by fitting to experimental data. Acquiring experimental data is a time-consuming and costly procedure, for some components even unfeasible. In this work we used neural networks (NNs) to predict PC-SAFT pure-component parameters without the need of experimental data.

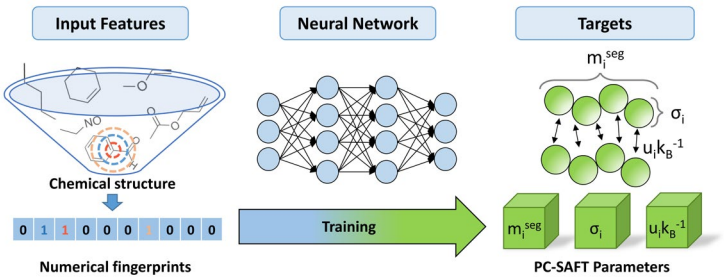

Figure 1: ML-framework to predict PC-SAFT pure-component parameters based on numerical fingerprints.

Classical neural networks are designed to map any arbitrary input features to targets (Figure 1). These targets can be for instance facial recognition, recognition of handwriting, or in our case the prediction of PC-SAFT pure-component parameters (three parameters for a non-associating molecule). NNs are trained using a training set of available data and comparing the true targets with the current NN-outputs. This allows the NN to "learn" underlying patterns in the training data. Having the trained NN in hand, the targets can now be predicted for an unknown molecule without any additional (experimental) input. To increase the statistical validity, multiple NNs are trained on slightly different training sets, creating a so-called NN-ensemble.

Defining suitable input features is crucial, as they must be processible by the NN and per definition non-experimental. The chemical structure of a molecule serves as non-experimental starting point to develop input features for the NN. Unfortunately, the structure itself is not processible by a NN and needs a transformation to a numerical representation.

In this work, a numerical fingerprint has been used as representation of the chemical structure. Starting from a central atom, substructures are derived by iteratively increasing the radius of neighboring atoms to collect larger substructures. This procedure is repeated for every atom of a molecule to collect more substructures, which are all stored in the numerical fingerprint.

The NN-ensemble was then trained on a dataset of ~300 molecules. The success of the training is visualized in Figure 2 (exemplary for one of the three parameters/targets) showing that predicted and validation data are in excellent agreement. With the trained NN-ensemble now in hand, PC-SAFT pure-component parameters for new molecules were predicted within seconds without the need to generate any experimental data, excellently describing experimental thermodynamic properties. Prospectively, NN-ensembles based on numerical fingerprints as input features can be used in an early state of process design to estimate thermodynamic properties/ phase behavior just from the chemical structure of a molecule.

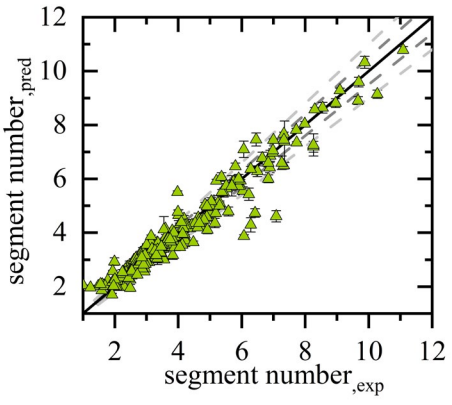

Figure 2: Parity plot for the predictions of the trained NN-ensemble for the segment number (target) compared to the original segment number.

Contacts:
jonas.habicht@tu-dortmund.de
christoph.brandenbusch@tu-dortmund.de
gabriele.sadowski@tu-dortmund.de

Publications:
J. Habicht, C. Brandenbusch, G. Sadowski, Fluid Phase Equilibria, 565, 113657 (2023)

Predicting CO_2 solubility in aqueous and organic electrolyte solutions with ePC -SAFT advanced

CO_2 solubility is predicted, and solvent-specific and ion-specific effects are evaluated

Daniel Schick, Lena Bierhaus, Alexander Strangmann, Paul Figiel, Christoph Held, and Gabriele Sadowski

CO_2 solubility in aqueous and organic electrolyte solutions is of special interest for carbon capture and storage (CCS) or utilization (CCU) processes. Unfortunately, the experimental determination at such conditions is rather laborious. Therefore, the ion-based model ePC-SAFT advanced was used in this work to predict the CO_2 solubility in such systems. We found that the model predictions were accurate. For the first time the salt effect on CO_2 solubility was predicted without the use of parameters that correlate the ion-CO_2 interactions. The mixtures under investigation were binary systems of CO_2 + solvent and higher systems comprised of water + organic solvent + salt (NaCl, KCl, CsCl, $MgCl_2$, $CaCl_2$, $NaNO_3$, KNO_3, $Mg(NO_3)_2$, $Ca(NO_3)_2$, Na_2SO_4, K_2SO_4, $MgSO_4$, $NaHCO_3$, and K_2CO_3).

Knowledge on CO_2 solubility is of crucial importance for process engineering. As the experimental determination is expensive, we used ePC-SAFT advanced to predict CO_2 solubility in various aqueous and organic electrolyte solutions. First, systems of CO_2 + solvent were considered (Figure 1), showing that the CO_2 solubility is highest in non-polar solvents. In a next step, more complex systems containing solvent mixtures and additional salts were studied.

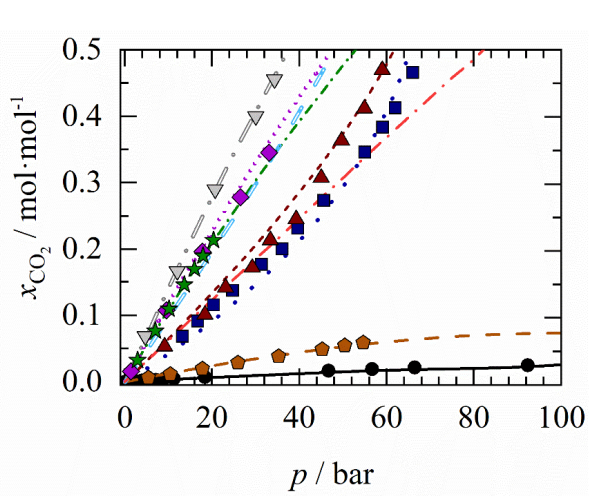

Figure 1: CO_2 solubility in mole fraction in different solvents plotted against the pressure at constant temperature T = 313.15 K. Symbols represent experimental data from the literature (solid circles: water, solid hexagons: GVL, solid squares: methanol, solid up-triangles: ethanol, solid stars: NMP, solid diamonds: DMF, and solid down-triangles: THF). Lines are modeling results (solid line: water, long-dashed line: GVL, dotted line: methanol, long-dash-dotted line: DMSO, short-dashed line: ethanol, empty-dashed line: MeCN, short-dash-dotted line: NMP, empty-dotted line: DMF, and empty-long-dash-dotted line: THF).

The nature of the considered systems required including dissociation reactions of carbonic acid (H_2CO_3/HCO_3^-/CO_3^{2-}) in the modeling framework, most importantly for the systems containing carbonate salts. The results showed that all salts caused salting-out effects on the CO_2 solubility except carbonates (an apparent salting-in due to a pH shift), as shown in Figure 2. The strength of the salting-out effect is related to the charge density of the ions. ePC-SAFT advanced was found to accurately predict the CO_2 solubility in aqueous and organic electrolyte solutions while accounting for solvent-specific effects and ion-specific effects for a broad range of conditions.

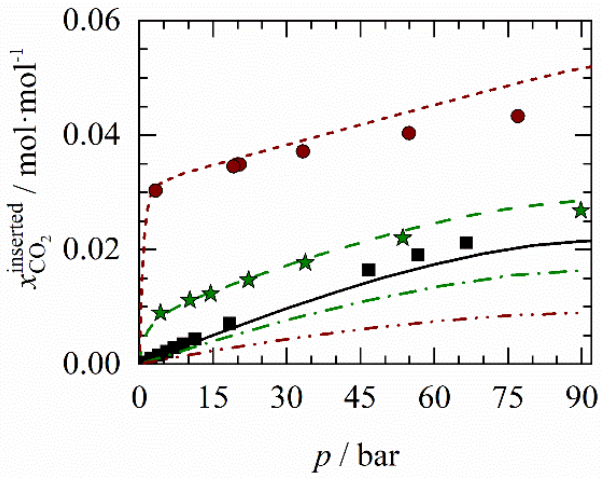

Figure 2: CO_2 solubility in aqueous electrolyte solutions in mole fraction plotted against the pressure at constant temperature T = 313.15 K. Symbols represent experimental data from the literature (solid squares: salt-free system, solid stars: 0.42 mol kg^{-1} K2CO3, and solid circles: 1.71 mol kg^{-1} K_2CO_3). Lines represent predictions (solid line: salt-free system, dash-dotted line: 0.42 mol kg^{-1} K_2CO_3 and dash-double-dotted line: 1.71 mol kg^{-1} K2CO3 while neglecting the dissociation of carbonic acid, dashed line: 0.42 mol kg^{-1} K_2CO_3 and dotted line: 1.71 mol kg^{-1} K_2CO_3 including the dissociation of carbonic acid).

Publications:
D. Schick, L. Bierhaus, A. Strangmann, P. Figiel, G. Sadowski, C. Held, Fluid Phase Equilibria 567, 113714 (2023)

Contact:
christoph.held@tu-dortmund.de

Prediction of pH in multiphase systems with ePC-SAFT advanced

The potential of a physical sound thermodynamic model

Moreno Ascani, Daniel Pabsch, Marcel Klinksiek, Nicolás Gajardo-Parra, Gabriele Sadowski and Christoph Held

The pH value expresses the proton activity, which is the crucial factor determining the species distribution in solution of weak electrolytes. Knowledge of the pH is mandatory, for instance, to assess enzyme activity in an Aqueous Two-Phase System (ATPS) or to estimate the CO_2 solubility in geological reservoirs. This work addresses the prediction of pH in multicomponent multiphase systems by solving the coupled reaction and phase equilibria, using the thermodynamic equation of state ePC-SAFT advanced to describe the nonideality in each phase. The predicted pH values were in excellent agreement with experimental data, using model parameters that were fitted exclusively to phase equilibrium properties.

pH is among the crucial properties that must be known for designing and operation of chemical and biochemical processes. However, pH measurements can be very challenging e.g. in deep geological aquifer systems or in the intracellular medium of living cells. According to the IUPAC definition, the pH value is defined as:

$$pH = -log_{10}\left(a_{H_3O^+}\right) = -log_{10}\left(\frac{\tilde{m}_{H_3O^+}\gamma^{*,\tilde{m}}_{H_3O^+}}{\tilde{m}^0}\right)$$

In Eq. 1, $\tilde{m}_{H_3O^+}$ is the proton molality in the system, $\tilde{m}^0$ is the standard molality (1 mol kg^{-1}) and $\gamma^{*,\tilde{m}}_{H_3O^+}$ is the molality-based activity coefficient of the proton, which at given temperature, pressure and composition is accessible by a thermodynamic model. This work considers two-phase systems with a distributed weak acid between an aqueous and an either organic or vapor phase. The equation of state ePC-SAFT advanced is used to calculate the pH in the aqueous phase, and to predict the chemical and phase equilibrium (CPE) composition of both phases at the experimental condition. Figure 1 provides a comparison between experimental and predicted pH-values in the pseudo-ternary system CO_2 + water + salt as function of the salt $\tilde{m}_{salt}$ molality for the salts KCl, NaCl and $NaHCO_3$. The main difference between the three systems is that $NaHCO_3$ takes part to the reaction equilibrium of CO_2, whereas KCl and NaCl only influence the activity of all the components. The behavior of the three systems is quantitatively captured in our calculations. Figure 2 shows experimental and predicted pH values in the aqueous phase of three pseudo-ternary systems carboxylic acid + water + organic solvent. Systems with acetic and citric acid contain toluene, whereas the systems with oxalic acid contains MIBK as solvents. In all the three systems the predictions are in excellent agreement with the experimental data.

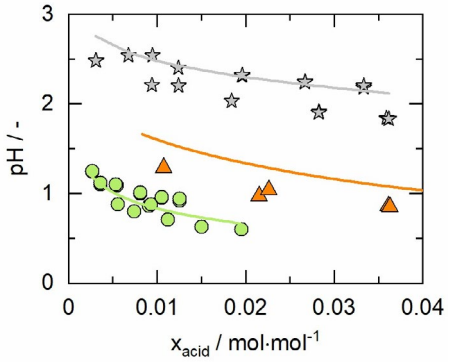

Figure 1: pH of the ternary system CO_2 + water + salt as function of salt molality. Predictions: solid lines. Experimental data: symbols (stars: $NaHCO_3$ at T = 308 K and p = 9.2 bar; hexagons: $NaHCO_3$ at T = 308 K and p = 43 bar; circles: NaCl at T = 343 K and p = 10 bar; triangles: KCl at T = 298 K and p = 9 bar). References: see publication.

In summary, ePC-SAFT advanced was able to quantitatively predict the influence of salts and organic solvents on the pH in multiphase systems. No parameter fitting to the experimental pH values was required.

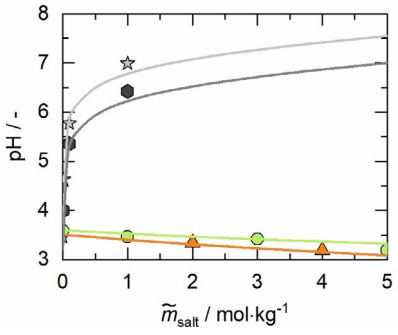

Figure 2: pH of the ternary system carboxylic acid + water + organic solvent as function of the water concentration in the aqueous phase. Predictions: solid lines. Experimental data: symbols. (stars: acetic acid; triangles: citric acid; circles: oxalic acid. The experimental condition is for the three systems T = 298 K and p = 1 bar) References: see publication.

Contacts:
christoph.held@tu-dortmund.de
moreno.ascani@tu-dortmund.de

Publication:
M. Ascani, D. Pabsch, M. Klinksiek, N.F. Gajardo-Parra, G. Sadowski, C. Held, ChemComm 58, 8436-8439 (2022)

Predicting the phase behavior during freeze-drying of biopharmaceuticals

A tool to optimize excipient selection in formulation and process development

Maximilian Zäh, Christoph Brandenbusch, Gerhard Winter, Gabriele Sadowski

Freeze-drying (lyophilization) remains one of the dominant strategies for long-term stabilization of biopharmaceuticals. The biopharmaceutical is thereby embedded in an amorphous phase of several excipients (e.g. cryoprotectants such as sugars), preserving its native state and activity during storage. Aside protein stability, choice of the excipients also defines process parameters of the lyophilization process, e.g. drying time. Choice of excipients and determination of these process parameters is usually performed through costly and time-consuming experiments. Within this work, we developed a hybrid (predictive) approach to facilitate the excipient choice and give easy access to the aforementioned process parameters.

Freeze-drying (lyophilization) is frequently used as the formulation method of choice when it comes to sensitive biopharmaceutics. The lyophilization process can be divided into two major process steps. The first step is freezing. During this step, the solid (ice) phase is formed, leading to a concentrated amorphous (excipient) phase surrounding the ice particles. The excipients, the biopharmaceutical, and a bit of water are then present in the amorphous phase. The second step is the actual drying, where the majority of water is sublimated by reducing the pressure below the sublimation pressure of ice at the given freezing temperature. Most important parameters that need to be known are: (1) the lowest possible temperature at which freezing should be performed, (2) the amount of residual water that is present after freezing. The latter intrinsically defines the drying time.

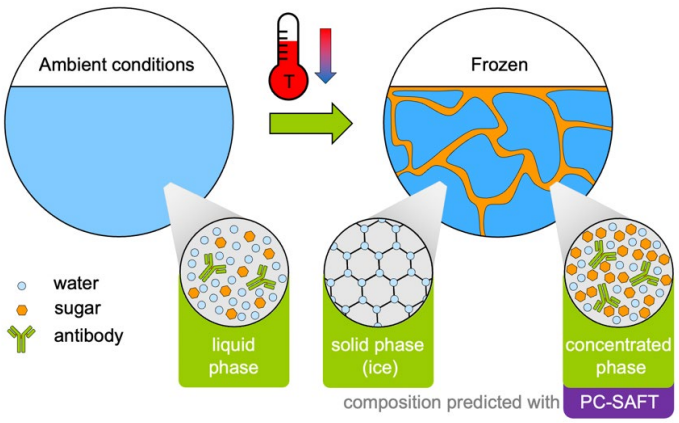

Figure 1: Schematic representation of the freezing step during freeze drying. Initial state at ambient conditions is shown on the left. Sugar and antibody are dissolved in water. The state after freezing is shown on the right. An ice phase and a concentrated amorphous phase have formed. The excipients initially dissolved in the liquid phase can now be found in the amorphous phase.

For a given excipient (mixture), the exact amount of excipients in the amorphous phase (vice versa the residual amount of water in the amorphous phase) is defined by the intercept of the glass-transition temperature (of the amorphous phase) and the solubility of water (being a function of temperature and type of excipient(s)). This process step is nicely visualized in Figure 1 and the two separate phases are illustrated in blue and orange.

Applying our hybrid approach, we determined the glass-transition temperature of the amorphous phase using one single experiment. This then allowed us to calculate the composition of the amorphous phase after freezing using the thermodynamic model PC-SAFT. We experimentally validated the approach for common single excipients used in freeze-drying e.g. sucrose and trehalose, for excipient mixtures of sucrose with the osmolyte ectoine and for excipient/protein mixtures of sucrose/BSA. It was shown that the approach precisely predicts the composition of the amorphous phase after freezing and thus dramatically reduces the effort required in state-of-the-art approaches. It can therefore be used for fast screening of potential formulation compositions during formulation and process development.

Publication:
M. Zäh, C. Brandenbusch, G. Winter, G. Sadowski, Int. J. Pharm., 636, 122836 (2023)

Contacts:
maximilian.zaeh@tu-dortmund.de
christoph.brandenbusch@tu-dortmund.de
gabriele.sadowski@tu-dortmund.de

Boosting the Kinetic Efficiency of Formate Dehydrogenase

Kinetic Efficiency is Increased by 300 % by Combined Effects of High Pressure and Co-solvent Mixtures

Nicolás Gajardo-Parra, Gabriele Sadowski, Christoph Held

The efficiency of homogenous liquid biocatalytic reactions depends on the environment of the catalyst (here: an enzyme) in the solution. This work evaluated the combined effects of temperature, pressure, and co-solvents to increase the kinetic efficiency of NADH synthesis. NADH is a high-value compound (> 10€/g NADH). The synthesis uses formate as substrate, which is oxidized in an aqueous solution with the enzyme formate dehydrogenase. The kinetic efficiency could be increased by 300 % applying a pressure of 2 kbar and a mixture of the co-solvents dextran and trimethylamine N-oxide (TMAO), compared to an aqueous buffer solution at 1 bar. The thermodynamic framework based on the equation of state ePC-SAFT allowed correctly predicting the combined effects of high pressure and co-solvent mixture on the kinetic efficiency without fitting any model parameters to the experimental kinetic data of the co-solvent mixtures.

The application of co-solvents and high pressure is an efficient means to modify the kinetics of enzyme-catalyzed reactions in aqueous solutions without decreasing enzyme stability. This is usually not possible by temperature treatment. FDH (formate dehydrogenase) catalyzes the formate oxidation to CO_2 via a complex mechanism partially limited by an irreversible hydride transfer. From a process perspective, it is most important to tune the macroscopic kinetic parameters at steady state. Thus, the kinetic parameters catalytic constant (k_{cat}), Michaelis constant (K_M), and catalytic efficiency ($K_{eff} = k_{cat}/K_M$) were studied in this work. It was known from literature (cf. publication) that K_{eff} was increased by a factor of three upon raising temperature from 25 °C to 45 °C. We were then keen on studying further the benefit of high pressure and cosolvent addition. TMAO and dextran were used as they improve the thermal stability of FDH. The combined effects of pressure and co-solvent on K_{eff} are shown in Figure 1.

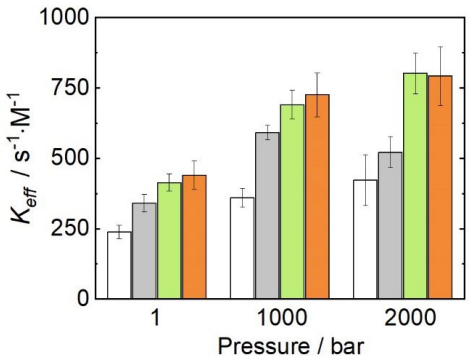

Figure 1: Experimental pressure dependence of kinetic efficiency K_{eff} for the FDH-catalyzed reaction at 25 °C and pH = 7.5 in aqueous buffer solution (white bars) and in aqueous solutions containing co-solvent dextran (gray, 13 mmol/kg), TMAO (green, 1 mol/kg), and a mixture of both co-solvents (orange).

Ultimately, the combined effect of co-solvent addition and high pressure increases K_{eff} by 300 % compared to a buffer solution at 1 bar. This boost is mainly caused by favored interactions of formate and TMAO and by mitigating conformational changes in the active pocket of FDH at high pressures. Conversely, dextran causes favorable FDH-solvent interactions to increase k_{cat}. To conclude, the mixture of the co-solvents positively affects both, kinetics and stability of FDH. However, there is a huge matrix to study the kind and concentration of co-solvent candidates. Thus, a thermodynamic activity-based framework was applied to predict the impact of cosolvent mixtures on the kinetic parameters beforehand. ePCSAFT was applied to predict interactions between formate/solvent and FDH/solvent as a function of pressure and co-solvent mixture. As shown in Figure 2, the ePC-SAFT predicted K_{eff} values are in accurate agreement with the experimental data. This is an excellent result as no ePC-SAFT parameters were fitted to the experimental kinetic data of the co-solvent mixtures. The predictions require only K_{eff} data in buffer as input data.

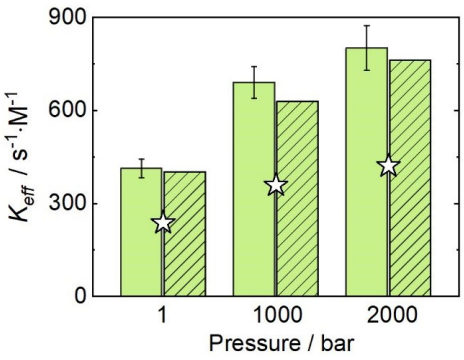

Figure 2: ePC-SAFT modeling of kinetic efficiency. Conditions: 25 °C, pH = 7.5 and 1 mol/kg of TMAO in water. Experimental data (green), ePC-SAFT (green striped), and the TMAO-free values (white stars).

Thus, combining experimental data and thermodynamic predictions allows boosting the kinetic parameters of enzyme-catalyzed reactions. This approach will further contribute to a broader insight into enzyme-catalyzed reactions at crowded cellular conditions, which still remain largely unexplored.

Contacts:
nicolas.gajardo@tu-dortmund.de
christoph.held@tu-dortmund.de
gabriele.sadowski@tu-dortmund.de

Publication:
M. Jaworek, N. Gajardo-Parra, G. Sadowski, R. Winter, C. Held, Colloids Surf. B. 208, 112127 (2021)

Publications 2020 –2022

2022

Peer-reviewed Journal Articles

- Arroyo-Avirama, N. Gajardo-Parra, V. Espinoza-Carmona, J. M. Garrido, C. Held, R. Canales
  Solvent Selection for the Extraction of 2-Phenylethanol from Aqueous Phases: Density and Viscosity Studies
  Journal of Chemical & Engineering Data, 355, 118936 (2022)

- A. Krummnow, A. Danzer, K. Voges, S. Dohrn, S. Kyeremateng, M. Degenhardt, G. Sadowski
  Explaining the Release Mechanism of Ritonavir/PVPVA Amorphous Solid Dispersion
  Pharmaceutics,14, 1904 (2022)

- A. C. Kufner, A. Krummnow, A. Danzer, K. Wohlgemuth
  Strategy for Fast Decision on Material System Suitability for Continuous Crystallization Inside a Slug Flow Crystallizer
  Micromachines, 13, 1795 (2022)

- D. Borrmann, A. Danzer, G. Sadowski
  Anomalous Water-Sorption Kinetics in ASDs
  Pharmaceutics, 14, 1897 (2022)

- D. Borrmann, A. Danzer, G. Sadowski
  Measuring and Modeling Water Sorption in Amorphous Indomethacin and Ritonavir Molecular
  Pharmaceutics, 19, 998-1007 (2022)

- D. Borrmann, A. Danzer, G. Sadowski
  Predicting the Water Sorption in ASDs
  Pharmaceutics, 14, 1181 (2022)

- D. Borrmann, A. Danzer, G. Sadowski
  Water Sorption in Glassy Polyvinylpyrrolidone-Based Polymers
  Membranes, 12, 434 (2022)

- D. Pabsch, J. Lindfeld, J. Schwalm, A. Strangmann, P. Figiel, G. Sadowski, C. Held
  Influence of solvent and salt on kinetics and equilibrium of esterification reactions
  Chemical Engineering Science, 263, 118046 (2022)

- D. Pabsch, P. Figiel, G. Sadowski, C. Held
  Solubility of Electrolytes in Organic Solvents: Solvent-Specific Effects and Ion-Specific Effects
  Journal of Chemical & Engineering Data, 67, 2706-2718 (2022)

- E. Cea-Klapp, N. Gajardo-Parra, P. Aravena, H. Quinteros-Lama, C. Held, R. Canales, J. M. Garrido
  Interfacial Properties of Deep Eutectic Solvents by Density Gradient Theory Industrial & Engineering
  Chemistry Research, 61, 2580-2591 (2022)

- F. Huxoll, A. Kampwerth, T. Seidensticker, D. Vogt, G. Sadowski
  Predicting Solvent Effects on Homogeneity and Kinetics of the Hydroaminomethylation: A Thermodynamic Approach Using PC-SAFT
  Industrial & Engineering Chemistry Research, 61, 2323-2332 (2022)

- F. Wolbert, I. Fahrig, T. Gottschalk, C. Luebbert, M. Thommes, G. Sadowski
  Factors Influencing the Crystallization-Onset Time of Metastable ASDs
  Pharmaceutics, 14, 269 (2022)

- F. Wolbert, K. Nikoleit, M. Steinbrink, C. Luebbert, G. Sadowski
  The Shelf Life of ASDs: 1. Measuring the Crystallization Kinetics at Humid Conditions Molecular
  Pharmaceutics, 19, 2483-2494 (2022)

- N. Gajardo-Parra, H. Akrofi-Mantey, M. Ascani, E. Cea-Klapp, J. M. Garrido, G. Sadowski, C. Held
  Osmolyte effect on enzymatic stability and reaction equilibrium of formate dehydrogenase Physical Chemistry
  Chemical Physics, 24, 27930-27939, (2022)

- J. Delgado, W. Vasquez, G. Bronzetti, V. Casson-Moreno, M. Mignot, J. Legros, C. Held, H. Grénman, S. Leveneur
  Kinetic model assessment for the synthesis of - -valerolactone from n-butyl levulinate and levulinic acid hydrogenation over the synergy effect of dual catalysts Ru/C and Amberlite IR-120
  Chemical Engineering Journal, 430, 133053 (2022)

- J. Sauer, H.-D. Kühl
  Performance improvements in Stirling cycle machines by a modified appendix gap geometry
  International Journal of Energy Research, 46, 1180- 1197 (2022)

- K. Ge, R. Paus, V. Penner, G. Sadowski, Y. Ji
  Theoretical modeling and prediction of biorelevant solubility of poorly soluble pharmaceuticals
  Chemical Engineering Journal, 444, 136678 (2022)

- L. Janssen, G. Sadowski, C. Brandenbusch
  Long-term stable bioprocess-derived Pickering-type emulsions: Identification of key parameters for emulsion stability based on cell interaction at interface
  Chemical Engineering Science, 264, 118164 (2022)

- L. Nolte, C. Brandenbusch
  Monitoring and investigating reactive extraction of (di–)carboxylic acids using online FTIR – Part II: Reaction equilibria, reaction kinetics and competition within the complex formation between itaconic acid and several amine extractants
  Journal of Molecular Liquids, 366, 120223 (2022)

- L. Nolte, M. Nowaczyk, C. Brandenbusch
  Monitoring and investigating reactive extraction of (di–)carboxylic acids using online FTIR – Part I: Characterization of the complex formed between itaconic acid and tri-n-octylamine Journal of Molecular Liquids, 352, 118721 (2022)

- M. Ascani, D. Pabsch, M. Klinksiek, N. Gajardo-Parra, G. Sadowski, C. Held
  Prediction of pH in multiphase multicomponent systems with ePC-SAFT advanced
  Chemical Communications, 58, 8436-8439 (2022)

- M. Ascani, G. Sadowski, C. Held
  Calculation of Multiphase Equilibria Containing Mixed Solvents and Mixed Electrolytes: General Formulation and Case Studies
  Journal of Chemical & Engineering Data, 67, 1972-1984 (2022)

- M. Keppler, S. Moser, H. J. Jessen, C. Held, J. N. Andexer
  Make or break: the thermodynamic equilibrium of polyphosphate kinase-catalysed reactions
  Beilstein Journal of Organic Chemistry, 18, 1278-1288 (2022)

- N. Gajardo-Parra, L. Meneses, A. Duarte, A. Paiva, C. Held
  Assessing the Influence of Betaine-Based Natural Deep Eutectic Systems on Horseradish Peroxidase ACS Sustainable
  Chemistry & Engineering, 10, 12873-12881 (2022)

- P. Kroll, G. Sadowski, C. Brandenbusch
Solubilization of Aldehydes and Amines in Aqueous CiEj Surfactant Aggregates: Solubilization Capacity and Aggregate Properties
Langmuir, 38, 10022-10031 (2022)

- P. Kroll, J. Benke, S. Enders, C. Brandenbusch, G. Sadowski
Influence of Temperature and Concentration on the Self-Assembly of Nonionic CiEj Surfactants: A Light Scattering Study
ACS Omega, 7, 7057-7065 (2022)

- S. Baco, M. Klinksiek, R. Ismail, A. Garcia-Hernandez, M. Mignot, J. Legros, C. Held, V. Casson, S. Leveneur
Solvent effect investigation on the acid-catalyzed esterification of levulinic acid by ethanol aided by a Linear Solvation Energy Relationship
Chemical Engineering Science, 260, 117928 (2022)

- S. Schlüter, F. Huxoll, K. Grenningloh, G. Sadowski, M. Petzold, L. Böhm, M. Kraume, M. Skiborowski
Unraveling the influence of dissolved gases on permeate flux in organic solvent nanofiltration – Experimental analysis
Separation and Purification Technology, 295, 121265 (2022)

- T. Gottschalk, B. Grönniger, E. Ludwig, F. Wolbert, T. Feuerbach, G. Sadowski, M. Thommes
Influence of process temperature and residence time on the manufacturing of amorphous solid dispersions in hot melt extrusion
Pharmaceutical Development and Technology, 27, 1-6 (2022)

- T. Stolzke, C. Brandenbusch
Simplified choice of suitable excipients within biologics formulation design using protein-protein interaction- and water activity-maps
European Journal of Pharmaceutics and Biopharmaceutics, 176, 153-167 (2022)

2021

Peer-reviewed Journal Articles

- A. B. Morales, C. Luebbert, S. Enders, G. Sadowski, I. Smirnova
Production of polylactic acid aerogels via phase separation and supercritical CO2 drying: thermodynamic analysis of the gelation and drying process
Journal of Materials Science, 56, 18926-18945 (2021)

- A. Jastram, T. Lindner, C. Luebbert, G. Sadowski, U. Kragl
Swelling and Diffusion in Polymerized Ionic Liquids-Based Hydrogels
Polymers, 13, 1834 (2021)

- A. Roda, F. Santos, Y. Chua, A. Kumar, H. T. Do, A. Paiva, A. Duarte, C. Held
Unravelling the nature of citric acid:l-arginine:water mixtures: the bifunctional role of water
Physical Chemistry Chemical Physics, 23, 1706-1717 (2021)

- A. Sosa, J. Ortega, L. Fernández, N. Haarmann, G. Sadowski
Methodology Based on the Theory of Information to Describe the Representation Ability of the DMC + Alkane Behavior
Industrial & Engineering Chemistry Research, 60, 1036-1054 (2021)

- A. Schmitz, M. Bulow, D. Schmidt, D. H. Zaitsau, F. Junglas, T. O. Knedel, S. P. Verevkin, C. Held, C. Janiak
Tetrahydrothiophene-Based Ionic Liquids: Synthesis and Thermodynamic Characterizations
ChemistryOpen, 10, 153-163 (2021)

- B. Sepúlveda-Orellana, N. Gajardo-Parra, H. T. Do, J. Pérez-Correa, C. Held, G. Sadowski, R. Canales
Measurement and PC-SAFT Modeling of the Solubility of Gallic Acid in Aqueous Mixtures of Deep Eutectic Solvents
Journal of Chemical & Engineering Data, 66, 958-967 (2021)

- C. Luebbert, G. Sadowski, E. Stoyanov
Phase behavior of ASDs based on hydroxypropyl cellulose
International Journal of Pharmaceutics: X, 3, 100070 (2021)

- C. Prell, T. Busche, C. Rückert, L. Nolte, C. Brandenbusch, V. Wendisch
Adaptive laboratory evolution accelerated glutarate production by Corynebacterium glutamicum
Microbial Cell Factories, 20, 97 (2021)

- D. Borrmann, A. Danzer, G. Sadowski
Generalized Diffusion–Relaxation Model for Solvent Sorption in Polymers
Industrial & Engineering Chemistry Research, 60, 15766-15781 (2021)

- D. Sleziona, A. Mattusch, G. Schaldach, D. Ely, G. Sadowski, M. Thommes
Determination of Inherent Dissolution Performance of Drug Substances
Pharmaceutics, 13, 146 (2021)

- D. Zaitsau, R. Siewert, A. Pimerzin, M. Bülow, C. Held, M. Loor, S. Schulz, S. Verevkin
From volatility to solubility: Thermodynamics of imidazolium-based ionic liquids containing chloride and bromide anions
Journal of Molecular Liquids, 323, 114998 (2021)

- F. Fischer, H.-D. Kühl
Generation of compressed air by cascaded thermocompressors – project status
E3S Web Conf., 313, 04003 (2021)

- F. Huxoll, F. Jameel, J. Bianga, T. Seidensticker, M. Stein, G. Sadowski, D. Vogt
Solvent Selection in Homogeneous Catalysis—Optimization of Kinetics and Reaction Performance
ACS Catalysis, 11, 590-594 (2021)

- F. Huxoll, M. Heyng, I. Andreeva, S. Verevkin, G. Sadowski
Thermodynamic Properties of Biogenic Amines and Their Solutions
Journal of Chemical & Engineering Data, 66, 2822-2831 (2021)

- F. Huxoll, S. Schlüter, R. Budde, M. Skiborowski, M. Petzold, L. Böhm, M. Kraume, G. Sadowski
Phase Equilibria for the Hydroaminomethylation of 1-Decene
Journal of Chemical & Engineering Data, 66, 4484-4495 (2021)

- H. Veith, C. Luebbert, G. Sadowski
Predicting Deliquescence Relative Humidities of Crystals and Crystal Mixtures
Molecules, 26, 3176 (2021)

- H. Veith, C. Luebbert, N. Rodríguez-Hornedo, G. Sadowski
Co-Crystal Screening by Vapor Sorption of Organic Solvents
Crystal Growth & Design, 21, 4445-4455 (2021)

- H. Veith, F. Wiechert, C. Luebbert, G. Sadowski
Combining crystalline and polymeric excipients in API solid dispersions - Opportunity or risk?
European Journal of Pharmaceutics and Biopharmaceutics, 158, 323-335 (2021)

- H. Veith, M. Zaeh, C. Luebbert, N. Rodríguez-Hornedo, G. Sadowski
Stability of Pharmaceutical Co-Crystals at Humid Conditions Can Be Predicted
Pharmaceutics, 13, 433 (2021)

- H.-D. Kühl, J. Sauer
Appendix gap losses in Stirling engines – review of recent findings
E3S Web Conf., 313, 03001 (2021)

- J. Brinkmann, I. Becker, P. Kroll, C. Luebbert, G. Sadowski
Predicting the API partitioning between lipid-based drug delivery systems and water
International Journal of Pharmaceutics, 595, 120266 (2021)

- J. Brinkmann, L. Exner, S. Verevkin, C. Luebbert, G. Sadowski
PC-SAFT Modeling of Phase Equilibria Relevant for Lipid-Based Drug Delivery Systems
Journal of Chemical & Engineering Data, 66, 1280-1289 (2021)

- J. Delgado, W. Salcedo, G. Bronzetti, V. Casson-Moreno, M. Mignot, J. Legros, C. Held, H. Grénman, S. Leveneur
Kinetic model assessment for the synthesis of - -valerolactone from n-butyl levulinate and levulinic acid hydrogenation over the synergy effect of dual catalysts Ru/C and Amberlite IR-120
Chemical Engineering Journal, 133053 (2021)

- J. Sauer, H.-D. Kühl
Performance improvements in Stirling cycle machines by a modified appendix gap
geometry International Journal of Energy Research, 45, 1-18 (2021)

- K. Wysoczanska, B. Nierhauve, G. Sadowski, E. Macedo, C. Held
Solubility of DNP-amino acids and their partitioning in biodegradable ATPS: Experimental and ePC-SAFT modeling
Fluid Phase Equilibria, 527, 112830 (2021)

- M. Ascani, C. Held
Prediction of salting-out in liquid-liquid two-phase systems with ePC-SAFT: Effect of the Born term and of a concentration-dependent dielectric constant
Zeitschrift für anorganische und allgemeine Chemie, 647, 1305 (2021)

- M. Bülow, M. Ascani, C. Held
ePC-SAFT advanced - Part I: Physical meaning of including a concentration-dependent dielectric constant in the born term and in the Debye-Hückel theory
Fluid Phase Equilibria, 535, 112967 (2021); ibid 548, 113184

- M. Bülow, M. Ascani, C. Held
ePC-SAFT advanced – Part II: Application to Salt Solubility in Ionic and Organic Solvents and the Impact of Ion Pairing
Fluid Phase Equilibria, 537, 112989 (2021); ibid 548, 113183

- M. Bülow, M. Greive, D. Zaitsau, S. Verevkin, C. Held
Extremely Low Vapor-Pressure Data as Access to PC-SAFT Parameter Estimation for Ionic Liquids and Modeling of Precursor Solubility in Ionic Liquids
ChemistryOpen, 10, 216-226 (2021)

- M. Bülow, N. Gerek Ince, S. Hirohama, G. Sadowski, C. Held
Predicting Vapor–Liquid Equilibria for Sour-Gas Absorption in Aqueous Mixtures of Chemical and Physical Solvents or Ionic Liquids with ePC-SAFT
Industrial & Engineering Chemistry Research, 60, 6327-6336 (2021)

- M. Jaworek, N. Gajardo-Parra, G. Sadowski, R. Winter, C. Held
Boosting the Kinetic Efficiency of Formate Dehydrogenase by Combining the Effects of Temperature, High Pressure and Co-solvent Mixtures
Colloids and Surfaces B: Biointerfaces, 208, 112127 (2021)

- M. Wessner, B. Bommarius, C. Brandenbusch, A. Bommarius
Purification of chimeric amine dehydrogenase using a tailor-made aqueous two-phase system - A case study
Journal of Molecular Liquids, 323, 114991 (2021)

- M. Wessner, M. Meier, B. Bommarius, A. Bommarius, C. Brandenbusch
Intensifying aqueous two-phase extraction by adding decisive excipients for enhancement of stability and solubility of biomolecules
Chemical Engineering and Processing - Process Intensification, 167, 108534 (2021)

- N. Gajardo-Parra, H. T. Do, M. Yang, J. Pérez-Correa, J. M. Garrido, G. Sadowski, C. Held, R. Canales
Impact of deep eutectic solvents and their constituents on the aqueous solubility of phloroglucinol dihydrate
Journal of Molecular Liquids, 344, 117932 (2021)

- S. Dohrn, C. Luebbert, K. Lehmkemper, S. Kyeremateng, M. Degenhardt, G. Sadowski G.
Solvent influence on the phase behavior and glass transition of Amorphous Solid Dispersions
European Journal of Pharmaceutics and Biopharmaceutics, 158, 132-142 (2021)

- S. Dohrn, C. Luebbert, K. Lehmkemper, S. Kyeremateng, M. Degenhardt, G. Sadowski
Solvent mixtures in pharmaceutical development: Maximizing the API solubility and avoiding phase separation
Fluid Phase Equilibria, 548, 113200 (2021)

- S. Dohrn, P. Rawal, C. Luebbert, K. Lehmkemper, S. Kyeremateng, M. Degenhardt, G. Sadowski
Predicting process design spaces for spray drying amorphous solid dispersions
International Journal of Pharmaceutics: X, 100072 (2021)

- H.-T. Do, P. Franke, S. Volpert, M. Klinksiek, M. Thome, C. Held
Measurement and modelling solubility of amino acids and peptides in aqueous 2-propanol solutions
Physical Chemistry Chemical Physics, (2021)

- H.-T. Do, S. Chakrabarty, C. Held
Modeling solubility of amino acids and peptides in water and in water+2-propanol mixtures: PC-SAFT vs. gE models
Fluid Phase Equilibria, 113087 (2021)

- H.-T. Do, Y. Chua, J. Habicht, M. Klinksiek, S. Volpert, M. Hallermann, M. Thome, D. Pabsch, D. Zaitsau, C. Schick, C. Held
Melting Properties of Peptides and Their Solubility in Water. Part 2: Di- and Tripeptides Based on Glycine, Alanine, Leucine, Proline, and Serine
Industrial & Engineering Chemistry Research, 60 (12), 4693-4704 (2021)

- T. Greinert, K. Vogel, T. Maskow, C. Held
New thermodynamic activity-based approach allows predicting the feasibility of glycolysis
Scientific Reports, 11, 6125 (2021)

- Y. Ji, D. Hao, C. Luebbert, G. Sadowski
Insights into influence mechanism of polymeric excipients on dissolution drug formulations: A molecular interaction-based theoretical model analysis and prediction
AIChE Journal, 67, e17372 (2021)

- Y. Sun, Z. Zuo, G. Shen, C. Held, X. Lu, X. Ji
Modeling interfacial properties of ionic liquids with ePC-SAFT combined with density gradient theory
Fluid Phase Equilibria, 536, 112984 (2021)

- S. Capecci, Y. Wang, VC Moreno, C. Held, S. Leveneur
Solvent effect on the kinetics of the hydrogenation of n-butyl levulinate to ß-valerolactone
Chemical Engineering Science 231, 116315

2020

Peer-reviewed Journal Articles

- T. Weinbender, M. Knierbein, L. Bittorf, C. Held, R. Siewert, S. P. Verevkin, S. Sadowski, O. Reiser
High-pressure-mediated thiourea-organocatalyzed Michael addition to (hetero) aromatic nitroolefins: Prediction of reaction parameters by PCP-SAFT modelling
ChemPlusChem, 85, 6, 1292-1296 (2020)

- T. Greinert, K. Vogel, J. K. Mühlenweg, G. Sadowski, T. Maskow, C. Held
Standard Gibbs energy of metabolic reactions: VI. Glyceraldehyde 3-phosphate dehydrogenase reaction
Fluid Phase Equilibria, 517,112597 (2020)

- T. Greinert, K. Vogel, A. I. Seifert, R. Siewert, I. V. Andreeva, S. P. Verevkin, T. Maskow, G. Sadowski, C. Held
  Standard Gibbs energy of metabolic reactions: V. Enolase reaction
  Biochimica et Biophysica Acta (BBA)-Proteins and Proteomics, 1868 (2020)

- T. Greinert, K. Baumhove, G. Sadowski, C. Held
  Standard Gibbs energy of metabolic reactions: IV. Triosephosphate isomerase reaction
  Biophysical Chemistry, 258, 106330 (2020)

- R. Schneider, J. Kerkhoff, A. Danzer, A. Mattusch, A. Ohmann, M. Thommes, G. Sadowski
  The interplay of dissolution, solution crystallization and solid-state transformation of amorphous indomethacin in aqueous solution
  International Journal of Pharmaceutics: X, 100063 (2020)

- S. Dohrn, P. Reimer, C. Lübbert, K. Lehmkemper, S. O. Kyerematen, M. Degenhardt, S. Sadowski
  Thermodynamic modeling the solvent-impact on phase separation of amorphous solid dispersions during drying
  Molecular Pharmaceutics, In Press, 17, 7, 2721-2733 (2020)

- S. Dohrn, C. Lübbert, K. Lehmkemper, S. O. Kyerematen, M. Degenhardt, G. Sadowski
  Phase behavior of pharmaceutically relevant polymer/solvent mixtures
  International Journal of Pharmaceutics, 577, 119065 (2020)

- S. Capecci, Y. Wang, V. Casson Moreno, C. Held, S. Leveneur
  Solvent effect on the kinetics of the hydrogenation of n-butyl levulinate to g-valerolactone
  Chemical Engineering Science, 116315 (2020)

- R. Schneider, L. Taspinar, Y. Ji, G. Sadowski
  The influence of polymeric excipients on desupersaturation profiles of active pharmaceutical ingredients. 1: Polyethylene glycol
  International Journal of Pharmaceutics, 582, 119317 (2020)

- N. Haarmann, A. Reinhardt, A. Danzer, G. Sadowski, S. Enders
  Modeling of Interfacial Tensions of Long-Chain Molecules and Related Mixtures using PC-SAFT and the Density Gradient Theory
  J. Chem. Eng. Data, 65, 1005-1018 (2020)

- M. Wessner, M. Nowaczyk, C. Brandenbusch
  Rapid identification of tailor-made aqueous two-phase systems for the extractive purification of high-value biomolecules
  Journal of Molecular Liquids, In Press (2020)

- M. Wessner, K. Diederich, C. Brandenbusch
  Influence of Sodium Chloride and Lithium Bromide on the Phase Behavior of a Citrate–Polyethylene Glycol 2000 Aqueous Two-Phase System
  Journal of Chemical & Engineering Data, In Press, 65, 8, 4009-4017 (2020)

- M. Schleinitz, L. Nolte, C. Brandenbusch
  Predicting protein-protein interactions using the ePC-SAFT equation-of-state
  Journal of Molecular Liquids, 298 (2020)

- M. Knierbein, M. Voges, C. Held
  5-Hydroxymethylfurfural Synthesis in Nonaqueous Two-Phase Systems (NTPS)–PC-SAFT Predictions and Validation
  Organic Process Research & Development, In Press, 24, 6, 1052-1062 (2020)

- M. Knierbein, C. Held, G. Sadowski
  The Role of Molecular Interactions on Michaelis Constants of ß-Chymotrypsin Catalyzed Peptide Hydrolyses
  The Journal of Chemical Thermodynamics, 148, 106142 (2020)

- M. Bülow, A. Schmitz, T. Mahmoudi, D. Schmidt, F. Junglas, C. Janiak, C. Held
  Odd–even effect for efficient bioreactions of chiral alcohols and boosted stability of the enzyme
  RSC Advances, 10, 28351-28354 (2020)

- K. Wysoczanska, H. T. Do, G. Sadowski, E. A. Macedo, C. Held
  Partitioning of water-soluble vitamins in biodegradable aqueous two-phase systems: Electrolyte Perturbed-Chain Statistical Associating Fluid Theory predictions and experimental validation
  AIChE Journal, 66, e16984 (2020)

- K. Vogel, T. Greinert, M. Reichard, C. Held, H. Harms, T. Maskow
  Thermodynamics and Kinetics of Glycolytic Reactions. Part I: Kinetic Modeling Based on Irreversible Thermodynamics and Validation by Calorimetry
  International Journal of Molecular Sciences, 21, 8341 (2020)

- K. Vogel, T. Greinert, M. Reichard, C. Held, H. Harms, T. Maskow
  Thermodynamics and Kinetics of Glycolytic Reactions. Part II: Influence of Cytosolic Conditions on Thermodynamic State Variables and Kinetic Parameters
  International Journal of Molecular Sciences, 21, 7921 (2020)

- K. Vogel, T. Greinert, H. Harms, G. Sadowski, C. Held, T. Maskow
  Influence of cytosolic conditions on the reaction equilibrium and the reaction enthalpy of the enolase reaction accessed by calorimetry and van't Hoff
  Biochimica et Biophysica Acta (BBA) - General Subjects, 1864, 129675 (2020)

- K. Vogel, T. Greinert, C. Held, H. Harms, T. Maskow
  Application of Irreversible Thermodynamics to Determine the Influence of Cell Mimicking Conditions on the Kinetics of Equilibrium Reactions of the Glycolysis
  Biophysical Journal, 118, 346a-347a (2020)

- J. Sauer, H.-D. Kühl
  Theoretically and experimentally founded simulation of the appendix gap in regenerative machines
  Applied Thermal Engineering, 166, 114530 (2020)

- M. J. Lubben, R. I. Canales, Y. Lyu, C. Held, M. Gonzalez-Miquel, M. A. Stadtherr, J. F. Brennecke
  Promising Thiolanium Ionic Liquid for Extraction of Aromatics from Aliphatics: Experiments and Modeling
  Industrial & Engineering Chemistry Research, 59, 15707-15717 (2020)

- J. Brinkmann, L. Exner, C. Lübbert, G. Sadowski
  In-Silico Screening of Lipid-Based Drug Delivery Systems
  Pharmaceutical Research, 37, 249 (2020)

- J. Brinkmann, F. Rest, C. Lübbert, G. Sadowski
  Solubility of Pharmaceutical Ingredients in Natural Edible Oils
  Molecular Pharmaceutics, In Press, 17, 7, 2499–2507 (2020)

- D. H. Zaitsau, R. Siewert, A. A. Pimerzin, M. Bülow, C. Held, M. Loor, S. Schulz, S. P. Verevkin
  Paving the way to solubility through volatility: Thermodynamics of imidazolium-based ionic liquids of the type [CnC1Im][I]
  Fluid Phase Equilibria, 522, 112767 (2020)

- H. Veith, E. Turan, C. Lübbert, G. Sadowski
  Hydrate formation in polymer-based pharmaceutical formulations
  Fluid Phase Equilibria, 112677 (2020)

- H. Veith, C. Lübbert, G. Sadowski
  Correctly Measuring and Predicting Solubilities of Solvates, Hydrates, and Polymorphs
  Crystal Growth & Design, 20, 723-735 (2020)

- F. Wolbert, J. Stecker, C. Lübbert, G. Sadowski
  Viscosity of ASDs at humid conditions
  European Journal of Pharmaceutics and Biopharmaceutics, 154, 387-396 (2020)

- F. Fischer, H.-D. Kühl
  Analytical model for an overdriven free-displacer thermos compressor
  Applied Thermal Engineering, 116251 (2020)

- D. Pabsch, C. Held, G. Sadowski
  Modeling the CO2 Solubility in Aqueous Electrolyte Solutions Using ePC-SAFT
  Journal of Chemical & Engineering Data, 65, 12, 5768-5777 (2020)

- C. Held
  Thermodynamic gE Models and Equations of State for Electrolytes in a Water-Poor Medium: A Review
  Journal of Chemical & Engineering Data, 65, 5073-5082 (2020)

- A. Reinhardt, N. Haarmann, G. Sadowski, S. Enders
  Application of PC-SAFT and DGT for the Prediction of Self-Assembly
  Journal of Chemical & Engineering Data, 65, 5897-5908 (2020)

SCIENTIFIC HIGHLIGHTS 2022

Impressum
TU Dortmund
www.bci.tu-dortmund.de
Redaktion: Prof. Joerg C. Tiller
Publication date: September 2023